1956

An investigation of the effect of wave slope on the angle of pitch of ships of various forms

McKibben, Ferney M.; Volz, Robert L.

Massachusetts Institute of Technology

AN INVESTIGATION OF THE EFFECT OF WAVE SLOPE ON THE ANGLE OF PITCH OF SHIPS OF VARIOUS FORMS

Ferney M. McKibben
and
Robert L. Volz

AN INVESTIGATION OF THE EFFECT OF WAVE SLOPE ON THE ANGLE OF PITCH OF SHIPS OF VARIOUS FORMS

by

FERNEY M. McKIBBEN, Lieutenant, U.S. Coast Guard
B.S., U.S. Coast Guard Academy
(1950)

and

ROBERT L. VOLZ, Lieutenant, U.S. Navy
B.S., U.S. Naval Academy
(1949)

SUBMITTED IN PARTIAL FULFILLMENT
OF THE REQUIREMENTS FOR THE
DEGREE OF NAVAL ENGINEER
at the
MASSACHUSETTS INSTITUTE OF TECHNOLOGY
May 1956

Department of Naval Architecture and
Marine Engineering, May 21, 1956

Signature of Authors _____

_____

Certified by _____
Thesis Supervisor

Accepted by _____
Chairman, Departmental Committee
on Graduate Students

ABSTRACT

AN INVESTIGATION OF THE EFFECT OF WAVE SLOPE ON THE ANGLE OF PITCH OF SHIPS OF VARIOUS FORMS

by

Ferney M. McKibben and Robert L. Volz

Submitted to the Department of Naval Architecture and Marine Engineering on 21 May 1956 in partial fulfillment of the requirements for the degree of Naval Engineer.

A study is made of the behavior in head seas of three different ships, a destroyer (Model 1), a cruiser (Model 2), and an aircraft carrier with bulbous bow (Model 3). Pitch angles were measured by means of an angular motion gyroscope capable of determining angles to close tolerances. Pitching angle, heave, and speed reduction are presented in the form of dimensional and dimensionless graphs.

The models were run in waves covering the range $.5 < \lambda/L < 2.335$, with wave slopes of $70 < \lambda/a < 25$. Model 1 was run at towing forces corresponding to three still-water speeds, while Models 2 and 3 were run at one still-water speed.

For a number of runs, experimental values of pitch angle were compared with those given by the theory of Weinblum and St. Denis in their paper "On the Motions of Ships at Sea," Transactions SNAME, Vol. 58, 1950. The theory was found to be satisfactory for predicting pitch angles at values of λ/L below 1.3. Correlation for the destroyer was excellent at all wave lengths; the other two models showed some marked discrepancies between theoretical and experimental values for λ/L above 1.0.

The primary purpose of this investigation was to determine the extent of linear variation between angle of pitch and wave slope. The authors conclude that pitch-angle is a non-linear function of wave slope for all of the models tested. Below values of $a/\lambda = .02$ a linear approximation is valid, but at higher values such an approximation will predict pitch angles greater than those actually observed. Heave is also found to be non-linear with wave slope, but for $a/\lambda < .025$ a linear approximation will give reasonable values. Since these limits of wave slope exclude the higher waves, it is concluded that the linear approximation cannot be used in the region of greatest interest.

The following general conclusions are also drawn:

1. Maximum pitching amplitudes do not necessarily occur at synchronism, where the ratio of still-water pitching period to period of wave encounter equals one. Maximum pitch angles occurred for all three models at values of tuning factor below .75. Since maximum velocities and accelerations normally occur near synchronism, the importance of this condition is not diminished.

2. All three models behaved substantially alike in pitching, heaving, and speed loss. Behavior of Models 1 and 2 was very similar, while Model 3 in general experienced greater motions. This is attributed to the somewhat finer waterline of Model 3 as compared with Models 1 and 2.

3. Since heave and pitch increased markedly with increasing values of λ/L for all three models, the standard ratio $\lambda/L = 1$ cannot be used as a limiting case when investigating seaworthiness.

Thesis Supervisor: Martin A. Abkowitz
Title: Associate Professor of Naval Architecture

ACKNOWLEDGEMENTS

The authors wish to acknowledge the contributions of the following persons in making this thesis possible:

Professor M. A. Abkowitz, who suggested the problem and guided our footsteps throughout its investigation.

Dr. V. G. Szebehely and the David Taylor Model Basin for graciously allowing us to use model number 2.

Mr. George Wachnik who by his knowledge and understanding of the complexities of the Ship Model Towing Tank saved us at least an extra semester's work and provided us with invaluable assistance and advice in performing our experiments.

Our families who by calm acceptance of endless discussion, late hours and meals, and lost weekends provided inspiration in our darkest hours.

TABLE OF CONTENTS

LIST OF FIGURES

LIST OF FIGURES (Cont.)

SYMBOLS

a	Wave height
b	Ship's half beam
f	Reduced exciting force
g	Acceleration of gravity
h	Damping coefficient
k	Spring constant
k_y	Longitudinal radius of gyration
ℓ	Distance from center of gravity of model to springs in determination of k_y
m	Mass
n	Strobe setting in flashes per minute
q	Logarithmic decrement
r	Wave ordinate ($\frac{1}{2}$ wave height)
s	General coordinate of displacement - either linear or angular
t	Time
x	Peak amplitude of extinction curve
z	Heave
J_y	Longitudinal moment of inertia of the waterplane
L	Ship or model length
M_ψ	Exciting moment in pitch
N	Number of spaces between lines in 7-ft. length on stroboscopic photograph
T_e	Period of encounter
T_p	Natural pitching period
T_r	Period of angular motion in determination of k_y
T_t	Period of translation in determination of k_y

SYMBOLS (Cont.)

V	Ship or model speed
X	Longitudinal coordinate of ships surface, measured along fore and aft axis from center of gravity
Y	Vertical coordinate of ships surface, measured along vertical axis from center of gravity
γ	Wave length parameter
ϵ_1, ϵ_2	Partial phase angles
ϕ	Wave slope
$\varkappa$	Dimensionless damping factor
λ	Wave length
μ_z	Magnification factor
ν	Frequency of free oscillation
ρ	Density
$\frac{1}{2}\psi$	Angle of pitch (angle of inclination from horizontal)
ω	Frequency of exciting force
ω_r	Frequency of angular motion in determination of k_y
ω_t	Frequency of translation in determination of k_y
Λ	Tuning factor = T_p/T_e
$\Psi_t(\gamma)$	Corrected pitch function

Superscripts

'	Value actually measured (uncorrected value)

Subscripts

avg.	Average
o	Open water
m,max.	Maximum
s	Still water

I. INTRODUCTION

As an isolated motion, pitching of a ship in calm water is a practical impossibility because of the large magnitude of its longitudinal moment of inertia. The introduction of waves provides an exciting force capable of overcoming the longitudinal moment of inertia of the ship and causing it to pitch. The magnitude of the resulting pitching motion, for a particular ship, will be a function of the size of the wave and the angle of encounter between the ship and the wave.

It is the intent of this thesis to investigate for waves of different lengths the effect of varying the wave slope on pitching, heaving, and sea speed of three different hull forms.

The wave slope used as a measure of wave amplitude is effective wave slope. This is based on the Froude-Krylov hypothesis that the pressure acting at every point on the submerged surface of a ship is that pressure at a corresponding depth in a free wave. This considers the effect of the wave upon the ship but does not consider the effect of the ship upon the wave. This hypothesis is a simplification of the true case, since the presence of a ship in the wave does influence the pressure distribution over the submerged surface of the hull.

Reference (11) indicates that distortion of the wave will be such that the wave height along the entrance will be increased and will be reduced along the run. The effect will be less pronounced for long waves or for slender vessels.

Methods for the analytical calculation of the actual pressure distribution over the ship's hull for use in determining effective wave slope are reported in references (7), (12) and (13). The procedures used in these references are complicated and tedious since they involve integrations of the pressure at the several stations shown on the body plan and the subsequent integration of the pressure for the ship as a whole. The process yields the pressure for one position of the wave with respect to the ship's profile. Repetition of the process is necessary to determine a point of maximum effective wave slope.

A detailed analysis such as the one just outlined is beyond the time allowed for such investigations in the preliminary design of a ship. Therefore, if an engineering estimate of the pitching produced by the nominal effective wave slope can be made, the designer can then proceed having some indication of the seaworthiness of his vessel. A knowledge of the region of linearity between wave slope and pitching motion will define the limits wherein an engineering estimate may be made of the pitch expected for a given wave slope in regular waves.

An alternate method of predicting the pitch of a ship would be direct computation using the relation

$$\frac{\frac{1}{2}\psi_m}{\phi_m} = \Psi(\gamma)\mu_z \qquad (1)$$

which is equation 121 from "On The Motions of Ships at Sea" by Weinblum and St. Denis, (Reference 13). In this relation $\Psi(\gamma)$ is dependent on the shape of the waterline of the

ship and the relative length of the ship and the wave. The magnification factor μ_z is dependent upon the ratio of pitching period (T_p) to the period of encounter (T_e) and the damping factor (χ).

Pitching and heaving will be analyzed as uncoupled motions; however, this is a simplification of the actual case. The magnitude of the effect of the coupling of pitch and heave has not been fully established. Reference (11) indicates that assumption of uncoupled motion between pitch and heave is valid where the center of flotation is near amidships. This would tend to exclude transom stern vessels.

The pitching and heaving motions of a ship traveling in head seas would naturally be expected to have an effect upon the ship's speed. Sustained sea speed is becoming a factor of considerable importance particularly for naval vessels which are required to maintain high speeds in all sea conditions. Pitch and heave cause a change in the wetted surface of the hull and thus change the frictional resistance. Wave making resistance is also affected since the major portion of damping of these motions is in the generation of waves. Increase in total resistance will obviously affect sea speed.

Only testing in head seas was done because the M.I.T. Towing Tank is equipped for the generation of regular waves traveling parallel to the path of the model. Head seas present the worst possible sea condition for the excitation of pitch and heave. In the extreme case, the deck may be submerged or the forefoot may emerge from the water. These

seas also give the greatest reduction in speed since all of the wave energy is expended in a fore and aft direction, and none is used to roll the ship.

It was desired to determine the effects of wave slope on the motions of naval ships of varied form normally operating at relatively high speeds. The models chosen for testing were a destroyer, a light cruiser, and an aircraft carrier. Details of the models and of the parent ships will be found in Appendix A.

II PROCEDURE

To provide a better comparison of ship performance in calm water and waves, the models were towed in head seas with a towing force corresponding to a constant still water speed.

Each model was run in the towing tank according to the following schedule:

1. Resistance tests in still water to determine towing force for 18 knots ship speed.
2. Tests in waves of following length/model length ratios and wave length/amplitude ratios, at a constant towing force for 18 knots still water speed:

λ/L	λ/a
.5	40
.75	40
1.0	30,40,50,60
1.1	40
1.3	30,40,50,60
1.5	40

The following additional runs were made:

a) Model No. 1:

1. Resistance tests in still water to determine towing force for 10 knots and 26 knots ship speed.
2. Tests in waves of characteristics given above, at constant towing forces for 10 knots and 26 knots, omitting λ/L ratios of .75, 1.1, and 1.5.
3. Tests in waves given below at a constant towing force for 18 knots still water speed.

λ/L	λ/a
1.0	20
1.3	25
1.75	40
2.0	40
2.335	30,40,50,60

b) Model No. 2:

Tests in waves given below at a constant towing force for 18 knots still water speed:

λ/L	λ/a
1.0	25
1.3	25
2.055	40
2.213	40
2.412	40

c) Model No. 3:

Tests in waves given below at a constant towing force for 18 knots still water speed:

λ/L	λ/a
1.0	25 and 70
1.3	70

The additional runs at 10 knots and 26 knots for Model No. 1 were made at the beginning of the test program. Due to time limitations, the two extra speeds were dropped for Models 2 and 3.

The change in wave characteristics to $\lambda/a = 70$ for Model No. 3 was made during the test program when it became apparent that running in λ/a ratios of 25 and below would result in swamping the model.

The speed of 18 knots was chosen as being one which was of practical importance to all three types of ship. This speed will be slightly higher than cruising speed for all three ships, and probably represents a maximum that such vessels would attempt in waves. At higher speeds, the vessels in many cases would pitch uncontrollably, while

speeds below 15 knots are not of much importance except in maneuvering.

The waves were obtained by changing speed and amplitude of the wave maker according to calibration curves. A fuller discussion of this procedure may be found in Reference (1). Length of wave was determined easily, but amplitude of each wave could only be obtained by trial-and-error procedure involving measurement of each height by means of a capacitance wire depth gauge connected to a Sanborn recorder. Obtaining the correct wave height setting consumed the most time of the entire test series, since the water in the tank had to be allowed to settle after each new wave was generated.

Before testing each model, longitudinal radius of gyration was calculated by the method described on page 92.

In addition, a pitch extinction curve was obtained by manual oscillation of the model in calm water. Pitching period and logarithmic decrement of pitch were obtained by analysis of the extinction curve, a sample of which may be found in Plate XIV. Pitching periods for each model are tabulated in Appendix A. A measure of the accuracy of the pitching period determined can be obtained by comparing the results obtained for Model No. 1 with a destroyer model of the same length described by E. V. Lewis in "Ships Speeds in Irregular Seas" SNAME (1955). The pitching period obtained for Model No. 1, .565 seconds, agrees very closely with the .56 second period obtained by Lewis.

Pitch of the model was measured using the angular

motion gyro described by Porter in Reference (9). This gyro presents a continuous time-base record of pitch angle, and may be adjusted for pitch angles of up to 15° (double amplitude). Mounting of gyro case and junction box in Model No. 3 is illustrated in Plate I.

Heave and sustained sea speed were obtained from photographs taken during the run using a stroboscope as a light source. A detailed description of the calculation of each quantity may be found in Appendix D. Comparison of the pitch angles obtained by gyro and also from measurement of the photograph was made for one run. Results of this comparison are presented in Part IV.

Accuracy of Results

Since number of intervals on the photographs can be read to within one-quarter of a space, sea speed can be computed accurately to within ± o.1 knots. Accuracy of pitch angle determination depends upon the calibration curve for the day in question; since the tape could be read to within one-half of a millimeter, and since 25 millimeters on the calibration curve were set equal to one degree, pitch could be read accurately to within $\frac{1}{2} \times \frac{1}{25}$ of a degree, or ± .02 degrees. Heave could be read to within .01 inches on the photographs; since it was scaled up to ship dimensions in accordance with the scale ratio, heave for Model No. 1, extrapolated to ship dimensions, was accurate to within ± .01 in. x 67.09 = ± .6709 in.

III. PRESENTATION OF RESULTS

The results of this thesis are presented in Figures I to XXX, which were obtained by plotting the data given in Tables I to V and Tables XXI to XXIII. The data is subject to the following limitations:

a) Pitch angles were taken from a mean calibration curve such as Plate VIII. A mean calibration curve was taken since the actual calibration was found to vary as indicated between morning and evening. This is attributed to the variation in temperature of the integrating gyroscope.

b) The temperature of the gyroscope is subject to slight changes during the run since the heating element is not connected during the run. This is considered to have a negligible effect on the results.

c) Choice of values of longitudinal radius of gyration was limited by the physical configuration of the model and the ballast available for movement after installation of the gyroscope. Also, the corresponding value of k_y for the parent ship was unknown.

d) Difficulty was experienced in obtaining the exact value of wave height desired for any particular run. In cases where the wave height was different from that desired, a linear interpolation was used to correct the measured values of pitch and heave to an amount corresponding to the desired value of wave

height. This in effect assumes a linear variation of pitch and heave with wave slope and can be considered accurate only where the difference between measured and desired wave heights is small.

e) Pitch angles are average values obtained by an arithmetic average at least ten cycles of pitch for each run.

f) The damping factor used to obtain the theoretical data shown in Figures XXVII-XXIX was obtained in calm water at zero speed. This in effect assumes that damping is independent of forward speed. The damping factor was calculated using the logarithmic decrement; however, a more exact method would have been to take the slope of a logarithmic plot of amplitude of pitch vs. time.

g) Heave was measured by taking the difference in vertical height of the reference line on the model. Vertical distances do not take into account the inclination of the reference line on the model. The correction is a cosine function and for angles under 5^{o} was considered negligible compared with the accuracy with which heave could be read from the multi exposure photographs.

FIGURE I

Pitch Angle vs Period of Encounter

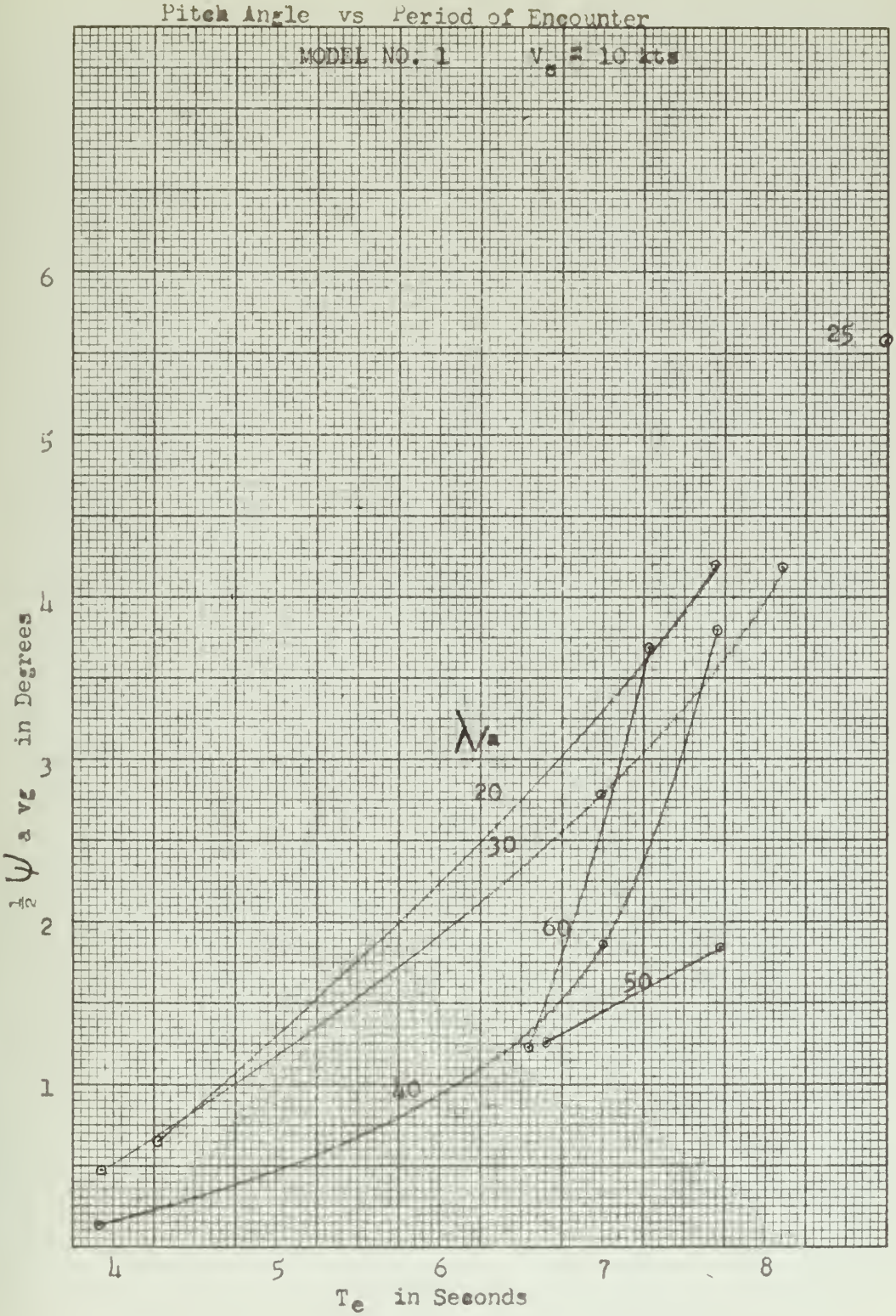

FIGURE II

Pitch Angle vs Period of Encounter

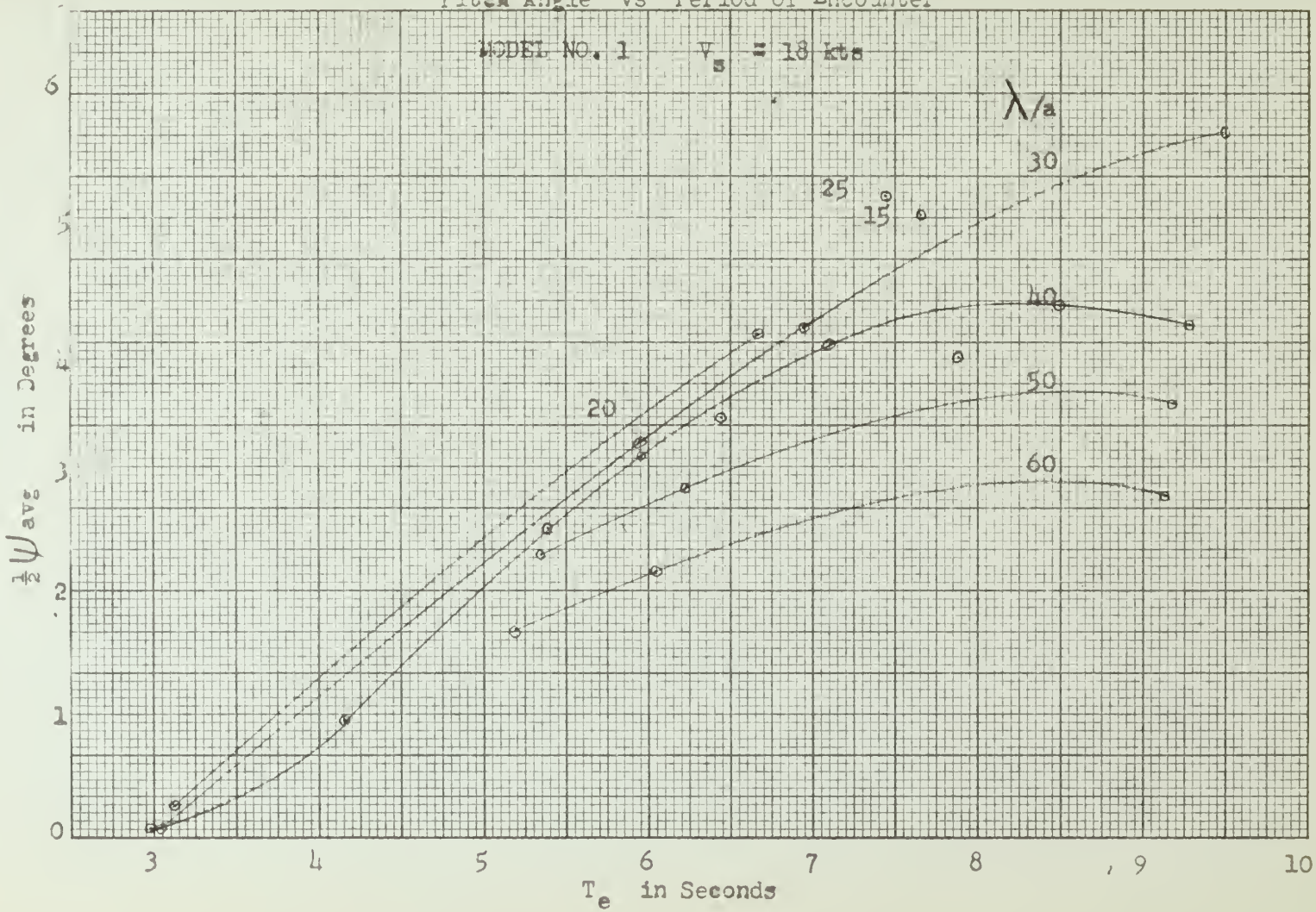

FIGURE III

Pitch Angle vs Period of Encounter

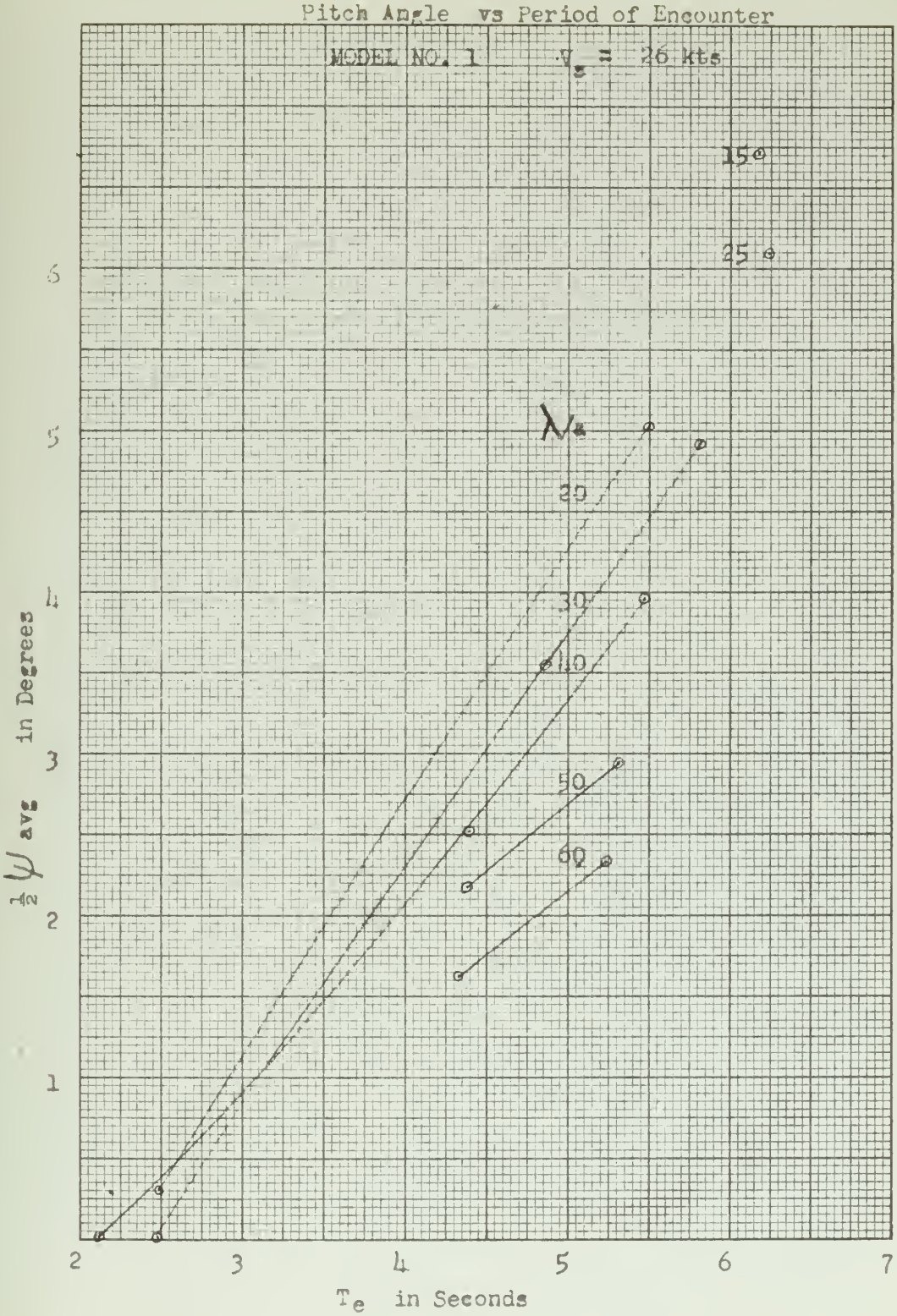

FIGURE IV

Pitch Angle vs Period of Encounter

MODEL NO. 2 V_0 = 16 kts

FIGURE V

Pitch Angle vs Period Of Encounter

FIGURE VI

Heave vs Period of Encounter

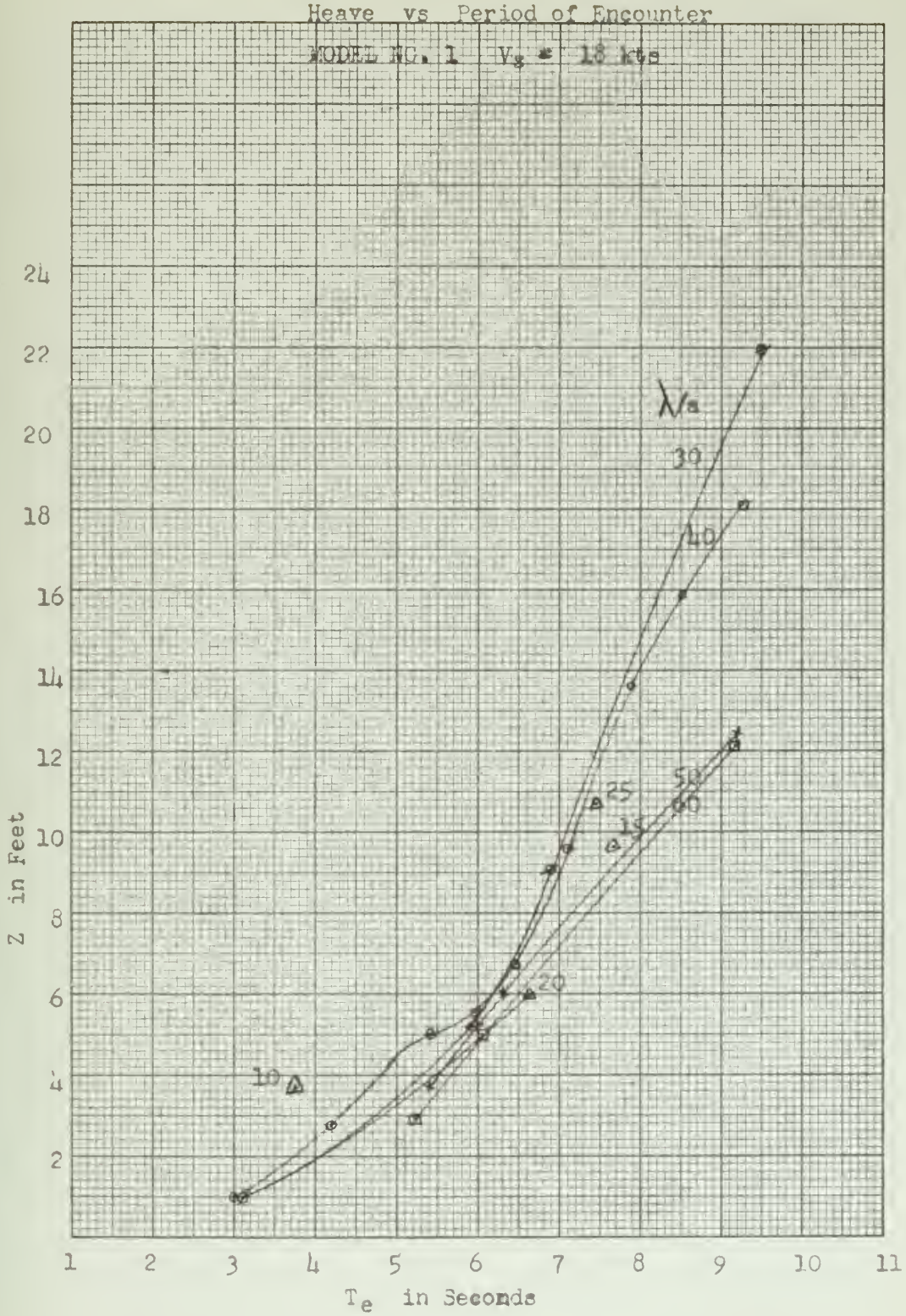

FIGURE VII

Heave vs Period Of Encounter

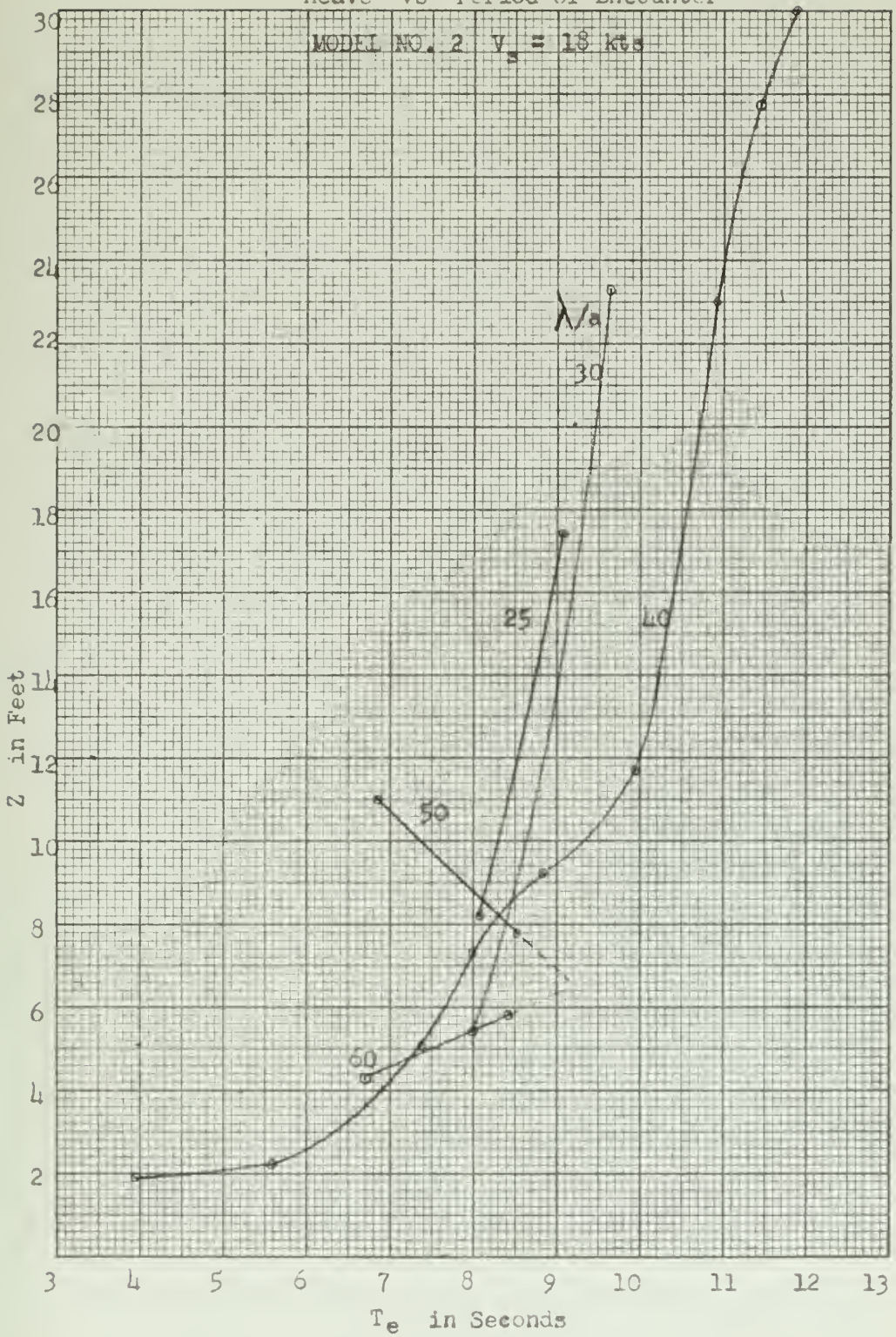

FIGURE VIII

Heave vs Period of Encounter

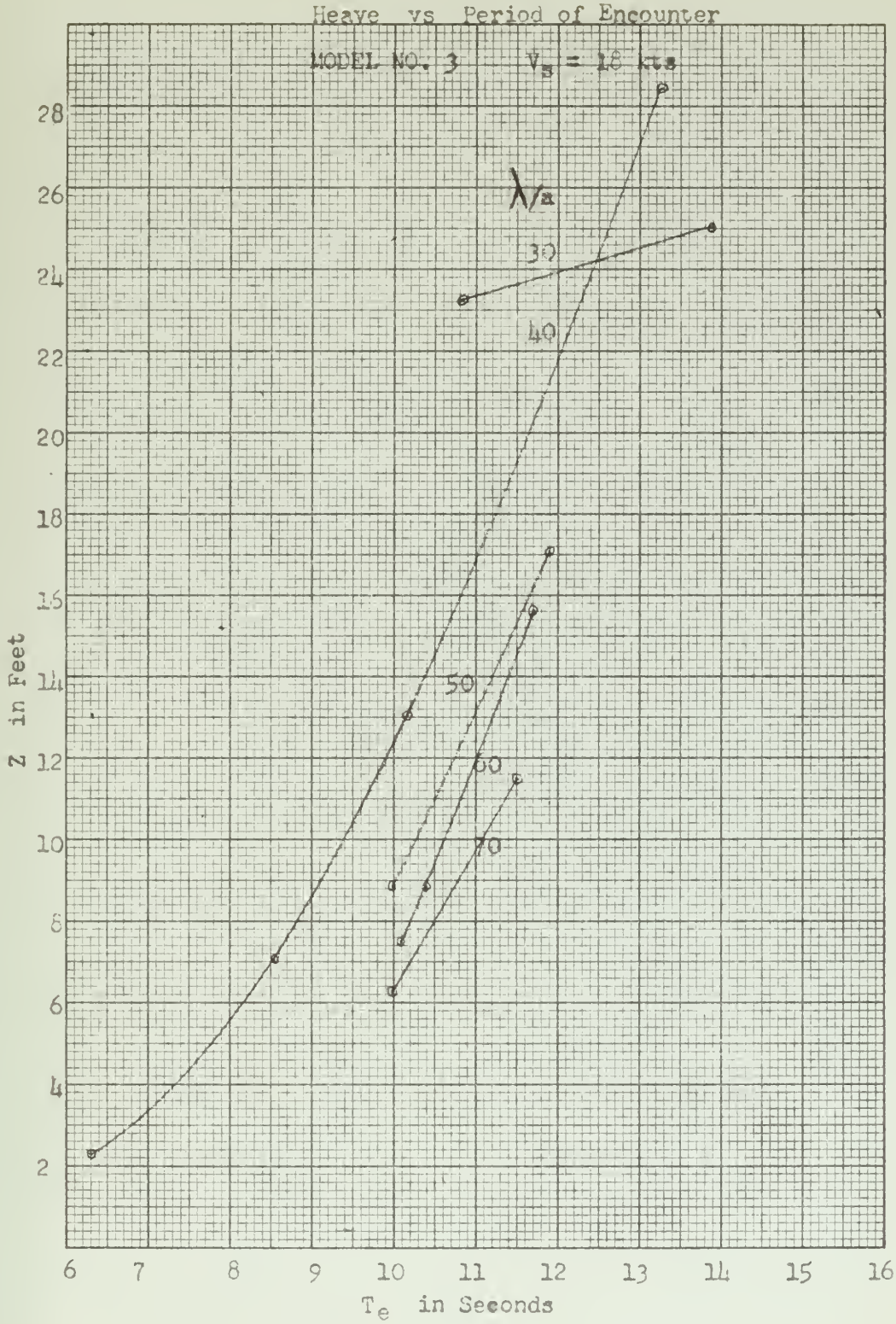

FIGURE IX

Sea Speed vs Wave Length

MODEL NO. 1 V_s = 10 kts

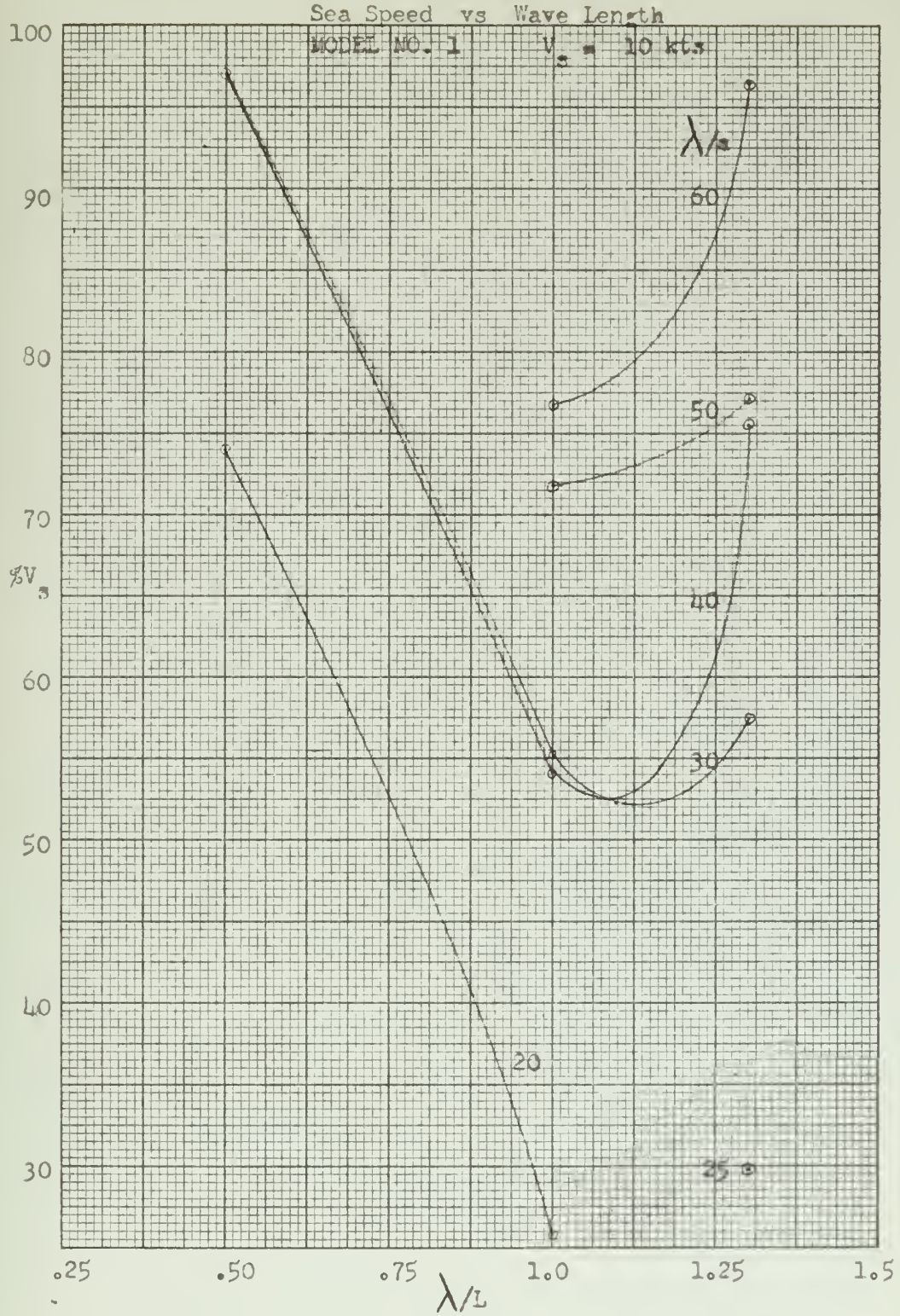

FIGURE X

Sea Speed vs Wave Length

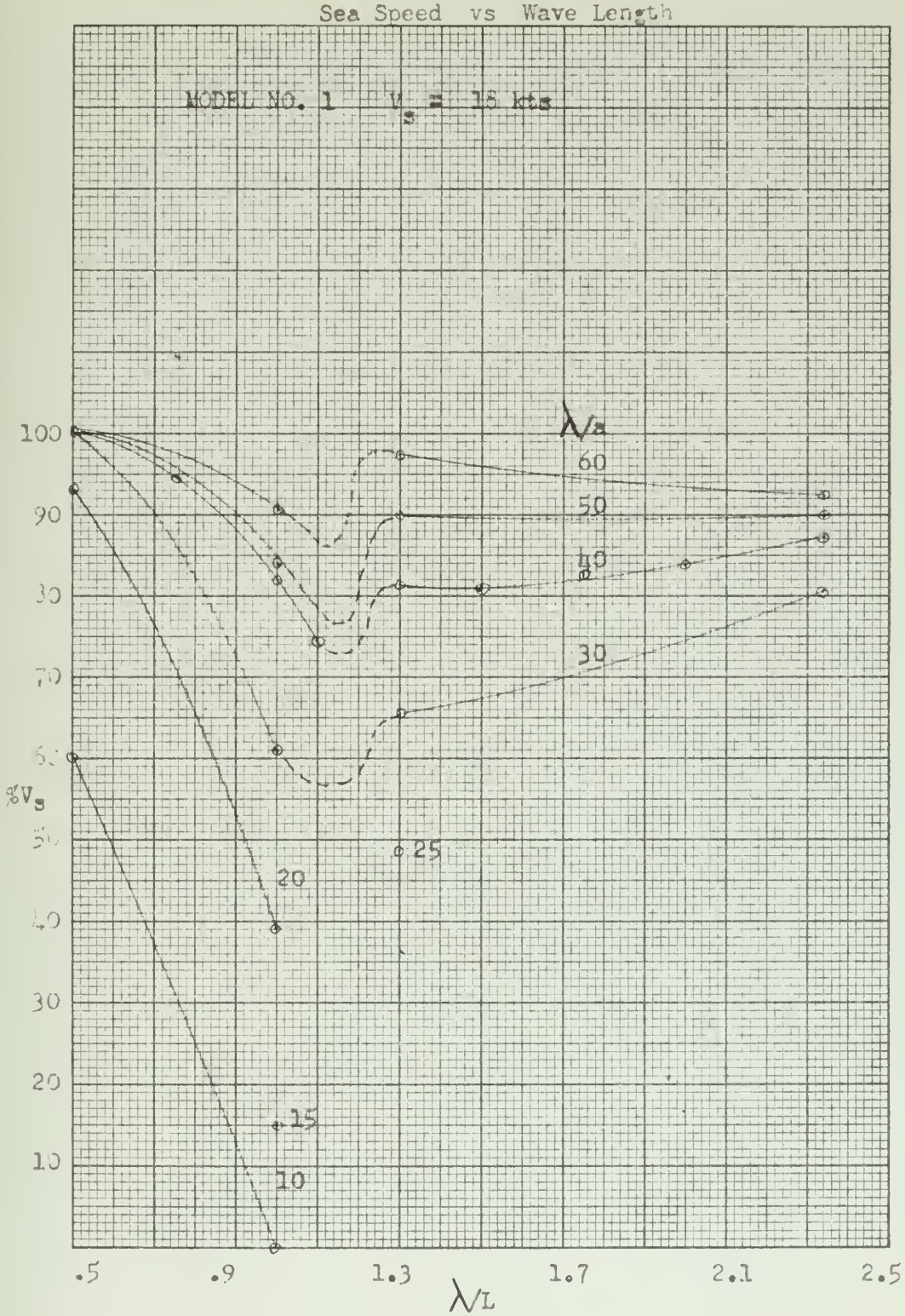

FIGURE XI

Sea Speed vs Wave Length

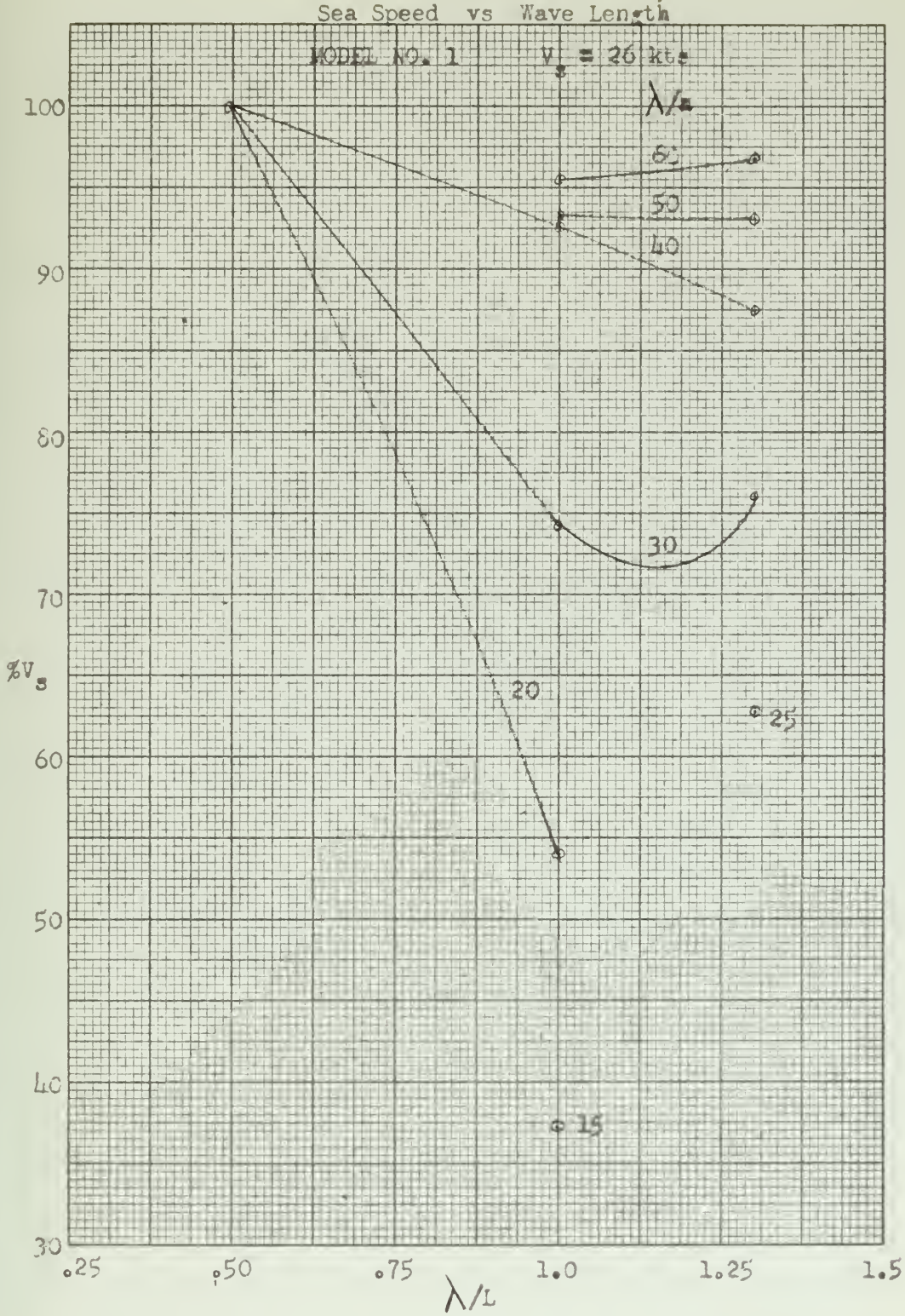

FIGURE XII

Sea Speed vs Wave Length

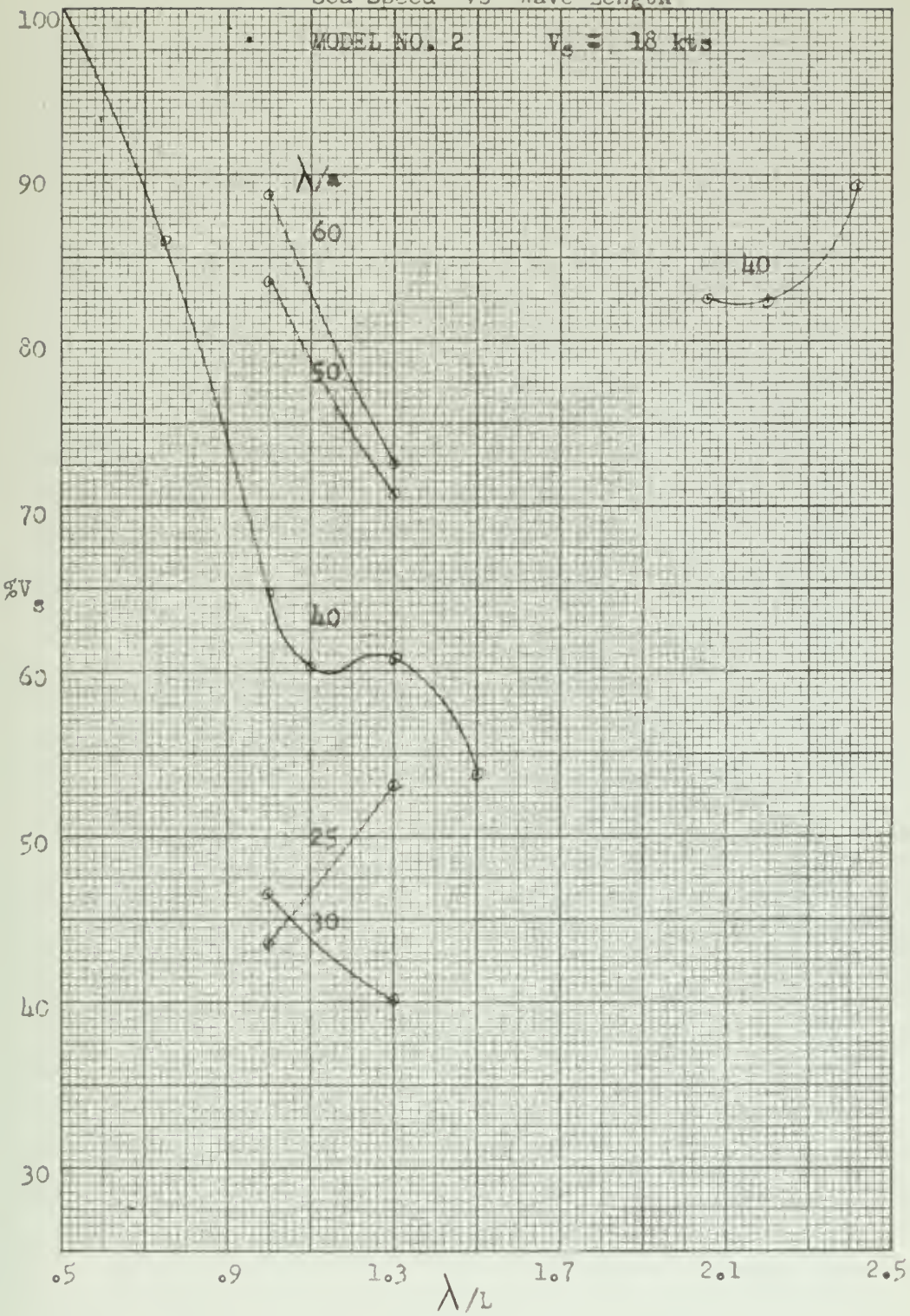

FIGURE XIII

Sea Speed vs Wave Length

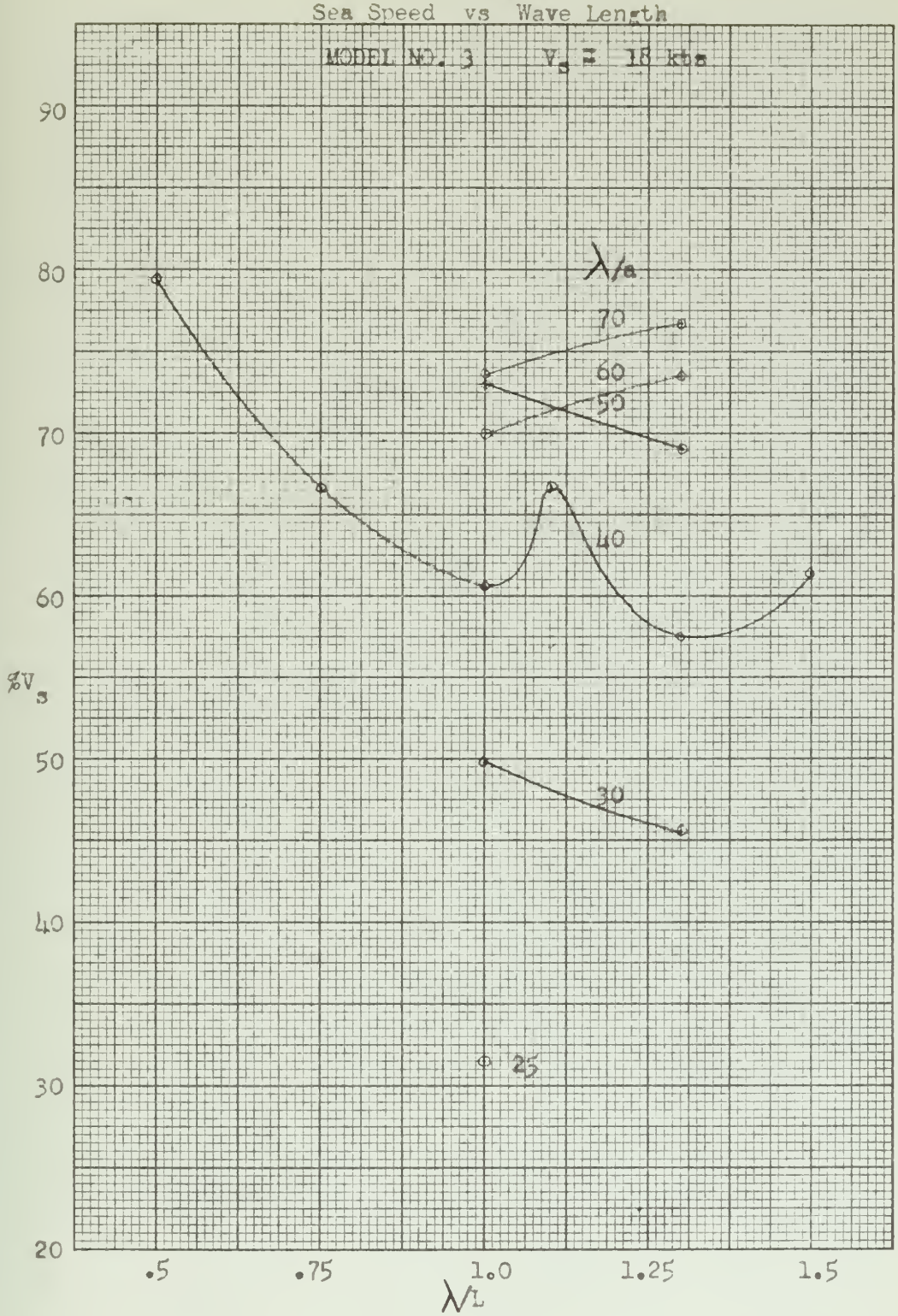

FIGURE XIV

Heave vs Wave Height

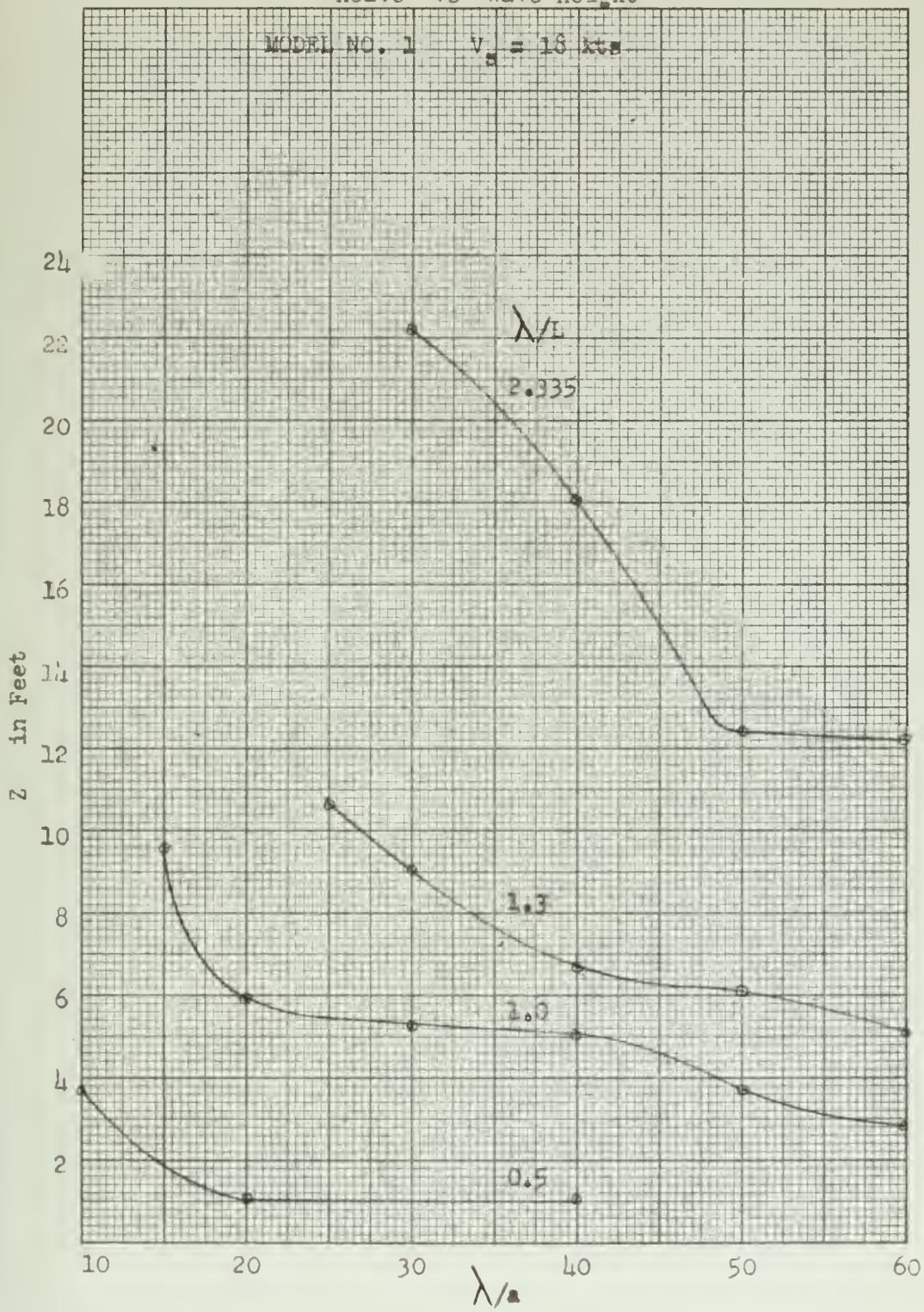

FIGURE XV

Heave vs Wave Height

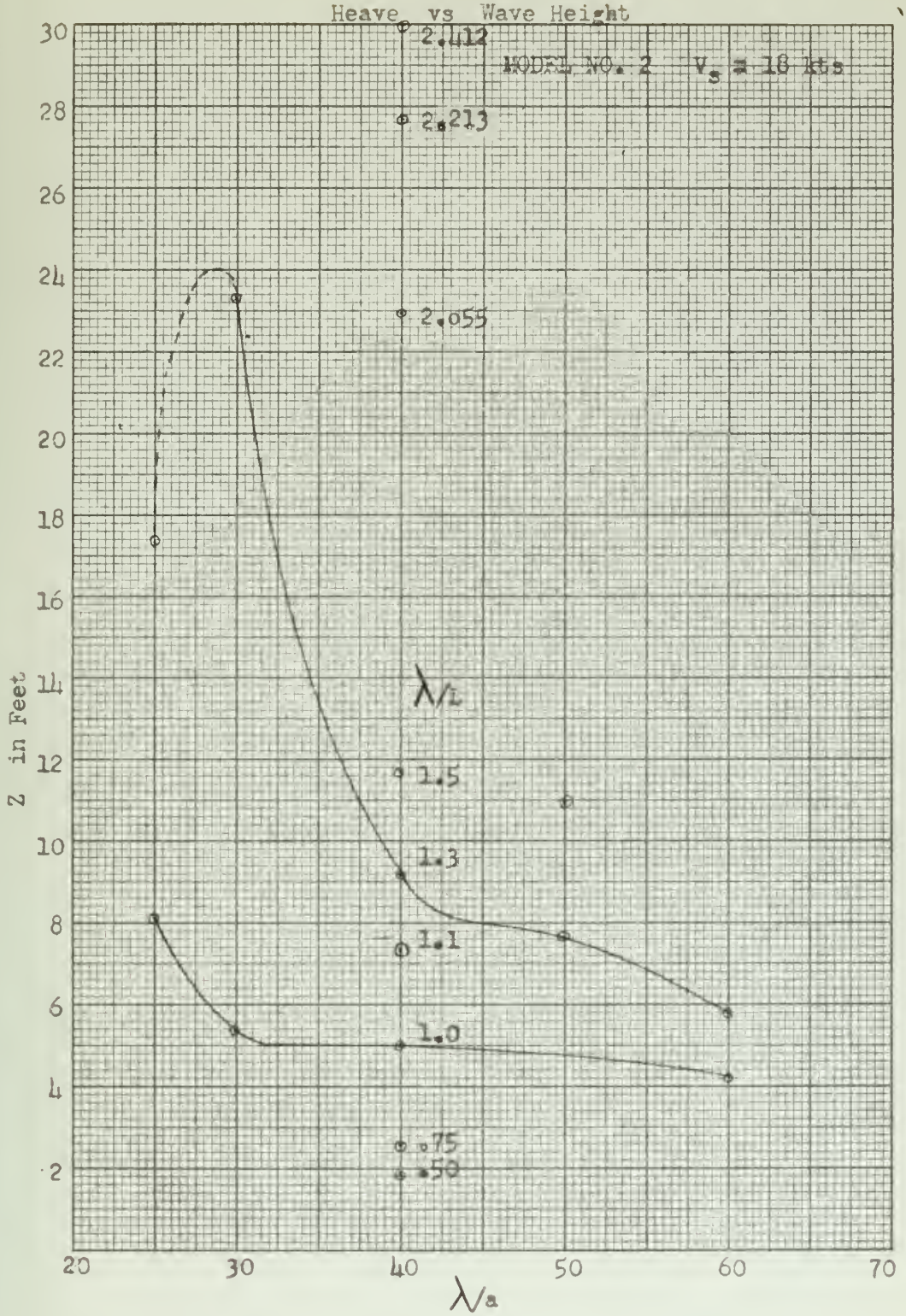

FIGURE XVI

Heave vs Wave Height

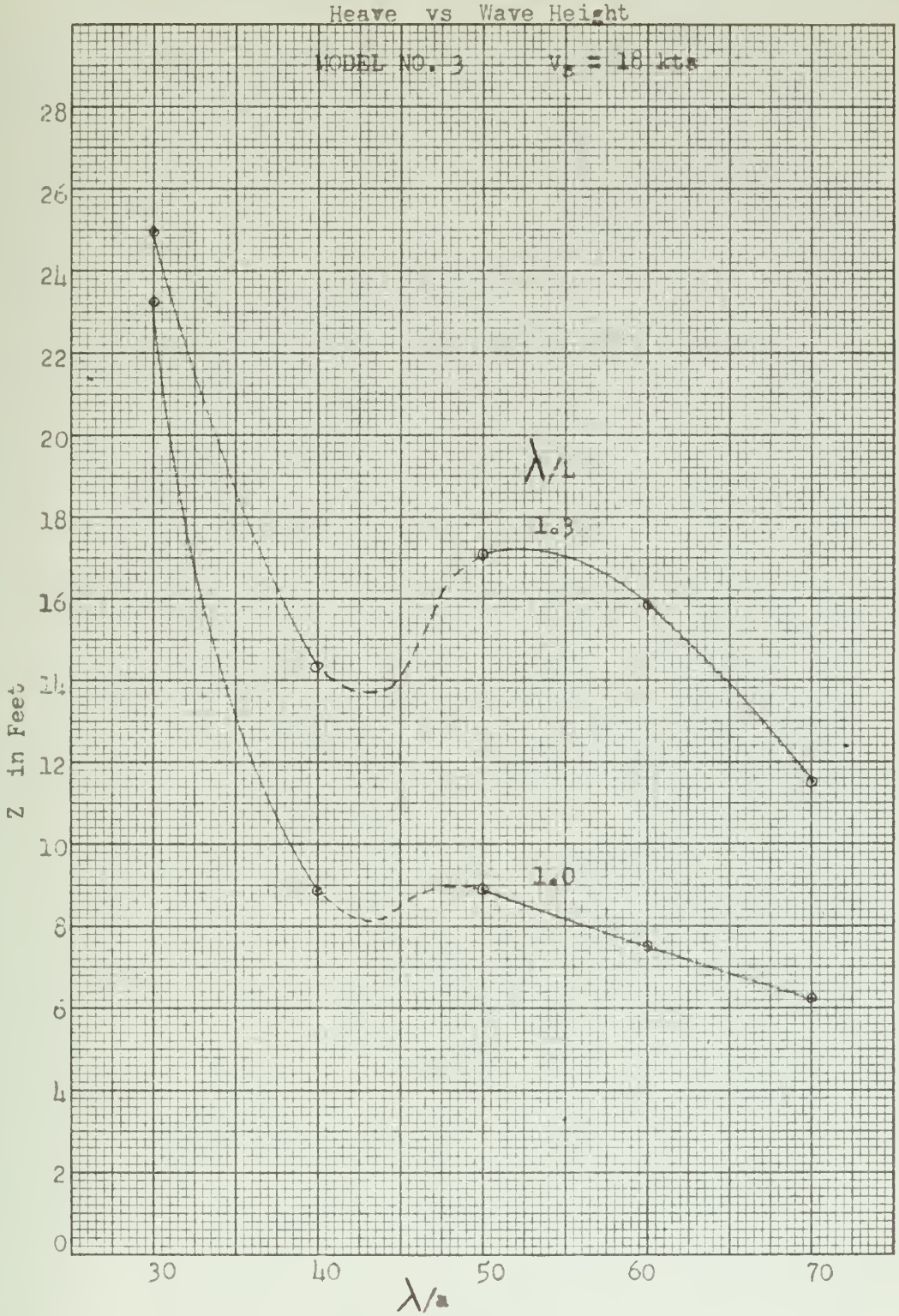

FIGURE XVII

Comparison of Heave vs Wave Length for Models 1, 2, & 3

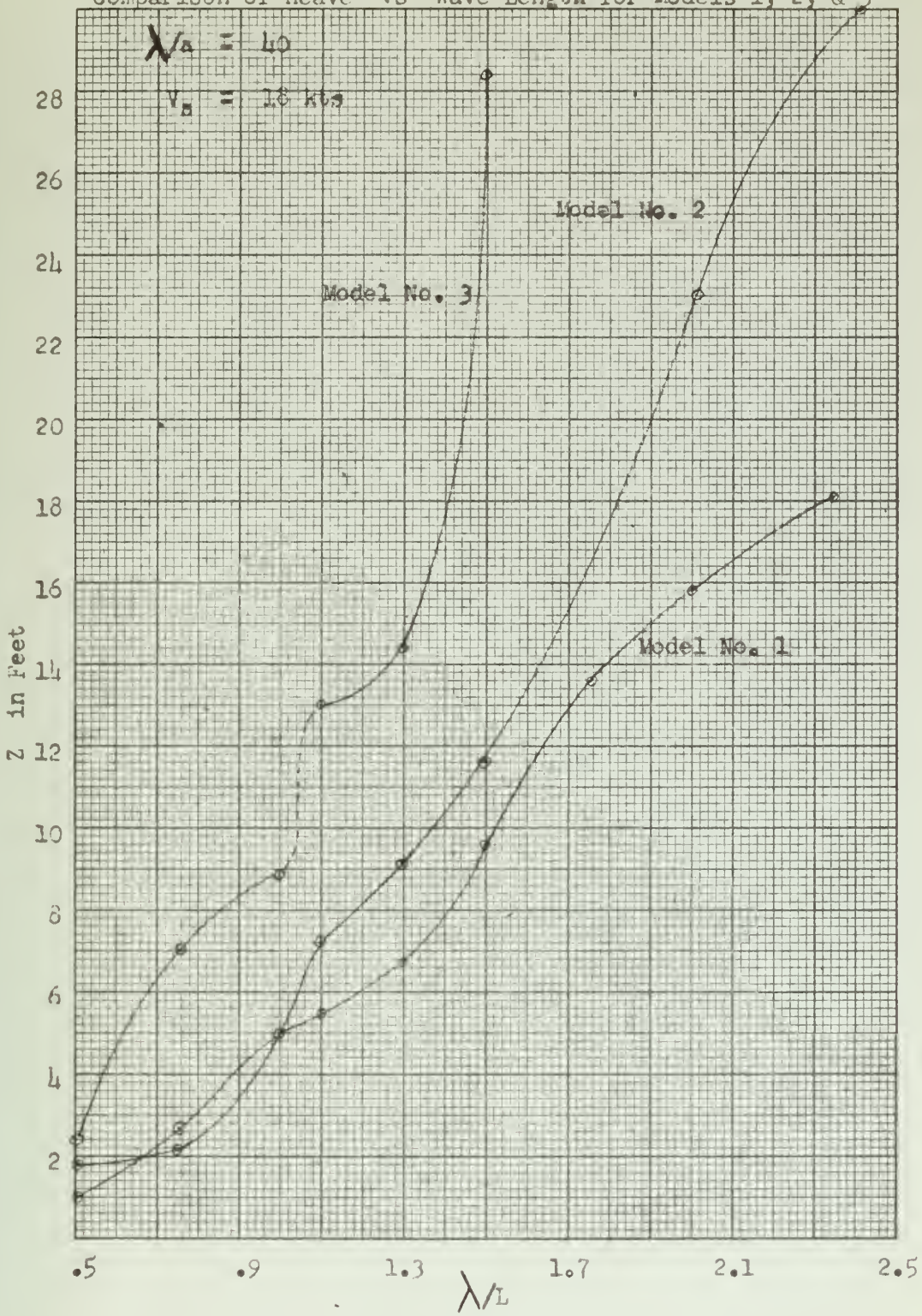

FIGURE XVIII

Comparison of Sea Speed vs Wave Length for Models 1, 2, & 3

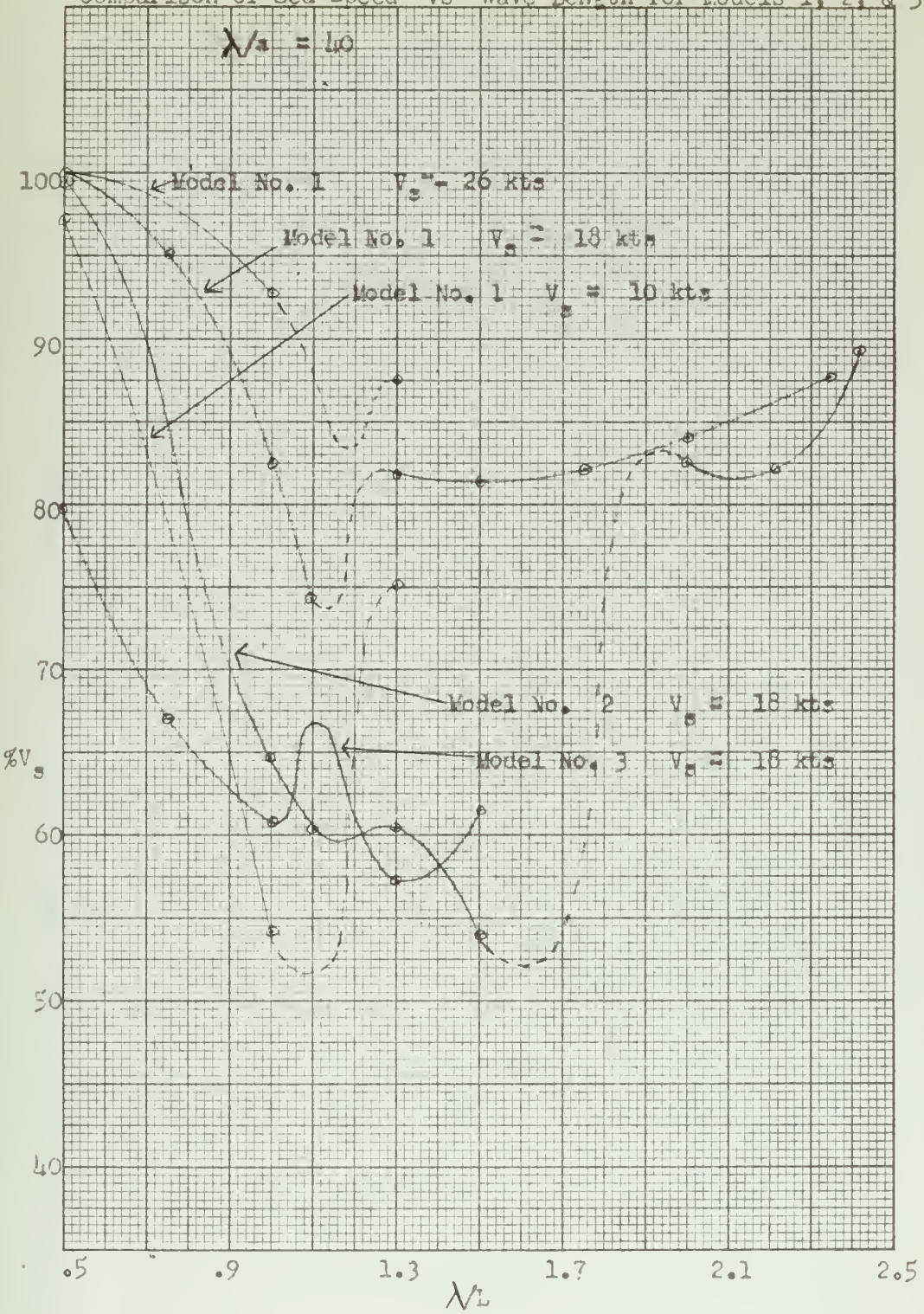

FIGURE XI X

Comparison of Pitch Angle vs Period of Encounter for Models 1, 2, & 3

$\lambda/a = 40$

Model No. 1 V_s = 26 kts

Model No. 1 V_s = 18 kts

Model No. 2 V_s = 18 kts

Model No. 1 V_s = 10 kts

Model No. 3 V_s = 18 kts

$\frac{1}{2}\psi_{avg}$ in Degrees

T_e in Seconds

FIGURE XXI

Heave vs Wave Slope

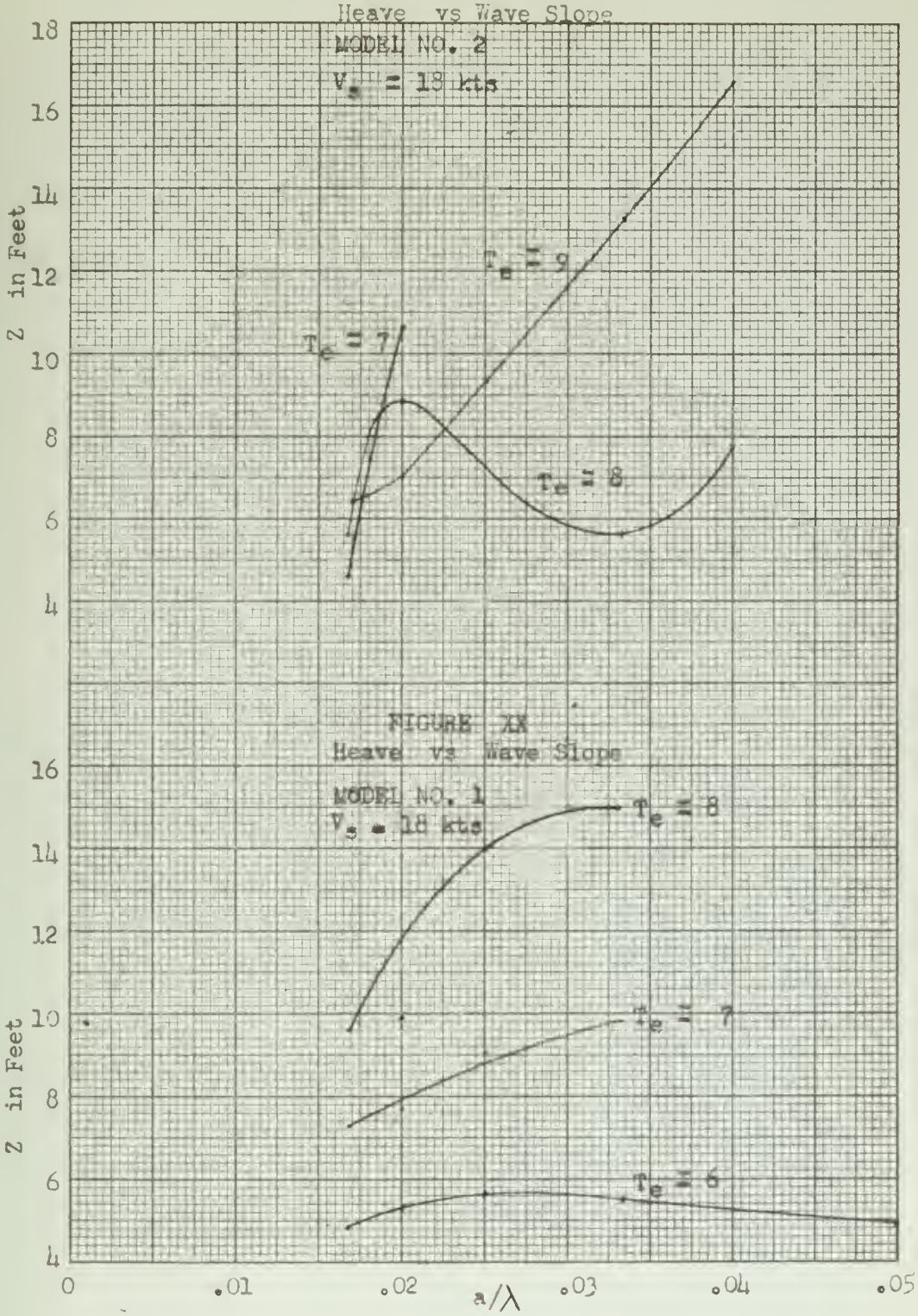

FIGURE XX

Heave vs Wave Slope

FIGURE XXII

Heave vs Wave Slope

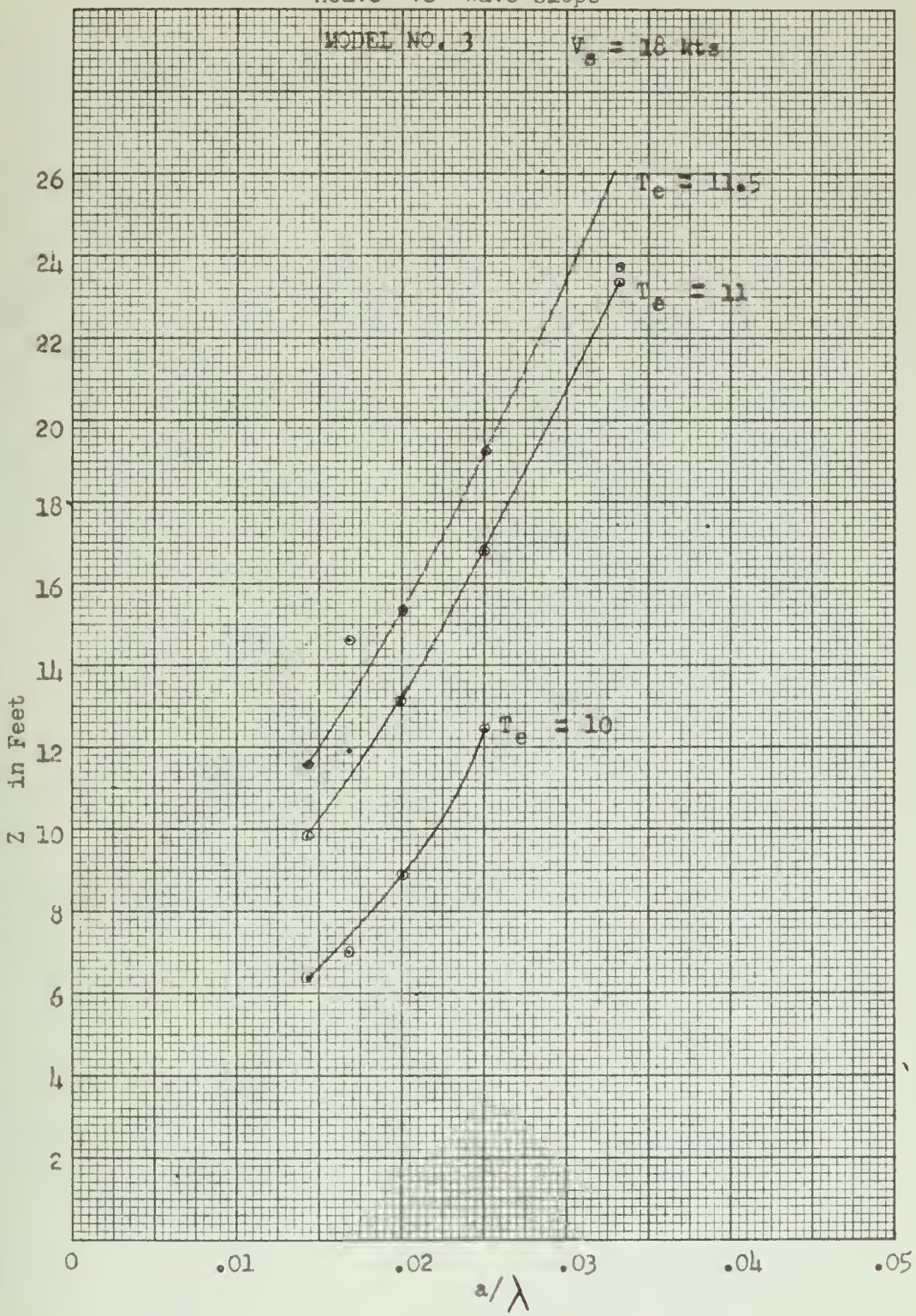

FIGURE XXIV

Pitch Angle vs Wave Slope

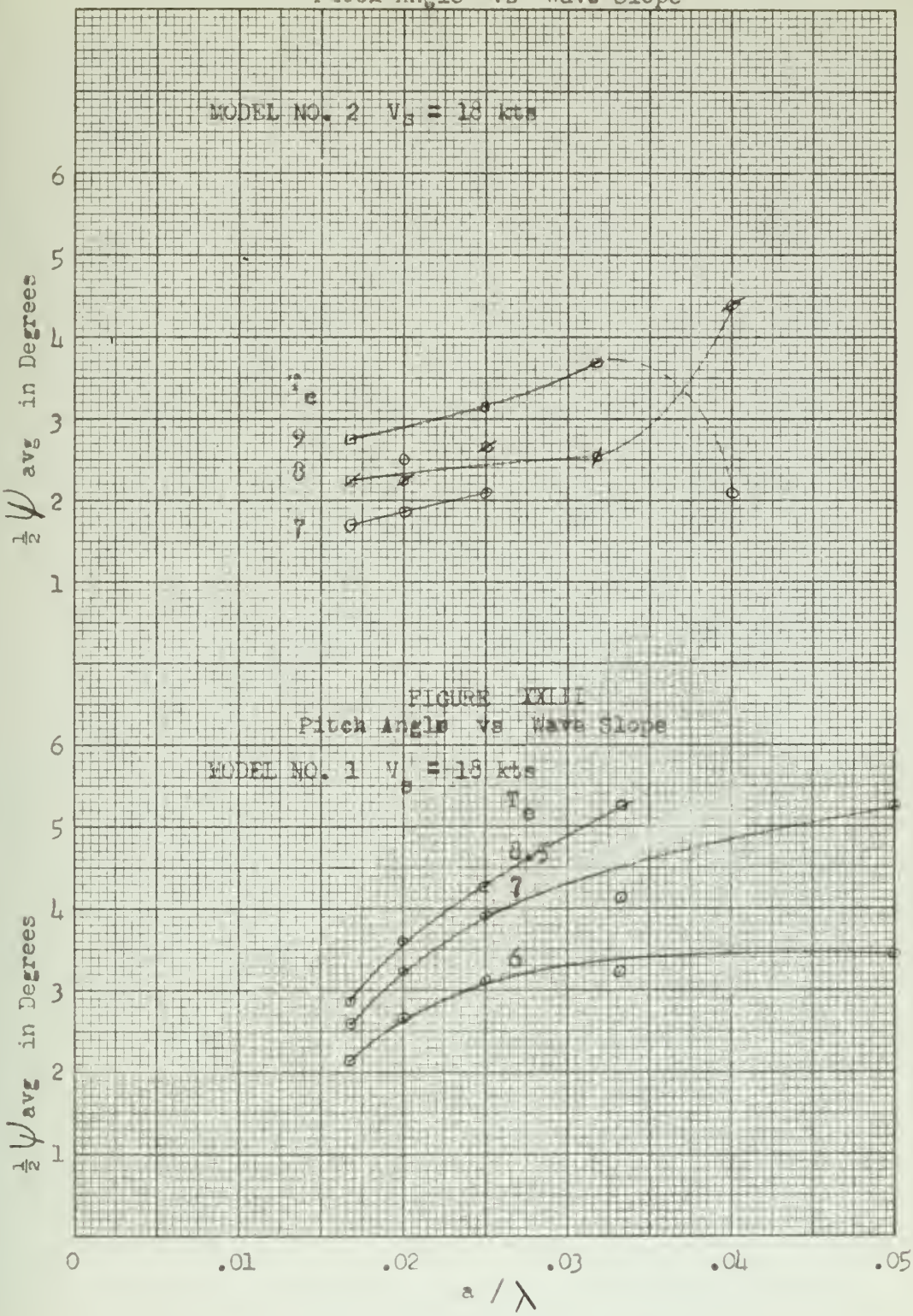

FIGURE XXIII

Pitch Angle vs Wave Slope

FIGURE XXV

Pitch Angle vs Wave Slope

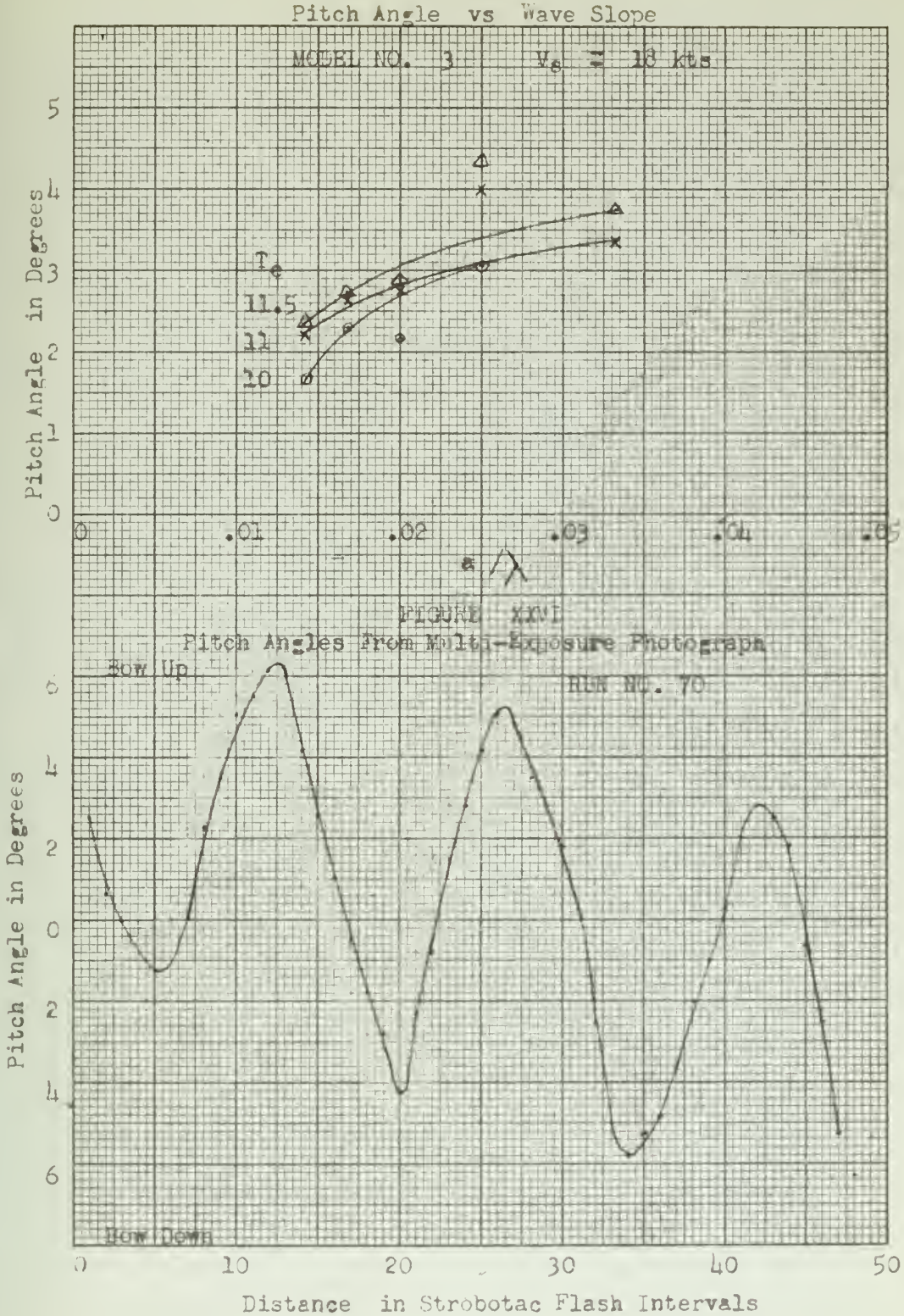

FIGURE XXVI

Pitch Angles From Multi-Exposure Photograph

FIGURE xxVII

Pitch Angle vs Tuning Factor

MODEL NO. 1 V_s = 12 kts

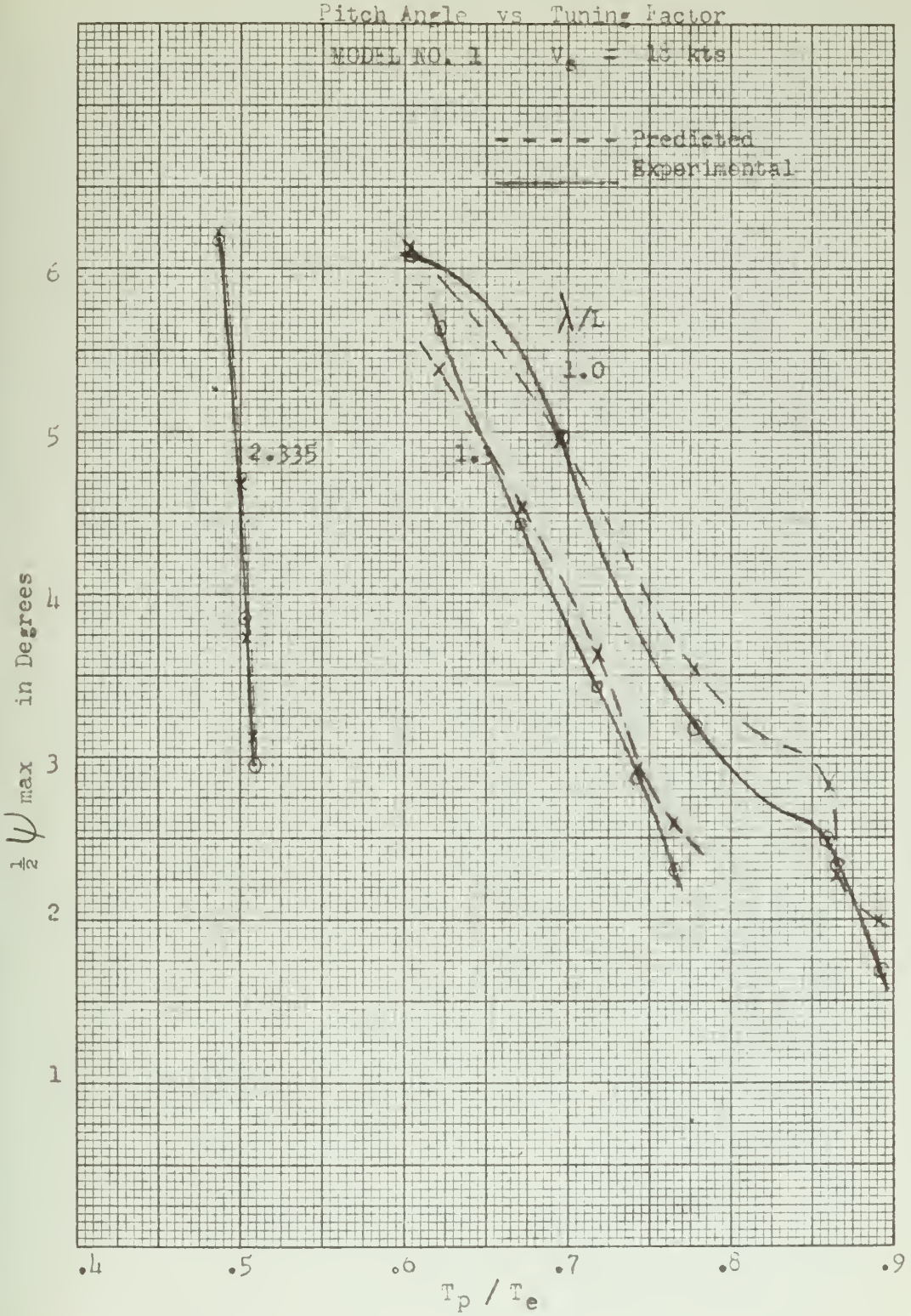

FIGURE XXVIII

Pitch Angle vs Tuning Factor

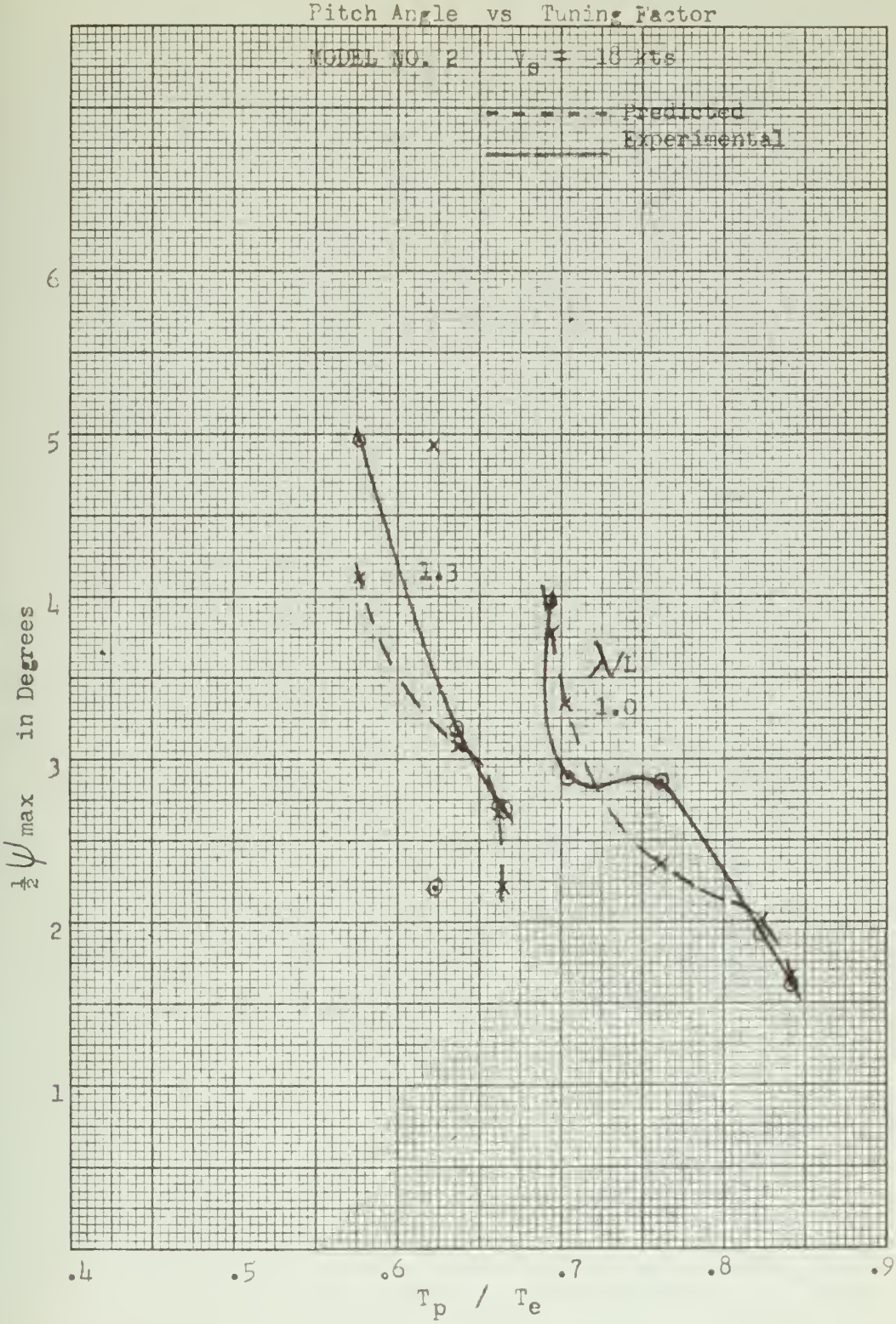

FIGURE XXIX

Pitch Angle vs Tuning Factor

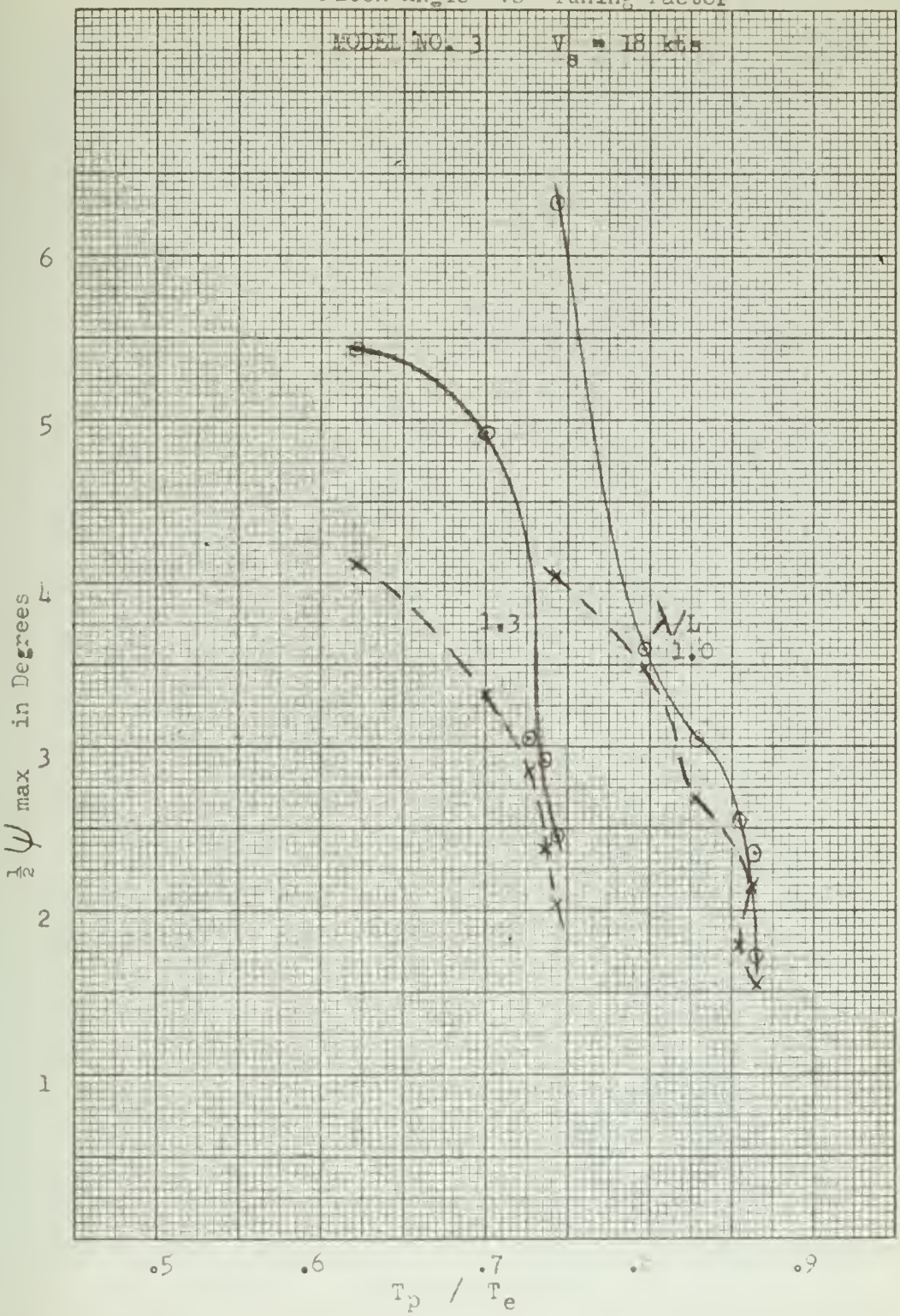

FIGURE XXX

Pitch Angle vs. Wave Length

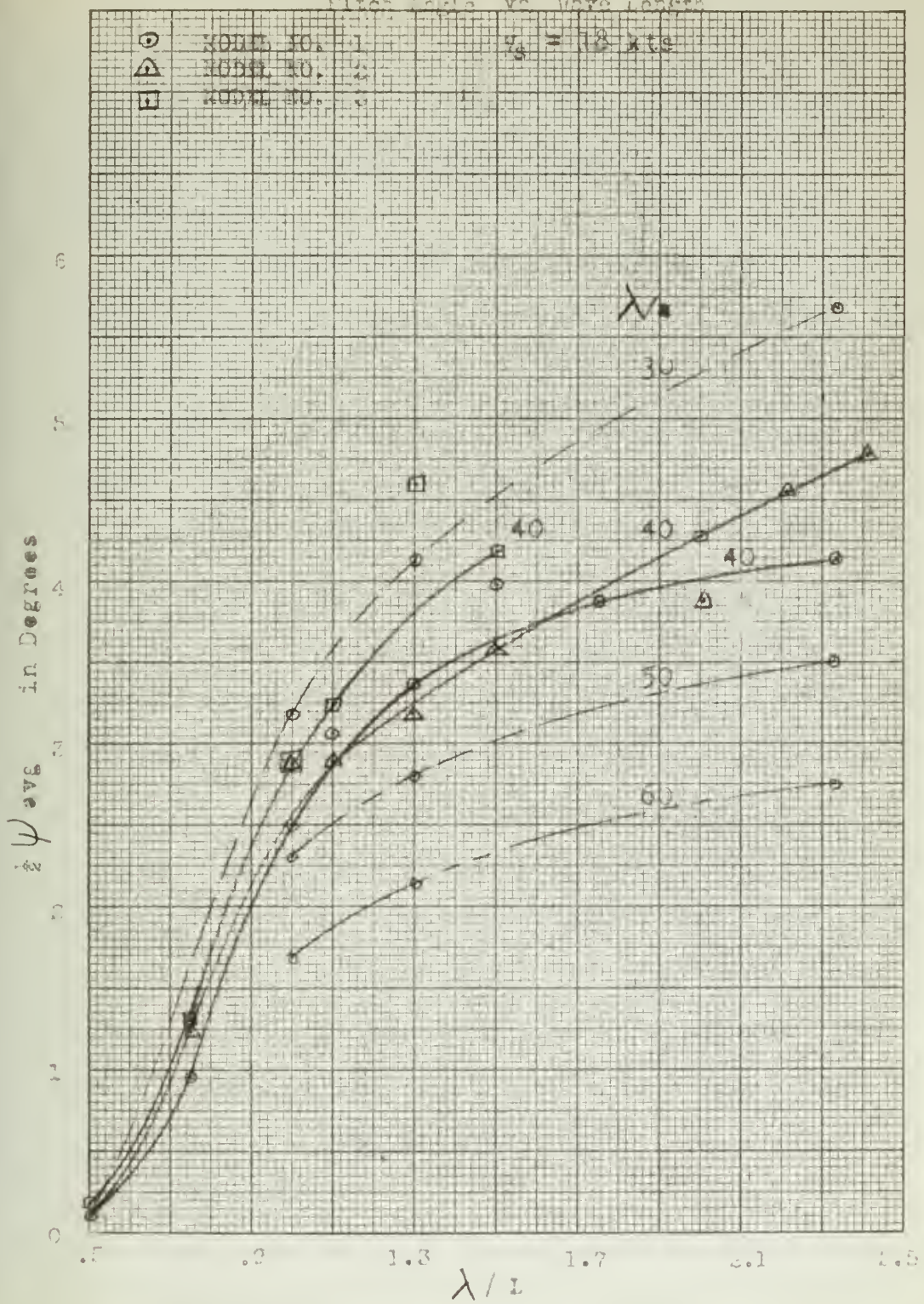

IV. DISCUSSION OF RESULTS

The results obtained from the investigation of the effects of wave slope on pitch, heave, and sea speed are presented in Chapter III as Figures I through XXX. The figures will be discussed by number.

Figures I-III

These figures illustrate the variation in pitch angle with period of encounter for Model No. 1 at three speeds. The pitch angle is seen to increase with period of encounter, and to be of the same order of magnitude for all three speeds. Figure II shows that there is some value for T_e, at which maximum pitching amplitudes are reached. With V_s = 18 knots, this value of T_e is about 8.25 seconds for λ/a ratios of 40, 50, and 60. This is a tuning factor, T_p/T_e of about .560. The strong dependence of pitching angle upon period of encounter is shown in all three graphs.

Another point of interest is the similarity of the curves for various speeds; the curves are very similar in shape and only absolute magnitudes of the pitch angles vary. As would be expected, higher pitch amplitudes occur for higher speeds at the same period of encounter. This shows that a faster moving ship is inherently more responsive to exciting forces than a slower one.

Figures IV and V

These figures show the variation in pitch angle with period of encounter for Models 2 and 3. The motion for the

same value of λ/a increases with increasing period of encounter, having the same general shape in most cases. Only in the case of Model No. 3, for $\lambda/a = 40$, was the maximum point of the curve reached, at $T_e = 12.5$. At this point the waves generated by the wavemaker were so long that much splashing occurred at the inboard end of the tank. Obtaining points on the other low side of the curve would have meant using even longer waves; it was felt that the extreme turbulence in the tank made it unwise to extend the wave length much beyond the point where maximum pitch amplitude was reached.

Figure IV shows a variation in shape of the pitching curve for $\lambda/a = 30$ and 25, as compared with other λ/a values. At these higher wave heights, from 3.25 in. to 3.90 in., the forefoot of the model was often out of the water. (See Plate VII). Since damping will be linear only when the forefoot is in the water, it is clear that such points represent conditions which are not the same as for other points on the curve, and therefore do not give a completely consistent picture of the motion.

Comparison of Figures II, IV, and V shows the similarity of model behavior in all three cases. Only in the case of Model 3, where periods of encounter are somewhat higher for maximum pitching amplitudes, is there a substantial difference. This similarity tends to substantiate Niedermair's observations in Reference (9), "In spite of some rather wide hull differences between individual models, all of the models behaved

substantially alike."

Figures VI, VII, VIII

These figures show the heave produced at various periods of encounter by different wave slopes. In general, increasing the period of encounter for a given wave slope will result in increased heaving motion.

Figures VI and VII show that heave increases sharply for values of T_e above 6 seconds, while Figure VIII shows that for Model No. 3 the curves are relatively linear for values of T_e above 10 seconds.

Figures IX, X, XI

These Figures show the reduction in speed resulting from operation of Model No. 1 at towing forces corresponding to still water speeds of 10, 18, and 26 knots. The greatest range of experimental data is presented in Figure X; however, the limited data presented in Figures IX and XI shows the same trends. For this reason these figures will be discussed as a group.

The greatest sea speed reduction will be encountered in the region where λ/L is between 1.0 and 1.3. The exact shape of the curves in this region was not determined; however, a curve faired through the observed points indicates marked decrease in this region. Increasing the wave slope for a constant value of λ/L results in a marked decrease in sea speed particularly for values of $\lambda/a < 40$. This can be explained in that the driving force of the model is applied at an angle to the horizontal dependent upon the wave slope.

The larger the wave slope, the smaller the horizontal component of the driving force which will produce forward speed.

Comparison of Figures IX, X, and XI shows that for increasing towing force (i.e. still water speed) the percentage loss in sea speed is less. This is explained from visual observation that at higher speeds the model had more of a tendency to drive through the waves rather than ride over them. This tendency will result in reduced motions of the ship; however, speed may not be increased indefinitely since the structural forces imposed by heavy seas will limit practical speeds. Reduction of pitching and heaving motions results in reduced wetted surface (i.e. frictional resistance) and increased sea speed.

Figure 9 of Reference (11) indicates a similar relation of resistance increasing for increasing speed and then falling off for a ship operated at a constant value of λ/L and λ/a.

Sea speed for these figures was obtained as indicated in Appendix E from multi-exposure photographs. A more detailed investigation of the relation between pitching and speed loss could be made by analysis of instantaneous speed, pitch, and wave height measured simultaneously. These values could be obtained by use of a multi channel Sanborn recorder. This item of equipment was not available in the M.I.T. towing tank at the time the results shown in Figures IX, X, and XI were obtained. Recording of simultaneous values of speed, pitch, and wave height would allow investi-

gation of the phase relations between excitation and ship response.

Figure XII

This figure shows the reduction in sea speed resulting from operation of Model No. 2 at a towing force corresponding to 18 knots still water speed. The curves show the same trends as those shown in Figures IX - XI for values of λ/L below 1.5. The shape of the curves between values of λ/L of 1.0 to 1.3 was not determined and should be the subject of further investigation to determine the maximum reduction of sea speed. Further investigation of speed loss in the region $1.5 < \lambda/L < 2.055$ should be made to establish the effect of very long waves on loss in sea speed.

Figure XIII

This figure shows the reduction in sea speed from operation of Model No. 3 at a towing force corresponding to 18 knots still water speed. These curves show the same trends as those in Figures IX - XII with the exception of an unexplainable increase in sea speed at $\lambda/L = 1.1$ for a wave height of $\lambda/a = 40$. The data obtained for this model was again not sufficient to establish the shape of the curve in the region of most severe speed reduction.

Figures XIV, XV, and XVI

These figures illustrate the strong dependence of heave upon wave height. For all three models, heaving increased markedly with increase in wave height; at values of λ/a less than 40, the increase was very rapid.

Figures XIV and XV support two of the theoretical deductions of Messrs. Weinblum and St. Denis, namely,

a) When the effective wave length is less than half the ship's length, the heaving force is small.

b) At an effective wave length equal to the ship's length the heaving force is moderate or even small. This point is not quite so obvious in the case of Model 3 but holds even here, if λ/a is greater than 40. The general idea that heaving increases with increase in wave length supports the conclusion of Weinblum and St. Denis that the standard ratio $\lambda/L = 1$, cannot be used as a limiting case when investigating the seaworthiness of ships.

The authors cannot explain the pronounced hollows in Curve No. XVI at λ/a between 40 and 50; they do offer the obvious solution that the curves in this region need more points before any conclusions can be drawn.

The similarity between the heave curves for $\lambda/L = 1.0$ and 1.3 in Models 1 and 2 is striking, making allowances for the different values of λ/a at which the slopes of the curves increase. The absolute magnitudes of their heave are about the same; this is an illustration of the dependency of heave on waterline shape. Models 1 and 2 have quite similar waterplane coefficients, while the coefficient for Model 3 is substantially lower.

Comparison of Figures XV and XVI shows that, in waves of $\lambda/L \geqq 1.0$, vessels with full waterlines are likely to

heave less than vessels with fine waterlines.

The theory that the heaving force has an important zero point at λ/L value close to the waterplane coefficient, Fig. 27, Reference (13), is certainly an interesting one and worthy of further investigation. This would mean that heave is zero at a certain value of λ/L; one point close to the waterplane coefficient was investigated for Model 2, but no diminution of heaving was observed.

Figure XVII

This heave curve agrees quite closely with the figures obtained by Ben-Nun and Harel in Reference (3). The general increase in heave with increasing λ/L ratios is shown, as well as the modified resonance points, where the curve has a pronounced hollow. This point occurs in the vicinity of $\lambda/L = 1.1$ for Models 2 and 3, and about $\lambda/L = 1.0$ for Model 1. The difference in behavior between Models 2 and 3 is of interest, since they have the same length and were therefore operating in waves of identical characteristics. Heave for Model 3 is much greater than that for Model 2, further supporting the idea that vessels with full waterlines heave less than vessels with fine waterlines. Values of heave for Models 1 and 2 show quite good agreement until a λ/L of about 1.7. At this point they begin to diverge until, at $\lambda/L = 2.3$, the difference is about 11 feet full scale. One possible theoretical explanation of this may be found in Fig. 27, Reference (13). Here the heaving force functions are seen to show fairly good agreement for different water-

lines until λ/L between 1.5 and 1.7 is reached. At this point they begin to diverge, and the divergence becomes more pronounced as higher values of λ/L are reached. Actually, the load waterlines of the two models do not correspond exactly to either one of the theoretical waterlines, but they are close enough to give a qualitative picture.

Figure XVIII

This figure, illustrating the effect of λ/L ratio upon loss of speed for the three models, permits comparison of the models in yet another way. Models 1 and 2 behave in a similar manner, with a sharp dip in sustained sea speed occurring at λ/L between 1.1 and 1.3, and the % loss in speed remaining fairly level at higher λ/L ratios. Model 3 shows dissimilar behavior, with a hump in the curve occurring at $\lambda/L = 1.1$, discussed under Figure XIII. The curves for Model 1 compare very well with those obtained by Vytlacil and Edstam for the same model. For a $V/\sqrt{L}$ of 1.81, they found the dip in the % V_S curve to occur at about $\lambda/L = 1.25$. Our highest $V/\sqrt{L}$ occurred at 26 knots ship speed, where $V/\sqrt{L} = 1.36$, with the dip in the curve occurring at about $\lambda/L = 1.2$. Study of the three curves for Model 1 and Figure 8 in Vytlacil's and Edstam's thesis indicate that, as still water speed increases, the point of greatest speed loss occurs at greater values of λ/L. This indication has not been verified, since the exact shape of our curves in the region from $\lambda/L = 1.1$ to 1.3 is not known.

Figure XIX

The curves of average pitch angle vs. period of encounter point out three facts:

1) Pitch angle is substantially a linear function of period of encounter, regardless of hull form. This is in agreement with the findings of Dillon and Lewis in Reference (4), Figure 17.

2) Peak amplitudes of pitching occurred at a lower period of encounter for the destroyer than for either the cruiser or carrier. Since T_e is most sensitive to the influence of λ, this again shows the strong dependence of pitching upon wave length.

3) Maximum amplitude of pitching is lowest for the destroyer, next highest for the carrier, and highest for the cruiser. Consideration of the exciting force relationship would indicate that Model 3 and Model 2 should have approximately the same amplitudes of pitch, with Model 3 pitching somewhat more. This has not been proved in this case, but the high points for Models 2 and 3 are so close that experimental errors might enter the picture. Moreover, the high periods of encounter used for Models 2 and 3 necessitated a much longer wave than was used for Model 1. This in turn resulted in much splashing of water at the inboard side of the wave maker and consequent production of a possible unstable condition. The M.I.T. Tank is not well equipped to handle waves

of over 12 feet in length, and this imposes a practical limit on the range of investigation.

Since the wave heights were so great at the longer periods of encounter, the plunging of the models into the water could easily introduce unfair points into the curves.

Figure XX

This figure shows for Model No. 1 the effect of wave slope on heaving motion for periods of encounter of 6, 7, and 8 seconds. At a period of encounter of 6 seconds, heaving motion is small, reaching a maximum at $a/\lambda = .0275$ and then decreasing. Since the period of encounter is so short, the vessel does not have time to fully react to the exciting force of the wave before encountering the succeeding wave and thus heaving is small. For larger wave slopes the model tends to go through the wave rather than riding over it with an accompanying vertical motion (i.e. heave).

Longer periods of encounter show maximum heave occurring at larger wave slopes and the absolute values of heave reach larger magnitudes. At a period of encounter of 7 seconds, heave is approximately linear with wave slope; however, for greater values of period of encounter heave shows a tendency to become non linear for values of a/λ above .025.

From this figure it can be seen that heave is not a linear function of wave slope but that a linear approximation will give reasonable values of heave for wave slopes less than .025.

Figure XXI

This figure shows, for Model No. 2, the effect of wave slope on heaving motion for periods of encounter of 7, 8, and 9 seconds. The results obtained are of little value, since there is no correlation between them. Further investigation of heave vs. wave slope for this model is recommended.

Figure XXII

This figure shows for Model No. 3 the effect of wave slope on heaving motion for periods of encounter of 10, 11, and 11.5 seconds. Within the limits of experimental error the results for Model 3 indicate that heave is essentially a linear function of wave slope in the range of wave slopes tested. Again it can be seen that with shorter periods of encounter less heave will result.

The range of wave lengths used in testing this model were extremely long and can be considered of academic value only since they would rarely, if ever, be actually encountered. It is therefore recommended that further testing be done with waves of length $\lambda/L < 1.0$ for this model.

Figures XXIII, XXIV, XXV

These figures show the effect of increasing wave slope on the angle of pitch for constant periods of encounter. These curves show comparable shapes regardless of the period of encounter and appear similar in shape for the three models tested. Shorter periods of encounter in all cases produce smaller amplitudes of pitch. The relation between pitch angle and wave slope is definitely of a non linear nature.

It appears that for wave slopes below $a/\lambda = .02$ a linear relation would closely approximate pitching; however, for larger wave slopes a linear assumption would result in excessive pitch prediction. This would result in over design for seaworthiness of an undetermined amount.

From these figures the authors conclude that a linear relation between pitch and wave slope is limited to wave slopes below $a/\lambda = .02$ and is of negligible importance, since the major problems in predicting seaworthiness occur for greater wave slopes.

The fact that pitch is not a linear function of wave slope is not unexpected, since pitching is dependent upon exciting forces (wave slope), inertia forces, and damping reactions. The linear approximation may be expected to hold for small wave slopes for the following reasons. A small wave slope will generate a small exciting force which will cause a small motion or response in the ship. Since the motion is small, the velocity and acceleration associated with it is correspondingly small. Damping is the result of the dissipation of the wave excitation energy in the generation of waves by pitching oscillation.

The total damping force must equal the exciting force plus any external force tending to cause motion of the ship. The inertia force of the ship is dependent upon its mass and its acceleration. Where the motions and resulting accelerations are small, the contribution of the inertia force to pitch excitation is small and damping is essentially linear

with wave slope. In the case of larger motions the damping force must again equal the sum of the exciting forces, but here the inertia force is no longer a small portion of the total. Thus, damping is greater than that required to overcome the excitation caused by the wave slope. This is graphically illustrated by the decrease in slope of the curves of pitch angle vs. wave slope presented in Figures XXIII-XXV.

Figures XXVII- XXIX

These figures are plots of maximum pitch angle versus tuning factor, T_p/T_e, for various values of λ/L. Heavy lines show experimental values, while the dashed lines are the theoretical values for maximum pitch angle predicted by Equation (121), Reference (13).

These plots are probably the most interesting part of the thesis, for they bring out several points which are of considerable interest and have caused much speculation and differences of opinion among authorities. First, all three of the curves show that maximum pitching amplitudes do not necessarily occur at synchronism, where $T_p/T_e = 1$. This statement may be modified somewhat by saying that maximum pitching amplitudes do not occur when the still-water period of pitching in waves is equal to the period of wave encounter. This suggests that natural period may vary considerably with such factors as the speed of the ship. Perhaps the data on natural pitching period is incorrect. This does not seem likely, since the three extinction curves obtained for any given model were almost identical. Furthermore, the close

agreement of T_p for Model 1 with that obtained by Lewis for a similar model, mentioned on Page 9 , indicates that our value is certainly very nearly the correct one. No, the answer will have to be found elsewhere, perhaps in Reference (13), where the authors state that there is no reason to expect the highest pitching angles to occur at resonance. Their theory helps to explain this fact, by virtue of the strong variation of the exciting moment with λ/L. Since the expression for $\frac{\frac{1}{2}\psi_m}{\phi_m}$ is made up of two terms, a magnification factor and a pitching function, both must be considered. Obviously the magnification factor μ_z will reach its highest value at resonance, assuming that damping does not change with speed. But what of the exciting factor? In general, it increases with increasing λ/L [Figure 30, Reference (13)], and, since increasing λ usually means increased period of encounter, the exciting factor will normally increase with <u>decreasing</u> values of T_p/T_e. As tuning factor is increased toward 1.0, there will be some point at which the exciting factor in combination with the magnification factor will produce highest pitching amplitudes; this point may or may not be where $T_p/T_e = 1.0$. Niedermair states, in Reference (9), that, in many cases, pitching amplitudes are not maximum until wave lengths well beyond those corresponding to synchronism have been reached. This statement is certainly substantiated by the results of our experiments. An obvious check is to obtain more points in the region of synchronism; that portion of the work will be left for those that follow.

The close agreement between experimental and theoretical values for Models 1 and 2 indicates that this theory is completely adequate to predict pitch angles in preliminary design work. Only in Models 2 and 3, at λ/L ratio of 1.3, are there marked differences between theoretical and actual values. In all other cases, $\frac{1}{2}\psi_m$ computed was between .641 and 1.18 times the actual $\frac{1}{2}\psi_m$. The agreement in the case of Model 1 is very good; the ratio of computed to actual values of $\frac{1}{2}\psi_m$ varies between .956 and 1.18. The discrepancies in the case of Models 2 and 3 at $\lambda/L = 1.3$ cannot be explained without further investigation, that is, obtaining more points. The difficulty may be due to a peculiarity of the towing tank, or to some experimental error. The fact that both discrepancies exist with waves of the same length (8.125 ft.) suggests an unstable condition in the wave setup. It will be noted that the theoretical calculations tend to overestimate the ratio $\frac{1}{2}\psi_m/\phi_m$ close to resonance, at least for Models 1 and 2. This is in accord with the conclusions reached by Weinblum and St. Denis.

Since there are two factors entering in the computation of $\frac{1}{2}\psi_m$ by the Weinblum-St. Denis theory, the reasons for the discrepancies will probably be found in either the damping factor or pitching function computation. This suggests

1) More concentrated investigation of the pitching period and damping factor, perhaps by some other method than the one used here. A particular area of investigation should be the possible change of these quantities with

speed or wave conditions.

2) A closer approximation to the actual waterline shape. Curves of pitching function have not been made for the transom stern waterline, and even the waterline of Model 3 varied considerably from the curves.

Had time permitted, we would have liked to extend our theoretical calculations to all the points that were obtained, and to complete a similar calculation for heave. Even without this additional evidence, our preliminary investigation shows that this theory is capable of accurately predicting pitch angles to a close enough approximation for design work, but such a prediction will not completely solve the ship motion problem. Williams points out in Reference (14) that the greatest velocities and accelerations are likely to arise much nearer to synchronism than the maximum amplitudes. Since the comfort of passengers and crew and the requirements for the stabilization of equipment depend upon these quantities, and particularly the effect of acceleration, the authors agree that the importance of synchronism is not diminished merely by observing that maximum amplitudes do not occur at this condition. The study of these velocities and accelerations is the next step, one which will require more complicated equipment than has been used heretofore in the M.I.T. Towing Tank.

Further investigation also should be made on the relationship between ship's pitching period in a seaway and the period of wave encounter. We feel that the angular

motion gyro offers an ideal means of determining ship's pitching period, by applying the method used to obtain the extinction curves.

Figure XXX

The variation of pitch with wave length for all three models is illustrated by Figure XXX. All three models behaved substantially the same in pitch, as they did in heave. The close agreement between the curves for all three models below $\lambda/L = 1.3$ at the same λ/a ratio is probably attributable to similarity of hull form. The curves for Models 1 and 2, which have relatively full lines and transom sterns, are almost concurrent until λ/L of 1.7 is reached, while the curve for Model 3 departs from the other two at considerably lower λ/L. In any case, the general trend of the curves indicates that pitching amplitudes increase with increasing λ/L, much as in the case of heave. The curves for Models 1 and 3 do not show the hollows at λ/L of about 1.2 which were obtained by Vytlacil and Edstam for the same models. This may be caused by either of two factors: 1) not enough points were taken in our experiments, or 2) our data is more accurate. We prefer to believe that the latter reason is the correct one, knowing that the gyro can be read to a much closer angle than the photographs. One way to substantiate our graphs would be to investigate more points near $\lambda/L = 1.2$. Unfortunately, time did not permit this in our case.

It can be seen from the curves that low values of the exciting forces at λ/L below .5 have restricted pitch angles to less than .25° for all three models; this indicates that this region is of such little importance that no further investigation is warranted.

V. CONCLUSIONS

From the foregoing discussion it is concluded that:

1) Pitch angle is a non linear function of wave slope for all of the models tested. Below values of $a/\lambda = .02$ a linear approximation is valid; however, above that wave slope a linear approximation predicts pitch greater than that actually observed. The region of linear approximation is of negligible importance since prediction of seaworthiness is desired at greater wave slopes.

2) Heave is a non linear function of wave slope: however, for values of $a/\lambda < .025$ a linear approximation will give reasonable values.

3) Maximum pitching amplitudes do not necessarily occur at synchronism, (tuning factor = 1). Maximum pitching amplitude for Model 1 occurred with $\Lambda = .6$, for Model 2 with $\Lambda = .575$, and for Model 3 with $\Lambda = .743$, all at 18 knots still water speed. This does not diminish the importance of synchronism, since maximum velocities and accelerations normally occur at this condition.

4) All three models behaved substantially alike in pitching, heaving, and speed loss. Models 1 and 2 behaved almost identically in most cases, while Model 3 in general experienced greater motions. This difference in behavior is attributed to the waterline shape of the models, and supports Weinblum's and St. Denis' contention that, above $\lambda/L = .8$, vessels with full waterlines are

likely to heave and pitch less than vessels with fine waterlines.

5) Both heave and pitch increased markedly with increasing values of λ/L for all three models.

6) Greatest sea speed reduction occurs in the region of $1.0 < \lambda/L < 1.3$ for all wave slopes.

7) For wave heights greater than $\lambda/a = 40$ sea speed is reduced to a greater extent for any particular wave length.

8) At higher ship thrusts the percentage loss in sea speed was in all cases less than that for low values of thrust (towing force).

9) The Weinblum-St. Denis theory contained in Reference (13) is completely satisfactory for predicting pitch angles in preliminary design work, for values of λ/L below 1.3. Theoretical values of $\frac{1}{2}\psi_m$ for Model 1 were between .956 and 1.18 times experimental values. Theoretical values for Models 2 and 3 varied from .641 and 1.18 times actual values for λ/L below 1.3. At $\lambda/L = 1.3$, the corresponding ratios varied from .825 to 2.24 for Model 2 and from .674 to .934 for Model 3; this may be an example of the growing discrepancy between theoretical and experimental values at higher λ/L ratios, as suggested by Weinblum and St. Denis. Theoretical calculations tended to overestimate the ratio $\frac{1}{2}\psi_m/\phi_m$ close to resonance for Models 1 and 2.

VI. RECOMMENDATIONS

The authors feel that the following areas of the pitching problem are particularly suitable for further study:

a) Determination of the effect of forward speed on the damping factor used in the theoretical prediction of pitch. Reference (11) states that damping is nearly independent of forward speed; however, this should be verified before extensive use of the theoretical pitch prediction is made.

b) Investigation of the actual period of pitching in waves using the angular motion gyro and a method similar to that used to obtain the natural still-water period (Page 91).

c) Calculation of further values of pitching and heaving functions in the Weinblum-St. Denis theory to approximate a greater variety of waterline forms (including transom sterns).

d) Investigation of the zero point of the heaving force function, Reference (13), which theoretically occurs at λ/L equal to waterplane coefficient.

e) Further investigation of sea speed loss in the region $1.0 < \lambda/L < 1.3$ to determine wave length where maximum speed loss occurs.

f) A more concentrated investigation of sea speed loss for model No. 2 in the region of $\lambda/L > 1.5$.

RECOMMENDATIONS (Cont.)

The following suggestions, if adopted, would improve the accuracy of future pitching experiments:

a) The sensitivity of the pitch recorder should be increased when operating in waves which give small amplitudes of pitch. A single calibration covering a range of pitch angles up to 6 degrees does not give enough detail to accurately read the small angles of pitch.

b) Any further investigations of the effects of wave slope on pitch, heave, and sea speed should be made using a multi channel recorder giving simultaneous plots of pitch, wave height and sea speed. This would enable the phase relations between excitation by the wave slope and response by the ship (pitching) to be obtained.

VII BIBLIOGRAPHY

1. Abkowitz, M. A., Paulling, J. R., "The Ship Model Towing Tank at M.I.T." Trans. SNAME*, vol. 61, 1953.

2. Bartlett, J. L., "The Motion of an Aircraft Carrier at Sea in Relation to the Operation of Naval Aircraft", Transactions of the Institution of Naval Architects, vol. 95, 1953.

3. Ben-Nun, Y. and Harel, J., "Seakeeping Tests of Series 60" S.B. Thesis M.I.T. 1954.

4. Dillon, E. Scott, and Lewis, Edward V., "Ships with Bulbous Bows in Smooth Water and in Waves," Paper presented before Chesapeake Section SNAME, March 3, 1955.

5. Kent, J. L., "Experiments on Mercantile Ship Models in Waves." Transactions of the Institution of Naval Architects vol. 64, 1922.

6. Kent, J. L., "Appropriate Ship Lengths for Minimum Pitching and Maximum Seaworthiness." Transactions of the Institution of Naval Architects, vol. 76, 1934.

7. Korvin-Kroukovsky, B. V., "Investigations of Ship Motions in Regular Waves." Trans. SNAME, vol. 63, 1955.

8. Manning, G. C., "The Motion of Ships among Waves." Principles of Naval Architecture, Volume II (edited by Rossell and Chapman) 1939.

9. Niedermair, J. A., "On the Motion of Ships." Transactions of the Institution of Naval Architects, vol. 93, 1951.

10. Porter, W. R., "A System of Angular Motion Instrumentation for Model Seaworthiness Testing," Naval Engineer Thesis, M.I.T. 1955.

11. St. Denis, M., "On Sustained Sea Speed" Trans. SNAME, vol. 59, 1951.

12. St. Denis, M., and Pierson, W. J. Jr., "On Motions of Ships in Confused Seas," Trans. SNAME, vol. 61, 1953.

13. Weinblum, G. P., and St. Denis, M., "On the Motions of Ships at Sea," Trans. SNAME, vol. 58, 1950.

14. Williams, A. J., "An Investigation into the Motions of Ships at Sea," Transactions of the Institution of Naval Architects, Vol. 94, 1952.

* Society of Naval Architects and Marine Engineers

VIII. APPENDIX

APPENDIX A

Model Characteristics

Model 1

Destroyer
Scale Ratio 67.09

	Model	Ship
Length	5.50 Ft.	369 Ft.
Displacement	20.51 pounds F.W.	2844 tons S.W.
Wetted Surface	3.523 Sq. Ft.	15,860 Sq. Ft.
Design Speed	4.268 Knots	35 Knots

Model 2

Light Cruiser
Scale Ratio 84.8

	Model	Ship
Length	6.25 Ft	530 Ft.
Beam	.610 Ft.	51.7 Ft.
Draft	.222 Ft.	18.8 Ft.
Displacement	26.44 Pounds F.W.	7400 tons S.W.
Design Speed	3.585 Knots	33 Knots

Model 3

Carrier
Scale Ratio 144 Block Coefficient .586

	Model	Ship
Length	6.25 Ft.	900 Ft.
Displacement	40.02 Pounds F.W.	55,000 tons S.W.
Wetted Surface	5.364 Sq. Ft.	111,220 Sq. Ft.
Design Speed	2.75 Knots	33.0 Knots

APPENDIX A (cont.)

Computed Model Characteristics

Model 1

k_y = 16.290 in.

T_p = .565 sec.

χ = .53

Approximate equation of design waterline:

$$\frac{Y}{b} = 1 - \left(\frac{X}{L/2}\right)^2$$

Model 2

k_y = 17.047 in.

T_p = .612 sec.

χ = .58

Approximate equation of design waterline:

$$\frac{Y}{b} \text{ between } \left[1 - \left(\frac{X}{L/2}\right)^2\right]^2 \text{ AND } \left[1 - \left(\frac{X}{L/2}\right)^4\right]$$

Model 3

k_y = 18.75 in.

T_p = .723 sec.

χ = .57

Approximate equation of design waterline:

$$\frac{Y}{b} = 1 - \left(\frac{X}{L/2}\right)^2$$

APPENDIX B

Supplementary Introduction

One of the most complete theoretical studies of ship motions in recent years has been presented by Messrs. Weinblum and St. Denis in Reference (13). The angle ψ referred to in Reference (13) corresponds to the angle $\frac{1}{2}\psi$, inclination from the horizontal, used in this paper. Our thesis has as an alternate objective the comparison of pitch angles predicted by this theory with those actually encountered in regular waves. The accuracy of the angular motion gyro offers an excellent means of evaluating pitch angles, and the wave characteristics can be measured. In practice, the evaluation of the theoretical pitch angles becomes difficult, because of

1) differences between model shape and those shapes for which pitch function has been tabulated, and
2) difficulty in obtaining damping factors for the models.

In order to better explain these difficulties, a summary of the pitching theory as presented in Reference (13) will be given.

The basic equations of motion for roll, pitch and heave are set up from consideration of the forces and moments which occur when the vessel is disturbed from the equilibrium position. For dynamic equilibrium, the exciting force or moment is resisted by the inertial, the damping, and the restoring reactions of the system. The major

portion of the paper consists of expressions for the various forces and moments, and specific solutions for the resulting motions. A further treatment of the subject is presented in reference (11), but the derived expressions are so complex that the 1950 paper was considered to be the more practical.

Following reference (13), the second order linear differential equation for ship motion is presented:

$$\frac{d^2s}{dt^2} + 2h\frac{ds}{dt} + v^2 s = f_1 \cos \omega t + f_2 \sin \omega t \qquad (2)$$

The forced motions in a seaway are obtained as particular solutions to equation (2) and are of the form

$$s = \frac{f}{v^2}\,\mu\,\cos(\omega t - \varepsilon_1 - \varepsilon_2) \qquad (3)$$

The amplitude $$s_m = \frac{f}{v^2}\,\mu \qquad (4)$$

$\frac{f}{v^2}$ represents static deflection under load, and μ is a magnification factor depending on the damping of the system, and the tuning factor, or ratio of natural period of the system to the exciting period. Values of μ plotted against tuning factor λ for various values of damping factor κ are presented in Figure 2, reference (13).

The second portion of the theory includes calculation of restoring moment in pitch. When a ship is rotated about its main transverse axis through an angle $\frac{1}{2}\psi$ from its position of equilibrium, the restoring moment resulting from the motion

is

$$M_\psi = -2\rho g \int_{-\ell}^{\ell} \tfrac{1}{2}\psi X^2 Y dX \cong -\rho g J_y (\tfrac{1}{2}\psi) \quad (5)$$

The angle ψ referred to in Reference (13) corresponds to the angle $\frac{1}{2}\psi$, inclination from the horizontal, used in this paper.

There is coupled to this moment a restoring force which is zero only when the abscissae of the center of flotation and center of gravity coincide. Since the magnitude of these coupled forces is not known, coupled motions are not considered in this theory.

The next step in computing the motion is to consider the exciting forces, or those due to wave action. The authors assume a wave of sinusoidal shape and consider the ship to be located normal to the wave crests (heading angle = 0° or 180°). The exciting moment is shown to be

$$M_\psi \cong 2\rho g \int_{-\ell}^{\ell} \gamma X Y_s dX \quad (6)$$

The exciting moment is then expressed in terms of maximum wave slope $\phi_m = \frac{2\pi r_m}{\lambda}$ and a pitch function $\Psi(\gamma)$ which is dependent upon the shape of the design waterline and the ratio of wave length to ship length λ/L. The pitch function is presented graphically in Fig. 30 of the paper. The maximum amplitude of the pitching moment is shown to be

$$(M_\psi)_m = \rho g \phi_m J_y \Psi(\gamma) \quad (7)$$

Setting pitching moment equal to the maximum value of restoring moment,

$$(M\psi)_m = \rho g \phi_m J_y \Psi(r) = -\rho g J_y (\tfrac{1}{2}\psi)_m$$

$$\phi_m \Psi(r) = -(\tfrac{1}{2}\psi)_m \tag{8}$$

The quantity $(\frac{1}{2}\psi)_m$, maximum pitch angle, is the static displacement due to the amplitude of the exciting force, and corresponds to the quantity $\frac{f}{\omega^2}$ in equation (3). Therefore, to find $(\frac{1}{2}\psi)_m$ under dynamic conditions, the magnification factor μ must be considered. Thus

$$(\tfrac{1}{2}\psi)_m = \phi_m \Psi(r) \mu_z \tag{9}$$

and the "pitch parameter" is

$$\frac{(\tfrac{1}{2}\psi)_m}{\phi_m} = \Psi(r) \mu_z \tag{10}$$

This equation is the basis for the theoretical calculations included in Appendix E.

APPENDIX C

Details of Procedure

A. Preparation of Models

Models 1 and 3 were prepared for testing by smoothing and repainting the hull and providing a space in the model large enough to hold the component parts of the gyro apparatus, (Plate I). In the case of Model 2, DTMB No. 4367, one coat of lacquer was applied to the hull and a small amount of wood removed from the interior of the model for the gyro case. Model 3 required a considerable amount of preparation, involving stripping off the old layers of paint and repainting several times. Covers were provided for the gyro equipment on all three models to prevent the entrance of water.

To provide means for evaluating motion of the model by photographs, a painted reference line was mounted in a vertical position at the center of gravity of each model. This reference line appears clearly in Plate III.

To obtain dynamic similarity between model and ship, the models were ballasted to give them a constant ratio of $\frac{k_y}{L}$ for ship and model.

For all three models, this ratio was taken to be .250. The model was then ballasted to give the correct radius of gyration. A detailed description of the method of calculation is contained in page 92. In the case of Model 2, the small amount of ballast remaining after the gyro was installed did not permit a ratio of .250 to be obtained; the final value

used in the tests was .227.

B. Determination of Pitching Period

In order to obtain natural pitching period (T_p) and damping factor (K) for each model, a pitch extinction curve was obtained using the angular motion gyro. The model with gyro installed was first attached to the towing cable and located at the middle of the towing tank. The pitch recorder was turned on, and marks were made at one-second intervals on the tape by means of a timing device contained in the recorder. After at least ten marks had been made on the tape, the bow of the model was depressed manually and suddenly released. The resulting pitch curve is the still-water pitch extinction curve; an example is shown in Plate XIV.

Three runs were made for each model and the results averaged to give the final values of T_p and K. Knowledge of recorder tape speed allowed computation of T_p by determining the distance on the tape between the peak pitching amplitudes. Taking the ratio of the maximum pitching amplitude in one cycle to the maximum amplitude in the next cycle, and averaging these values, led to determination of the logarithmic decrement q, since $q = \log_e \frac{x_1}{x_2}$.

The relationship $q \cong \pi K$ permitted determination of K.

C. Description of Runs

Before commencing each day's runs, the angular motion gyro was calibrated in the model, using the test setup shown in Plate II. The model with gyro installed was placed on the test stand and elevated and depressed to known angles. At

the same time, a mark was made on the pitch recording tape, as shown in Plate VIII. A calibration curve was made by plotting the known angle of movement vs. the half amplitude measured on the recorder tape.

Since the gyro output is known to vary somewhat with time, the calibration was repeated after concluding the day's runs. Values of pitch angle were taken using the mean of the two calibration lines. The error using the mean was $\pm$ 0.2° for pitch angles above 5°.

The wave height recorder was also calibrated before each day's runs, by depressing the capacitance wire to known depths in the water and marking the tape, as shown in Plate IX. The calibration curve was plotted immediately and used in the determination of wave height settings. Checks indicated that the wave height calibration curve did not change with time.

After the calibrations had been completed, a desired wave length was set on the wavemaker using the M.I.T. Towing Tank wave length calibration curve. The wave height was determined by the wave height recorder. When the correct setting had been finally determined, the run was started, using the known towing force for desired speed. During the run a photograph was taken and model pitch and wave height were recorded simultaneously. A sample photograph is included as Plate XII.

Pitch and wave height were computed from the recording tape using a number of consecutive maximum and minimum values. The range over which these were taken was chosen so

as to coincide with the range in which the photographs were taken. Model speed in waves was computed from the photographs, using known stroboscope setting and the number of reference line impressions appearing in a 7-foot length.

APPENDIX D

Summary of Data and Calculations

Table

I	Summary of Data	- Model No. 1	-	V_s = 10 Kts.
II	Summary of Data	- Model No. 1	-	V_s = 18 Kts.
III	Summary of Data	- Model No. 1	-	V_s = 26 Kts.
IV	Summary of Data	- Model No. 2	-	V_s = 18 Kts.
V	Summary of Data	- Model No. 3	-	V_s = 18 Kts.
VI	Calculation of T_e	- Model No. 1	-	V_s = 10 Kts.
VII	Corrected Pitch and Heave	- Model No. 1	-	V_s = 10 Kts.
VIII	Calculation of T_e	- Model No. 1	-	V_s = 18 Kts.
IX	Corrected Pitch and Heave	- Model No. 1	-	V_s = 18 Kts.
X	Calculation of T_e	- Model No. 1	-	V_s = 26 Kts.
XI	Corrected Pitch and Heave	- Model No. 1	-	V_s = 26 Kts.
XII	Calculation of T_e	- Model No. 2	-	V_s = 18 Kts.
XIII	Corrected Pitch and Heave	- Model No. 2	-	V_s = 18 Kts.
XIV	Calculation of T_e	- Model No. 3	-	V_s = 18 Kts.
XV	Corrected Pitch and Heave	- Model No. 3	-	V_s = 18 Kts.

TABLE I

Summary of Data

Model No. 1 V_s = 10 Kts.

Run No.	λ/L	λ/a	T_e Sec.	$\frac{1}{2}\psi_{avg.}$ Deg.	$\frac{1}{2}\psi_{max.}$ Deg.	V_o/V_s %
4	.5	20	4.272	.65	.87	74.0
25A	1.0	20	7.728	4.18	5.10	25.7
45	1.3	25	8.800	5.56	5.68	29.7
7	.5	30	3.919	.45	.54	97.0
22	1.0	30	7.000	2.76	3.56	55.0
44	1.3	30	8.104	4.08	4.26	57.4
10	.5	40	3.913	.14	.14	97.4
19	1.0	40	7.016	1.84	1.84	54.3
39	1.3	40	7.708	3.79	3.97	75.4
32	1.0	50	6.664	1.25	1.45	71.8
38	1.3	50	7.730	1.83	2.31	77.0
16	1.0	60	6.547	1.22	1.49	76.6
33	1.3	60	7.292	3.67	4.72	96.4

TABLE II

Summary of Data

Model No. 1 V_s = 18 Kts.

Run No.	λ/L	λ/a	T_e Sec.	$\frac{1}{2}\psi_{avg.}$ Deg.	$\frac{1}{2}\psi_{max.}$ Deg.	$Z_{avg.}$ Ft.	V_o/V_s %
2	.5	10	3.76	.375	.375	3.73	60.4
29	1.0	15	7.66	5.00	6.08	9.59	15.62
5	.5	20	3.12	.265	.326	1.13	93.7
26A	1.0	20	6.66	4.04	4.97	5.95	39.5
46	1.3	25	7.45	5.15	5.63	10.67	49.0
8A	.5	30	3.01	.10	.10	1.05	100.8
23C	1.0	30	5.95	3.18	3.18	5.25	61.4
43	1.3	30	6.90	4.12	4.44	9.07	66.0
85	2.335	30	9.50	5.69	6.20	22.22	80.3
11	.5	40	2.97	.104	.104	1.07	103.5
48	.75	40	4.16	.947	.985	2.70	95.0
20	1.0	40	5.38	2.50	2.50	5.08	82.7
49A	1.1	40	5.96	3.06	3.06	5.49	74.3
40	1.3	40	6.45	3.37	3.43	6.76	82.0
50	1.5	40	7.11	3.99	3.99	9.60	81.4
81A	1.75	40	7.88	3.87	3.99	13.59	82.9
80	2.00	40	8.49	4.27	4.95	15.89	84.0
82	2.335	40	9.27	4.14	4.70	18.10	87.7
31	1.0	50	5.35	2.29	2.34	3.73	84.2
37A	1.3	50	6.23	2.81	2.87	6.08	90.4
83A	2.335	50	9.19	3.50	3.85	12.43	90.2
17	1.0	60	5.19	1.69	1.69	2.88	91.0
34B	1.3	60	6.05	2.14	2.30	5.03	98.0
84	2.335	60	9.12	2.75	2.95	12.24	92.7

TABLE III

Summary of Data

Model No. 1 V_s = 26 Kts.

Run No.	λ/L	λ/a	T_e Sec.	$\frac{1}{2}\psi_{avg.}$ Deg.	$\frac{1}{2}\psi_{max.}$ Deg.	V_o/V_s %
3	.5	10	2.668	.25	.34	87.5
28	1.0	15	6.170	6.70	6.94	37.3
6	.5	20	2.475	.37	.63	99.9
27A	1.0	20	5.494	5.02	5.35	54.0
47	1.3	25	6.219	6.08	6.54	62.9
9A	.5	30	2.443	0	0	1.02
24A	1.0	30	4.849	3.55	3.75	74.4
42	1.3	30	5.784	4.90	4.90	76.0
12	.5	40	2.091	0	0	1.02
21	1.0	40	4.385	2.41	2.50	92.7
41B	1.3	40	5.455	3.80	3.94	87.5
30	1.0	50	4.372	2.15	2.22	93.4
36	1.3	50	5.306	2.93	3.07	93.1
18	1.0	60	4.323	1.61	1.69	95.5
35B	1.3	60	5.214	2.30	2.45	96.7

TABLE IV

Summary of Data

Model No. 2 V_s = 18 Kts.

Run No.	λ/L	λ/a	T_e Sec.	$\frac{1}{2}\psi_{avg.}$ Sec.	$\frac{1}{2}\psi_{max.}$ Sec.	$Z_{avg.}$ Ft.	V_o/V_s %
57	1.0	25	8.118	3.86	3.97	8.19	43.6
64C	1.3	25	9.045	2.10	2.20	17.38	55.5
56	1.0	30	8.010	2.57	2.89	5.39	46.5
63	1.3	30	9.637	4.39	4.96	23.27	40.1
51A	.5	40	3.948	.10	.10	1.90	99.7
52	.75	40	5.591	1.15	1.24	2.15	85.7
55A	1.0	40	7.391	2.66	2.87	5.075	64.7
58	1.1	40	7.994	2.79	2.89	7.31	60.4
59A	1.3	40	8.861	3.10	3.18	9.22	60.7
60	1.5	40	9.925	3.51	3.58	11.71	53.8
86A	2.055	40	10.93	3.87	4.56	23.02	82.5
88	2.213	40	11.456	4.55	4.71	27.68	82.2
87B	2.412	40	11.845	4.78	5.59	30.16	89.3
54	1.0	50	6.845	1.81	1.93	10.99	83.6
62	1.3	50	8.528	2.40	2.70	7.68	70.7
53	1.0	60	6.706	1.53	1.62	4.32	88.7
61A	1.3	60	8.469	2.47	2.68	5.83	72.5

TABLE V

Summary of Data

Model No.3 V_s = 18 Kts.

Run No.	λ/L	λ/a	Te Sec.	$\frac{1}{2}\psi$ avg. Deg.	$\frac{1}{2}\psi$ max. Deg.	Z Ft.	V_o/V_s %
67	1.0	25	11.63	5.94	6.32	7.26	31.6
66	1.0	30	10.84	3.20	3.60	23.28	50.1
73	1.3	30	13.90	4.93	5.44	25.07	45.7
75	.5	40	6.24	.17	.17	2.37	79.6
76	.75	40	8.53	1.30	1.36	7.12	67.0
65	1.0	40	10.42	2.87	3.05	8.89	60.9
68	1.1	40	10.17	3.25	3.35	13.09	66.7
69	1.3	40	12.35	4.60	4.92	14.40	57.2
70	1.5	40	13.26	4.19	4.70	28.38	61.6
78	1.0	50	10.00	2.18	2.35	8.94	73.0
72	1.3	50	11.90	2.87	3.05	17.14	69.1
77	1.0	60	10.10	2.34	2.54	7.58	70.1
71	1.3	60	11.73	2.71	2.91	15.80	73.6
79	1.0	70	9.98	1.66	1.73	6.29	73.6
74A	1.3	70	11.63	2.35	2.45	11.56	76.9

TABLE VI

Calculation of T_e

Model No. 1 V_s = 10 Kts.

Run No.	Spaces in 7 ft.	Strobe Setting Flash/min.	V_o f.p.s.	$\sqrt{\lambda}$ ft.$^{\frac{1}{2}}$	$2.26\sqrt{\lambda}$ ft.$^{\frac{1}{2}}$	T_e Sec.
4	91.7	1200	12.50	13.58	30.69	4.272
7	70.0	1200	16.39	13.58	30.69	3.919
10	69.7	1200	16.46	13.58	30.69	3.913
16	88.6	1200	12.95	19.21	43.41	6.547
19	125.0	1200	9.18	19.21	43.41	7.016
22	123.5	1200	9.30	19.21	43.41	7.000
25A	176.0	800	4.34	19.21	43.41	7.728
32	94.5	1200	12.13	19.21	43.41	6.644
33	88.0	1500	16.29	21.90	49.49	7.292
38	87.8	1200	13.06	21.90	49.49	7.669
39	90.0	1200	12.74	21.90	49.49	7.708
44	98.5	1000	9.70	21.90	49.49	8.104
45	152.5	800	5.02	21.90	49.49	8.800

TABLE VII

Corrected Pitch and Heave

Model No. 1 V_s = 10 Kts.

Run No.	a in.	$a'_{avg.}$ in.	a/a'	$\frac{1}{2}\psi'_{avg.}$ Deg.	$\frac{1}{2}\psi_{avg.}$ Deg.	$\frac{1}{2}\psi'_{max.}$ Deg.	$\frac{1}{2}$ max. Deg.
4	1.65	1.57	1.05	.625	.656	.83	.871
25A	3.30	3.40	.972	4.30	4.18	5.25	5.10
45	3.42	2.70	1.259	4.42	5.56	4.51	5.68
7	1.10	1.10	1.00	.45	.45	.54	.54
22	2.20	2.35	.936	2.95	2.76	3.80	3.56
44	2.86	2.80	1.021	4.00	4.08	4.17	4.26
10	.825	.86	.96	.15	.144	.15	.144
19	1.65	2.20	.75	2.45	1.84	2.45	1.84
39	2.15	1.90	1.13	3.35	3.79	3.51	3.97
32	1.32	1.85	.715	1.75	1.25	2.03	1.45
38	1.72	1.97	.874	2.10	1.83	2.65	2.31
16	1.10	1.40	.786	1.55	1.22	1.90	1.49
33	1.43	.78	1.835	2.00	3.67	2.57	4.72

TABLE VIII

Calculation of T_e

Model No. 1 V_s = 18 Kts.

Run No.	Spaces in 7 ft.	Strobe Setting Flash/min.	V_o f.p.s.	$\sqrt{\lambda}$ Ft.$^{\frac{1}{2}}$	$2.26\sqrt{\lambda}$ Ft.$^{\frac{1}{2}}$	T_e Sec.
2	78.0	1500	18.38	13.58	30.69	3.76
5	50.3	1500	28.49	13.58	30.69	3.12
8A	46.8	1500	30.62	13.58	30.69	3.01
11	45.5	1500	31.50	13.58	30.69	2.97
17	51.8	1500	27.67	19.21	43.41	5.19
20	57.0	1500	25.15	19.21	43.41	5.38
23C	77.0	1500	18.61	19.21	43.41	5.95
26A	95.5	1200	12.01	19.21	43.41	6.66
29	161.0	800	4.75	19.21	43.41	7.66
31	56.0	1500	25.61	19.21	43.41	5.35
34B	48.2	1500	29.74	21.90	49.49	6.05
37A	52.2	1500	27.46	21.90	49.49	6.23
40	57.6	1500	24.88	21.90	49.49	6.45
43	71.5	1500	20.05	21.90	49.49	6.90
46	77.0	1200	14.90	21.90	49.49	7.45
48	49.7	1500	28.85	16.64	37.61	4.16
49A	63.5	1500	22.58	20.15	45.54	5.96
50	58.0	1500	24.71	23.53	53.18	7.11
80	37.4	1000	25.55	27.17	61.40	8.49
81A	45.5	1200	25.20	25.12	56.77	7.88
82	43.0	1200	26.69	29.35	66.33	9.27
83A	41.8	1200	27.43	29.35	66.33	9.19
84	40.7	1200	28.17	29.35	66.33	9.12
85	47.0	1200	24.40	29.35	66.33	9.50

TABLE IX

Corrected Pitch and Heave

Model No. 1 V_S = 18 Kts.

Run No.	a	a′	a/a′	$\frac{1}{2}\psi'_{avg.}$	$\frac{1}{2}\psi_{avg.}$	$\frac{1}{2}\psi'_{max.}$	$\frac{1}{2}\psi_{max.}$	Z′	Z
	in.	in.		Deg.	Deg.	Deg.	Deg.	Ft.	Ft.
2	3.30	3.30	1.0	.375	.375	.375	.375	3.73	3.73
5	1.65	1.57	1.051	.252	.265	.310	.326	1.08	1.13
8A	1.10	1.10	1.0	.10	.100	.10	.10	1.05	1.05
11	.825	.79	1.044	.10	.104	.10	.104	1.03	1.07
17	1.10	1.40	.785	2.15	1.69	2.15	1.69	3.67	2.88
20	1.65	1.65	1.0	2.50	2.50	2.50	2.50	5.08	5.08
23C	2.20	2.18	1.009	3.15	3.18	3.15	3.18	5.20	5.25
26A	3.30	3.25	1.015	3.98	4.04	4.90	4.97	5.86	5.95
29	4.40	4.70	.936	5.35	5.00	6.50	6.08	10.25	9.59
31	1.32	1.41	.936	2.45	2.29	2.50	2.34	3.99	3.73
34B	1.43	1.40	1.021	2.10	2.14	2.25	2.30	4.93	5.03
37A	1.72	1.65	1.042	2.70	2.81	2.75	2.87	5.84	6.08
40	2.15	2.20	.977	3.45	3.37	3.51	3.43	6.92	6.76
43	2.86	2.80	1.021	4.04	4.12	4.35	4.44	8.88	9.07
46	3.42	3.40	1.006	5.12	5.15	5.60	5.63	10.61	10.67
48	1.238	1.32	.938	1.01	.947	1.05	.985	2.88	2.70
49A	1.815	1.82	.997	3.07	3.06	3.07	3.06	5.51	5.49
50	2.475	2.45	1.01	3.95	3.99	3.95	3.99	9.51	9.60
80	3.30	3.32	.994	4.30	4.27	4.98	4.95	15.99	15.89
81A	2.89	2.90	.997	3.88	3.87	4.00	3.99	13.63	13.59
82	3.85	3.85	1.00	4.14	4.14	4.70	4.70	18.10	18.10
83A	3.08	3.10	.994	3.50	3.48	3.85	3.83	12.51	12.43
84	2.57	2.57	1.00	2.75	2.75	2.95	2.95	12.24	12.24
85	5.14	4.97	1.034	5.50	5.69	6.00	6.20	21.49	22.22

TABLE X

Calculation of T_e

Model No. 1 V_s = 26 Kts.

Run No.	Spaces in 7 ft.	Strobe Setting Flash/min.	V_o f.p.s.	$\sqrt{\lambda}$ ft.$^{\frac{1}{2}}$	$2.26\sqrt{\lambda}$ ft.$^{\frac{1}{2}}$	T_e Sec.
3	37.3	1500	38.45	13.58	30.69	2.668
6	32.7	1500	43.85	13.58	30.69	2.475
9A	32.0	1500	44.82	13.58	30.69	2.443
12	32.0	1500	44.82	13.58	30.69	2.443
18	34.7	1500	41.95	19.21	43.41	4.326
21	35.2	1500	40.75	19.21	43.41	4.385
24A	35.1	1200	32.68	19.21	43.41	4.849
27A	48.2	1200	23.76	19.21	43.41	5.494
28	70.0	1200	16.39	19.21	43.41	6.170
30	35.0	1500	40.98	19.21	43.41	4.372
35B	37.8	1500	42.50	21.90	49.49	5.214
36	34.7	1485	40.91	21.90	49.49	5.306
41B	37.3	1500	38.45	21.90	49.49	5.455
42	43.0	1500	33.45	21.90	49.49	5.784
47	41.5	1200	27.65	21.90	49.49	6.219

TABLE XI

Corrected Pitch and Heave

Model No. 1 V_S = 26 Kts.

Run No.	a in.	a' in.	a/a'	$\frac{1}{2}\psi'_{avg.}$ Deg.	$\frac{1}{2}\psi_{avg.}$ Deg.	$\frac{1}{2}\psi'_{max.}$ Deg.	$\frac{1}{2}\psi_{max.}$ Deg.
3	3.3	3.35	.985	.25	.246	.34	.335
28	4.4	4.25	1.035	6.46	6.70	6.70	6.94
6	1.65	1.57	1.05	.35	.368	.60	.63
27A	3.30	3.25	1.015	4.95	5.02	5.27	5.35
47	3.42	3.35	1.02	5.95	6.08	6.40	6.54
9A	1.10	1.10	1.00	0	0	0	0
24A	2.20	2.14	1.03	3.45	3.55	3.65	3.75
42	2.86	2.80	1.02	4.80	4.90	4.80	4.90
12	.825	.83	.995	0	0	0	0
21	1.65	.65	1.00	2.41	2.41	2.50	2.50
41B	2.15	2.18	.985	3.85	3.80	4.00	3.94
30	1.32	1.32	1.00	2.15	2.15	2.22	2.22
36	1.72	1.85	.93	3.15	2.93	3.30	3.07
18	1.10	1.40	.786	2.05	1.61	2.15	1.69
35B	1.43	1.43	1.00	2.30	2.30	2.45	2.45

TABLE XII

Calculation of T_e

Model No. 2 V_s = 18 Kts.

Run No.	Spaces in 7 ft.	Strobe Setting Flash/min.	V_o f.p.s.	$\sqrt{\lambda}$ ft.$^{\frac{1}{2}}$	$2.26\sqrt{\lambda}$ ft.$^{\frac{1}{2}}$	T_e Sec.
51A	42.50	1200	30.33	16.281	36.80	3.948
52	49.50	1200	26.04	19.937	45.06	5.591
53	47.75	1200	27.00	23.022	52.03	6.706
54	50.75	1200	25.40	23.022	52.03	6.845
55A	65.50	1200	19.68	23.022	52.03	7.391
56	76.00	1000	14.14	23.022	52.03	8.010
57	81.00	1000	13.26	23.022	52.03	8.118
58	58.50	1000	18.36	24.146	54.57	7.994
59A	58.25	1000	18.44	26.245	59.31	8.861
60	78.25	1200	16.37	28.198	63.73	9.925
61A	58.50	1200	22.04	26.245	59.31	8.469
62	60.00	1200	21.48	26.245	59.31	8.528
63	88.25	1000	12.18	26.245	59.31	9.637
64C	63.75	1000	16.86	26.245	59.31	9.045
86A	51.4	1200	25.07	33.00	74.58	10.93
87B	47.5	1200	27.14	35.75	80.79	11.85
88	51.6	1200	24.98	34.25	77.40	11.46

TABLE XIII

Corrected Pitch and Heave

Model No. 2 V_s = 18 Kts.

Run No.	a	a'	a/a'	$\frac{1}{2}\psi'_{avg.}$	$\frac{1}{2}\psi_{avg.}$	$\frac{1}{2}\psi'_{max.}$	$\frac{1}{2}\psi_{max.}$	Z'	Z
	in.	in.		Deg.	Deg.	Deg.	Deg.	Ft.	Ft.
51A	.9375	.95	.987	.10	.099	.10	.099	1.93	1.90
52	1.406	1.47	.956	1.20	1.15	1.30	1.24	2.25	2.15
53	1.25	1.39	.899	1.70	1.53	1.80	1.62	4.80	4.32
54	1.50	1.49	1.007	1.80	1.81	1.92	1.93	10.92	10.99
55A	1.875	1.80	1.042	2.55	2.66	2.75	2.87	4.87	5.075
56	2.50	2.38	1.05	2.45	2.57	2.75	2.89	5.13	5.39
57	3.00	2.90	1.03	3.75	3.86	3.85	3.97	7.95	8.19
58	2.062	1.96	1.05	2.66	2.79	2.75	2.89	6.96	7.31
59A	2.438	2.45	.995	3.12	3.10	3.20	3.18	9.27	9.22
60	2.812	2.79	1.008	3.48	3.51	3.55	3.58	11.62	11.71
61A	1.625	1.62	1.003	2.46	2.47	2.67	2.68	5.81	5.83
62	1.95	1.93	1.010	2.38	2.40	2.67	2.70	7.61	7.68
63	3.25	2.96	1.098	4.00	4.39	4.52	4.96	21.20	23.27
64C	3.90	3.90	1.00	2.10	2.10	2.20	2.20	17.38	17.38
86A	3.85	3.88	.992	3.90	3.87	4.60	4.56	23.21	23.02
87B	4.52	4.65	.972	4.92	4.78	5.75	5.59	31.03	30.16
88	4.15	4.10	1.012	4.50	4.55	4.65	4.71	27.35	27.68

TABLE XIV

Calculation of T_e

Model No. 3 V_s = 18 Kts.

Run No.	Spaces in 7 ft.	Strobe Setting Flash/min.	V_o f.p.s.	$\sqrt{\lambda}$ ft.$^{\frac{1}{2}}$	$2.26\sqrt{\lambda}$ ft.$^{\frac{1}{2}}$	T_e Sec.
65	75.50	1000	18.55	30.00	67.80	10.42
66	92.00	1000	15.22	30.00	67.80	10.84
67	117.00	800	9.58	30.00	67.80	11.63
68	69.0	1000	20.28	31.46	71.10	10.17
69	80.5	1000	17.40	34.20	77.29	12.35
70	59.75	800	18.75	36.74	83.03	13.26
71	50.00	800	22.40	34.20	77.29	11.73
72	53.25	800	21.03	34.20	77.29	11.90
73	70.50	700	13.90	34.20	77.29	12.83
74A	60.00	1000	23.34	34.20	77.29	11.63
75	57.80	1000	24.22	21.21	47.93	6.24
76	68.75	1000	20.37	29.98	58.71	8.53
77	65.75	1000	21.30	30.00	67.80	10.10
78	63.00	1000	22.23	30.00	67.80	10.00
79	62.50	1000	22.40	30.00	67.80	9.98

TABLE XV

Corrected Pitch and Heave

Model No. 3 V_s = 18 Kts.

Run No.	a	a'	a/a'	$\frac{1}{2}\psi'_{avg.}$	$\frac{1}{2}\psi_{avg.}$	$\frac{1}{2}\psi'_{max.}$	$\frac{1}{2}\psi_{max.}$	Z'	Z
	in.	in.		Deg.	Deg.	Deg.	Deg.	Ft.	Ft.
65	1.875	1.85	1.014	2.83	2.87	3.00	3.04	8.73	8.89
66	2.500	2.50	1.000	3.20	3.20	3.60	3.60	23.28	23.28
67	3.000	2.55	1.176	5.05	5.94	5.37	6.32	6.17	7.26
68	2.060	2.06	1.000	3.25	3.25	3.35	3.35	13.09	13.09
69	2.438	2.44	.999	4.60	4.60	4.92	4.92	14.40	14.40
70	2.81	2.75	1.022	4.10	4.19	4.60	4.70	27.77	28.38
71	1.625	1.59	1.022	2.65	2.71	2.85	2.91	15.48	15.80
72	1.95	1.92	1.016	2.83	2.87	3.00	3.05	16.87	17.14
73	3.25	3.20	1.016	4.85	4.93	5.35	5.44	24.68	25.07
74A	1.39	1.36	1.022	2.30	2.35	2.40	2.45	11.31	11.56
75	.9375	.95	.987	0.17	.168	0.17	.168	2.40	2.37
76	1.046	1.40	1.004	1.30	1.30	1.36	1.36	7.09	7.12
77	1.25	1.24	1.008	2.32	2.34	2.52	2.54	7.52	7.58
78	1.50	1.42	1.056	2.07	2.18	2.23	2.35	8.47	8.94
79	1.07	1.08	.991	1.68	1.66	1.75	1.73	6.35	6.29

APPENDIX E

Sample Calculations

For Run 23C, Model No. 1:

$\frac{\lambda}{L} = 1.0 \qquad \lambda = 5.5$ Ft.

$\frac{\lambda}{a} = 30 \qquad a = \frac{\lambda}{30} = \frac{5.5 \text{ Ft.} \times \frac{12 \text{ in.}}{\text{Ft.}}}{30} = 2.20$ in.

Corrected Pitch Angle and Heave

a', actual wave height from tape = 2.18 in.

$\frac{1}{2}\psi'_{avg}$, average inclination from horizontal, from tape = 3.15°.

Applying linear extrapolation,

$\frac{1}{2}\psi_{avg}$, corrected inclination = $\frac{1}{2}\psi'_{avg.} \times \frac{a}{a'}$

$= 3.15^{\circ} \left(\frac{2.20}{2.18}\right) = 3.18^{\circ}$

Z', average ship heave from photograph = .930 in.

x scale ratio = .930 x 67.09 = 62.69 in. = 5.20 ft.

Z, corrected heave = $Z' \times \frac{a}{a'} = 5.20 \times \left(\frac{2.20}{2.18}\right) = 5.25$ ft.

Ship's Sea Speed and Period of Encounter

Since the stroboscopic photograph gives a series of impressions of the model marker at known time intervals and in a 7-foot length of run, sustained sea speed may be computed.

If n = strobe setting in flashes/min.

N = number of spaces between marks in a 7-ft. length = number of lines - 1

Model sea speed (ft. per min.) =

$$\frac{7 \text{ ft.}}{\frac{N \text{ spaces}}{n \frac{\text{flashes}}{\text{min.}}} \times 60 \frac{\text{sec.}}{\text{min.}}} = \frac{7}{60} \frac{n}{N} \frac{\text{ft.}}{\text{sec.}}$$

$$\text{Model sea speed (kts.)} = \frac{7}{60} \frac{n}{N} \frac{\text{ft.}}{\text{sec.}} \times \frac{1 \text{ kt.}}{1.689 \frac{\text{ft.}}{\text{sec.}}}$$

$$\text{For similarity, } \frac{V \text{ model}}{\sqrt{L \text{ model}}} = \frac{V \text{ ship}}{\sqrt{L \text{ ship}}}$$

$$\therefore V \text{ ship} = V \text{ model} \sqrt{\frac{L \text{ ship}}{L \text{ model}}} = V \text{ model} \sqrt{\text{Scale Ratio}}$$

$$\text{Ship sea speed (kts.)} = \frac{7}{60 \times 1.689} \frac{n}{N} \sqrt{\text{Scale Ratio}}$$

Natural Pitching Period, T_p, and Damping Factor, K

From extinction curve $\frac{1}{2} T_p = \frac{\text{no. of mm. between peaks}}{\text{tape speed (mm./sec.)}}$

For test run 1A, $T_p = \frac{2 \times 7 \text{ mm.}}{24.93 \text{ mm./sec.}} = .562$ sec.

For run 2A, $T_p = .577$ sec.

For run 3A, $T_p = .557$ sec.

$$T_p = \frac{.562 + .577 + .557}{3} = .565 \text{ sec.}$$

$$\text{Log. decrement} = \log_e \frac{\text{amplitude, cycle 1}}{\text{amplitude, cycle 2}} = \log_e \frac{x_1}{x_2}$$

Run 1A, $\frac{x_1}{x_2} = 5.12$

Run 2A, $\frac{x_1}{x_2} = 5.25$

Run 3A, $\frac{x_1}{x_2} = 5.4$

$$\frac{x_1}{x_2} = \frac{5.12 + 5.25 + 5.4}{3} = 5.26$$

log. decrement = $\log_e$ 5.26 = 1.66.

By formula (6), Reference (13),

log decrement $\simeq \pi\chi$

$1.66 = \pi\chi$

χ, damping factor = .53

For Run 23C with N = 77 spaces and n = 1500 $\frac{\text{flashes}}{\text{min.}}$

Ship sea speed (kts.) = $\frac{7}{60 \times 1.689} \frac{n}{N} \sqrt{\text{Scale Ratio}}$

$= \frac{7}{60 \times 1.689} \frac{1500}{77} \sqrt{67.09}$

V_o = 11.02 kts.

By formula (68), Reference (8), Page 26

T_e, Period of encounter, sec. = $\frac{\lambda}{2.26\sqrt{\lambda} + 1.689\ V_o(\text{knots})}$

λ extrapolated to ship length =

5.5 ft. x Scale Ratio = 5.5 ft. x 67.09 = 369 ft.

T_e (ship) = $\frac{369}{2.26\sqrt{369} + 1.689\ (11.02)}$

T_e = 5.95 sec.

Calculation of Longitudinal Radius of Gyration k_y

The following method of determining longitudinal radius of gyration, k_y, was developed by Mr. George Wachnik for use in the Ship Model Towing Tank at M.I.T. The model is suspended by two springs, of equal spring constants k, placed equal distances ℓ from the center of gravity of the model, as shown in Plate XIII.

Den Hartog's"Mechanical Vibrations", p. 106, gives expressions for the two natural frequencies of this system:

Calculation of Theoretical Pitch Angle by Reference (13)

For Run 23C:

T_e (ship) = 5.95 sec.

$$T_e \text{ (model)} = \frac{5.95}{\sqrt{\text{Scale Ratio}}} = \frac{5.95}{\sqrt{67.09}} = .726 \text{ sec.}$$

$$\text{Tuning factor } \frac{T_p}{T_e} = \frac{.565 \text{ sec.}}{.726} = .778$$

Entering Fig. 4, Reference (13), with $\frac{T_p}{T_e} = .778$

and $\chi = .53$ gives magnification factor $\mu_z = 1.8$

Entering Fig. 30, Reference (13), with $\frac{\lambda}{L} = 1.0$

and the equation of design waterline

$$\frac{Y}{b} = 1 - \left(\frac{X}{L/2}\right)^2, \text{ pitching function } \Psi_T = .37$$

By formula (121), Reference (13),

$$\frac{\frac{1}{2}\psi_m}{\phi_m} = \Psi_T(\gamma)\mu_z = (.37)\ (1.8) = .666$$

From Reference (13)

$$\tan \phi_m = \frac{2\pi r_m}{\lambda}$$

$$r_m \text{ (corrected)} = \frac{2.20 \text{ in.}}{2} = 1.10 \text{ in.}$$

$$\lambda = 5.5 \text{ ft.} \times 12 \frac{\text{in.}}{\text{ft.}} = 66 \text{ in.}$$

$$\tan \phi_m = \frac{2\pi(1.10)}{66} = .1047$$

$$\phi_m = 5.98^\circ$$

$$\frac{\frac{1}{2}\psi_m}{\phi_m} = .666$$

$$\frac{1}{2}\psi_m = \phi_m(.666) = 5.98\ (.666) = 3.98^\circ$$

$$\frac{1}{2}\psi_m = \text{(actual)} = 3.18^\circ$$

$$\text{Ratio } \frac{\frac{1}{2}\psi_m \text{ (computed)}}{\frac{1}{2}\psi_m \text{ (actual)}} = \frac{3.98^\circ}{3.18^\circ} = 1.25$$

APPENDIX F

Original Data

Table

TABLE XVI

Original Data

Model No. 1 V_s = 10 Kts.

Run No.	λ/L	λ/a	$a'_{max.}$ in.	$a'_{avg.}$ in.	$\frac{1}{2}\psi'_{max.}$ Deg.	$\frac{1}{2}\psi'_{avg.}$ Deg.
4	.5	20	1.65	1.57	.83	.625
7	.5	30	1.20	1.10	.54	.45
10	.5	40	.86	.86	.15	.15
16	1.0	60	1.45	1.40	1.90	1.55
19	1.0	40	2.20	2.20	2.45	2.45
22	1.0	30	2.35	2.35	3.80	2.95
25A	1.0	20	4.00	3.40	5.25	4.30
32	1.0	50	1.95	1.85	2.03	1.75
33	1.3	60	.88	.78	2.57	2.00
38	1.3	50	2.05	1.97	2.65	2.10
39	1.3	40	1.90	1.90	3.51	3.35
44	1.3	30	2.95	2.80	4.17	4.00
45	1.3	25	2.90	2.70	4.51	4.42

TABLE XVII

Original Data

Model No. 1 V_s = 18 Kts.

Run No.	λ/L	λ/a	$a'_{max.}$ in.	$a'_{avg.}$ in.	$\frac{1}{2}\psi'_{max.}$ Deg.	$\frac{1}{2}\psi'_{avg.}$ Deg.	Z' in.
2	.50	10	3.30	3.30	.375	.375	.667
5	.50	20	1.65	1.57	.310	.252	.194
8A	.50	30	1.10	1.10	.10	.10	.188
11	.50	40	.83	.79	.10	.10	.185
17	1.00	60	1.45	1.40	2.15	2.15	.656
20	1.00	40	1.65	1.65	2.50	2.50	.909
23C	1.00	30	2.18	2.18	3.15	3.15	.930
26A	1.00	20	3.75	3.25	4.90	3.98	1.048
29	1.00	15	3.00	2.90	5.60	5.15	1.818
31	1.00	50	2.02	1.95	2.50	2.45	.706
34B	1.30	60	1.54	1.40	2.25	2.10	.882
37A	1.30	50	1.75	1.65	2.75	2.70	1.044
40	1.30	40	2.25	2.20	3.51	3.45	1.238
43	1.30	30	2.95	2.80	4.35	4.04	1.588
46	1.30	25	3.70	3.40	5.60	5.12	1.897
48	.75	40	1.32	1.32	1.05	1.01	.514
49A	1.10	40	1.82	1.82	3.07	3.07	.985
50	1.50	40	2.45	2.45	3.95	3.95	1.702
80	2.00	40	3.40	3.32	4.98	4.30	2.86
81A	1.75	40	2.90	2.90	4.00	3.88	2.437
82	2.335	40	4.15	3.85	4.70	4.14	3.238
83A	2.335	50	3.30	3.10	3.85	3.50	2.238
84	2.335	60	2.85	2.57	2.95	2.75	2.190
85	2.335	30	5.15	4.97	6.00	5.50	3.844

TABLE XVIII

Original Data

Model No. 1 V_S = 26 Kts.

Run No.	λ/L	λ/a	$a'_{max.}$ in.	$a'_{avg.}$ in.	$\frac{1}{2}\psi'_{max.}$ Deg.	$\frac{1}{2}\psi'_{avg.}$ Deg.
3	.5	10	3.45	3.35	.34	.25
6	.5	20	1.65	1.57	.60	.35
9A	.5	30	1.10	1.10	0	0
12	.5	40	.83	.83	0	0
18	1.0	60	1.45	1.40	2.15	2.05
21	1.0	40	1.65	1.65	2.50	2.41
24A	1.0	30	2.20	2.14	3.65	3.45
27A	1.0	20	3.40	3.25	5.27	4.95
28	1.0	15	4.40	4.25	6.70	6.46
30	1.0	50	1.45	1.32	2.22	2.15
35B	1.3	60	1.55	1.43	2.45	2.30
36	1.3	50	2.15	1.85	3.30	3.15
41B	1.3	40	2.30	2.18	4.00	3.85
42	1.3	30	2.90	2.80	4.80	4.80
47	1.3	25	3.70	3.35	6.40	5.95

TABLE XIX

Original Data

Model No. 2 V_s = 18 Kts.

Run No.	λ/L	λ/a	$a'_{max.}$ in.	$a'_{avg.}$ in.	$\frac{1}{2}\psi'_{max.}$ Deg.	$\frac{1}{2}\psi'_{avg.}$ Deg.	z' in.
51A	.5	40	.95	.95	.10	.10	.273
52	.75	40	1.53	1.47	1.30	1.20	.318
53	1.0	60	1.48	1.39	1.80	1.70	.636
54	1.0	50	1.49	1.49	1.92	1.80	1.545
55A	1.0	40	1.80	1.80	2.75	2.55	.871
56	1.0	30	2.42	2.38	2.75	2.45	.726
57	1.0	25	2.98	2.90	3.85	3.75	1.125
58	1.10	40	1.96	1.96	2.75	2.66	.984
59A	1.3	40	2.53	2.45	3.20	3.12	1.312
60	1.5	40	2.83	2.79	3.55	3.48	1.645
61A	1.3	60	1.68	1.62	2.67	2.46	.822
62	1.3	50	2.02	1.93	2.67	2.38	1.01
63	1.3	30	3.15	2.96	4.52	4.00	3.00
64C	1.3	25	3.95	3.90	2.20	2.10	2.459
86A	2.055	40	3.88	4.05	4.60	3.90	3.285
87B	2.412	40	4.95	4.65	5.75	4.92	4.392
88	2.213	40	4.25	4.10	4.65	4.50	3.87

TABLE XX

Original Data

Model No. 3 V_s = 18 Kts.

Run No.	λ/L	λ/a	$a'_{max.}$ in.	$a'_{avg.}$ in.	$\frac{1}{2}\psi'_{max.}$ Deg.	$\frac{1}{2}\psi'_{avg.}$ Deg.	z' in.
65	1.0	40	1.87	1.85	3.00	2.83	.727
66	1.0	30	2.84	2.50	3.60	3.20	1.940
67	1.0	25	2.75	2.55	5.37	5.05	.514
68	1.1	40	2.13	2.06	3.35	3.25	1.091
69	1.3	40	2.48	2.44	4.92	4.60	1.200
70	1.5	40	2.80	2.75	4.60	4.10	2.314
71	1.3	60	1.63	1.59	2.85	2.65	1.29
72	1.3	50	1.98	1.92	3.00	2.83	1.406
73	1.3	30	3.23	3.20	5.35	4.85	2.057
74A	1.3	70	1.41	1.36	2.40	2.30	.943
75	.5	40	.95	.95	.17	.17	.20
76	.75	40	1.42	1.40	1.36	1.30	.591
77	1.0	60	1.26	1.24	2.52	2.32	.627
78	1.0	50	1.48	1.42	2.23	2.07	.706
79	1.0	70	1.10	1.08	1.75	1.68	.529

TABLE XXI

Model No. 1 — Theoretical Pitch Angles by Reference (13)

Run No.	Model T_e Sec.	T_p/T_e	Ψ_T	μ_z	$\Psi_T\mu_z$	tan ϕ_m	ϕ_m Deg.	$\frac{1}{2}\psi_m$ Comp. Deg.	$\frac{1}{2}\psi_m$ Act. Deg.	Ratio
					$\frac{\lambda}{L} = 1.0$					
17	.634	.891	.37	1.8	.666	.0524	3.00	2.00	1.69	1.18
20	.657	.860	.37	1.7	.629	.0786	4.50	2.83	2.50	1.13
23C	.726	.778	.37	1.6	.592	.1047	5.98	3.54	3.18	1.11
26A	.813	.695	.37	1.5	.555	.157	8.92	4.95	4.97	.996
29	.935	.604	.37	1.4	.518	.2095	11.83	6.13	6.08	1.01
31	.653	.865	.37	1.7	.629	.0628	3.60	2.26	2.34	.966
					$\frac{\lambda}{L} = 1.3$					
34B	.739	.765	.54	1.6	.864	.0524	3.00	2.59	2.30	1.13
37A	.760	.743	.54	1.5	.810	.0628	3.60	2.92	2.87	1.02
40	.787	.718	.54	1.5	.810	.0787	4.50	3.64	3.43	1.06
43	.842	.671	.54	1.4	.756	.1048	6.00	4.54	4.44	1.02
46	.910	.621	.54	1.4	.756	.125	7.12	5.38	5.63	.956
					$\frac{\lambda}{L} = 2.335$					
82	1.131	.500	.80	1.3	1.04	.0785	4.49	4.67	4.70	.994
83A	1.122	.504	.80	1.3	1.04	.0628	3.60	3.74	3.85	.971
84	1.113	.508	.80	1.3	1.04	.0524	3.00	3.12	2.95	1.06
85	1.160	.487	.80	1.3	1.04	.1048	6.00	6.22	6.20	1.003

TABLE XXII

Model No. 2 — Theoretical Pitch Angles by Reference (13)

Run No.	Model T_e Sec.	T_p/T_e	Ψ_T	μ_z	$\Psi_T \mu_z$	tan ϕ_m	ϕ_m Deg.	$\frac{1}{2}\psi_m$ Comp. Deg.	$\frac{1}{2}\psi_m$ Act. Deg.	Ratio
					$\frac{\lambda}{L} = 1.0$					
53	.728	.841	.35	1.6	.560	.0524	2.984	1.67	1.62	1.031
54	.743	.824	.35	1.6	.560	.0628	3.59	2.01	1.93	1.041
55A	.803	.762	.35	1.5	.525	.0785	4.472	2.35	2.87	.819
56	.870	.703	.35	1.6	.560	.1047	5.968	3.34	2.89	1.156
57	.882	.694	.35	1.5	.525	.1257	7.154	3.76	3.97	.947
					$\frac{\lambda}{L} = 1.3$					
59A	.962	.636	.53	1.3	.689	.0785	4.472	3.08	3.18	.969
61A	.920	.665	.53	1.4	.742	.0524	2.984	2.21	2.68	.825
62	.926	.661	.53	1.4	.742	.0628	3.59	2.66	2.70	.985
63	1.046	.576	.53	1.3	.689	.1047	5.968	4.11	4.96	.829
64C	.982	.623	.53	1.3	.689	.1257	7.154	4.93	2.20	2.24

TABLE XXIII

Model No. 3 — Theoretical Pitch Angles by Reference (13)

Run No.	Model T_e Sec.	T_{p/T_e}	Ψ_T	μ_z	$\Psi_T \mu_z$	tan ϕ_m	ϕ_m Deg.	$\frac{1}{2}\psi_m$ Comp. Deg.	$\frac{1}{2}\psi_m$ Act. Deg.	Ratio
				$\frac{\lambda}{L} = 1.0$						
65	.868	.829	.354	1.70	.602	.0785	4.472	2.69	3.05	.882
66	.903	.797	.354	1.65	.584	.1047	5.968	3.49	3.60	.969
67	.969	.743	.354	1.60	.566	.1257	7.154	4.05	6.32	.641
77	.842	.855	.354	1.70	.602	.0524	2.984	1.79	2.54	.705
78	.833	.864	.354	1.70	.602	.0628	3.59	2.16	2.35	.919
79	.832	.865	.354	1.70	.602	.0448	2.567	1.55	1.73	.896
				$\frac{\lambda}{L} = 1.3$						
69	1.029	.700	.53	1.40	.742	.0785	4.472	3.32	4.92	.674
71	.978	.736	.53	1.50	.795	.0524	2.984	2.37	2.91	.814
72	.992	.726	.53	1.50	.795	.0628	3.59	2.85	3.05	.934
73	1.158	.622	.53	1.30	.689	.1047	5.968	4.11	5.44	.756
74A	.969	.743	.53	1.50	.795	.0448	2.567	2.04	2.45	.833

APPENDIX G

Plates

Plate	
I	Installation of integrating gyroscope in model No. 3
II	Model No. 2 on pitch calibration stand
III	Model No. 2 in still water
IV	Model No. 3 in still water
V	Model No. 1
VI	Model No. 3
VII	Model No. 2 in waves
VIII	Sample of pitch calibration data and resulting calibration curve
IX	Sample of wave height calibration curve and resulting calibration curve
X	Sample pitch record
XI	Sample wave height record
XII	Typical multi-exposure photograph
XIII	Sketch of procedure for determining longitudinal radius of gyration
XIV	Pitch extinction curve for model No. 2

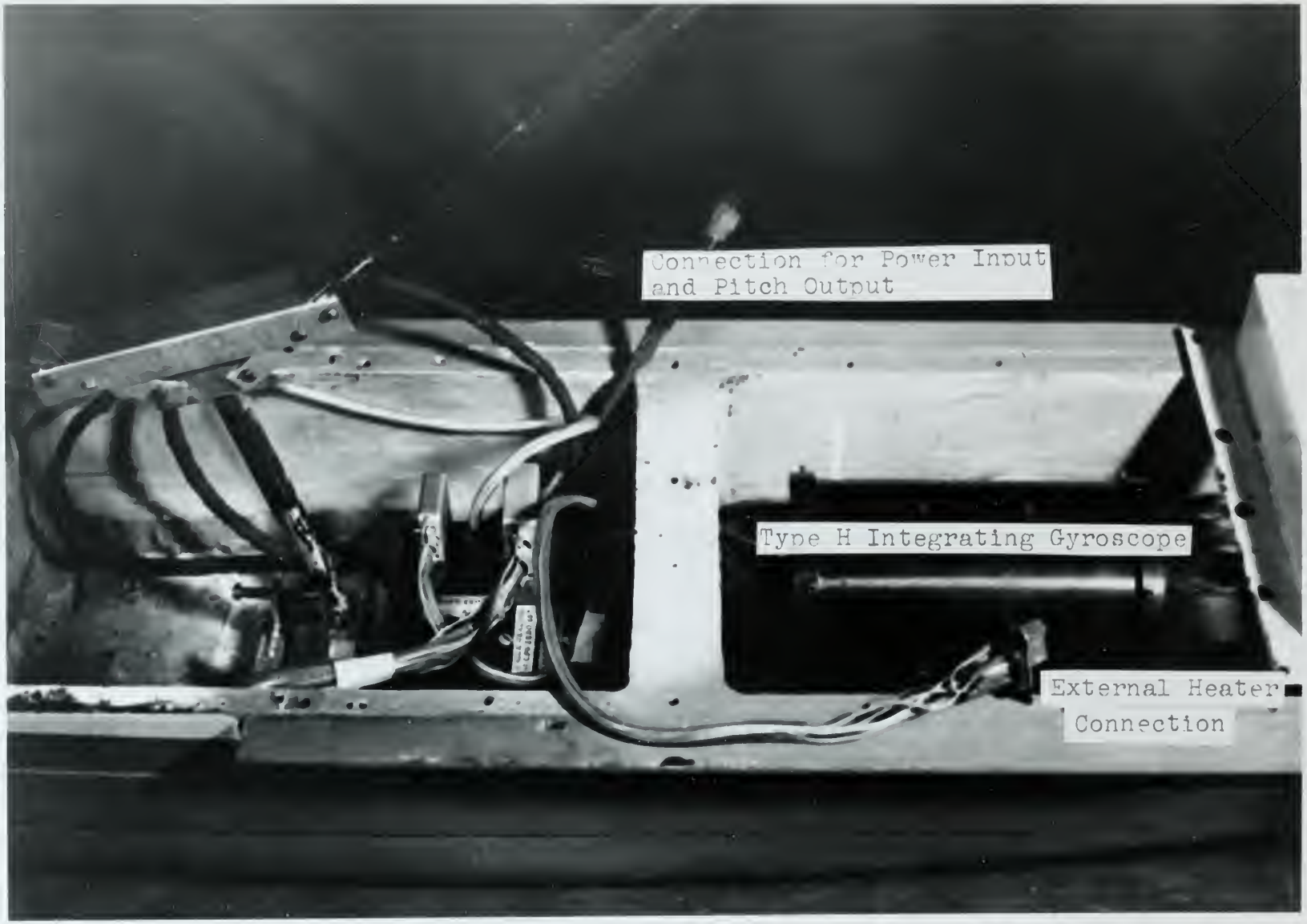

PLATE I INSTALLATION OF INTEGRATING GYROSCOPE IN MODEL NO. 3

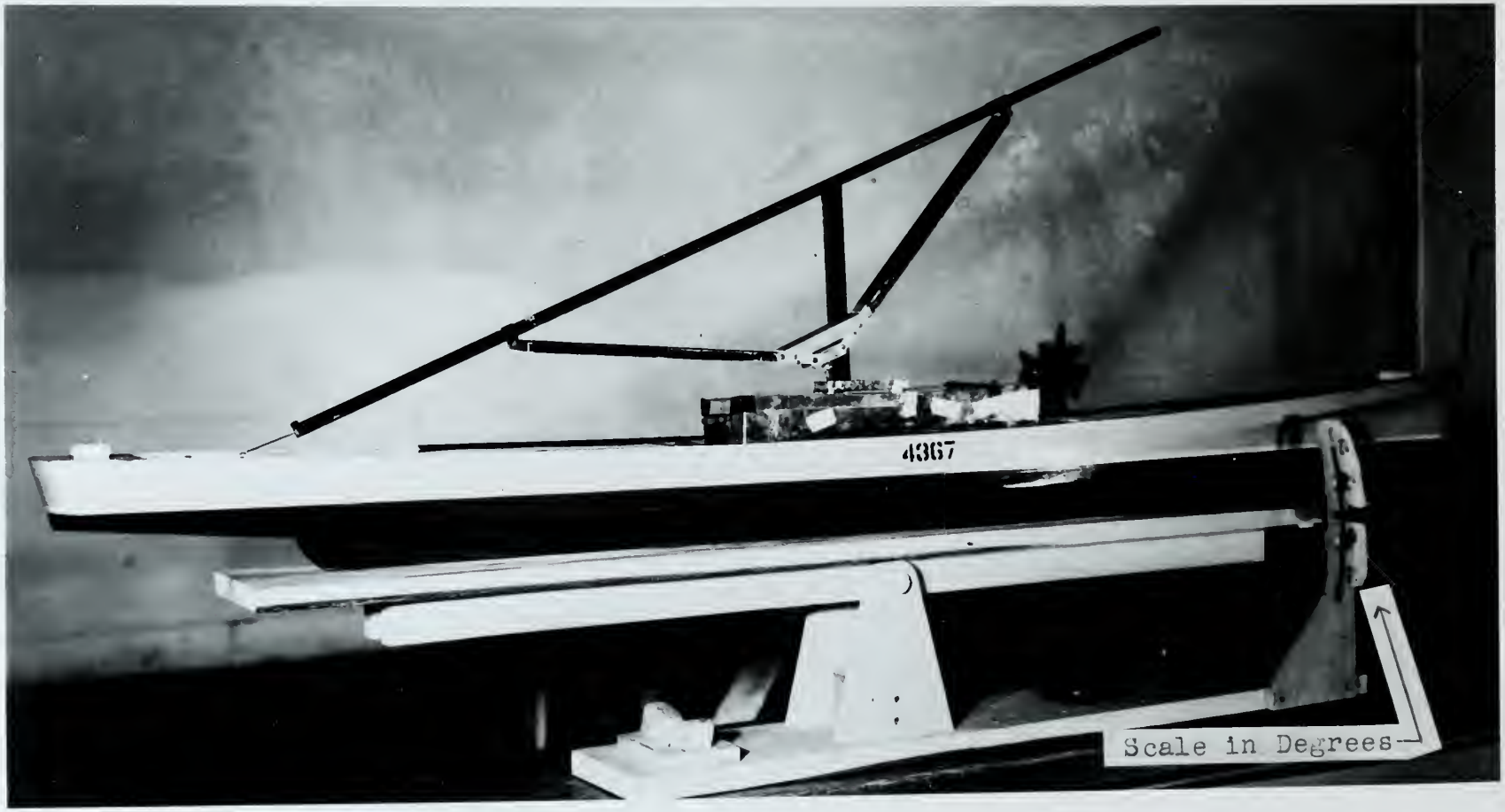

PLATE II MODEL NO. 2 ON PITCH CALIBRATION STAND

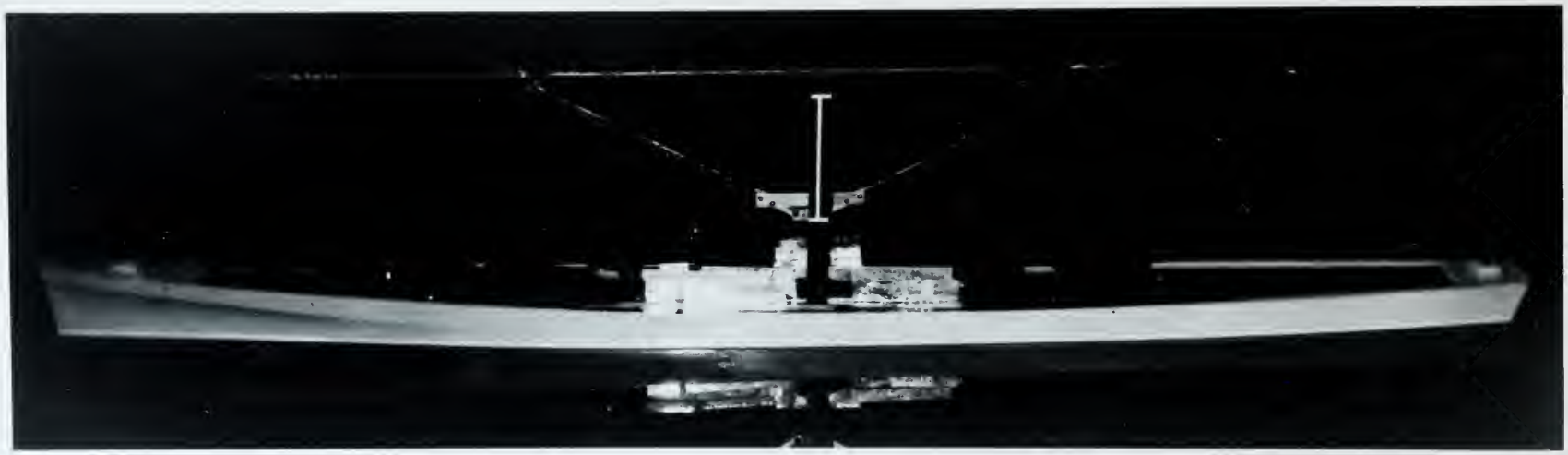

PLATE III MODEL NO. 2 IN STILL WATER

PLATE IV MODEL NO. 3 IN STILL WATER

PLATE V MODEL NO. 1

PLATE VI MODEL NO. 3

PLATE VII MODEL NO. 2 IN WAVES

PLATE VIII

SAMPLE OF PITCH CALIBRATION TAPE and CALIBRATION CURVE

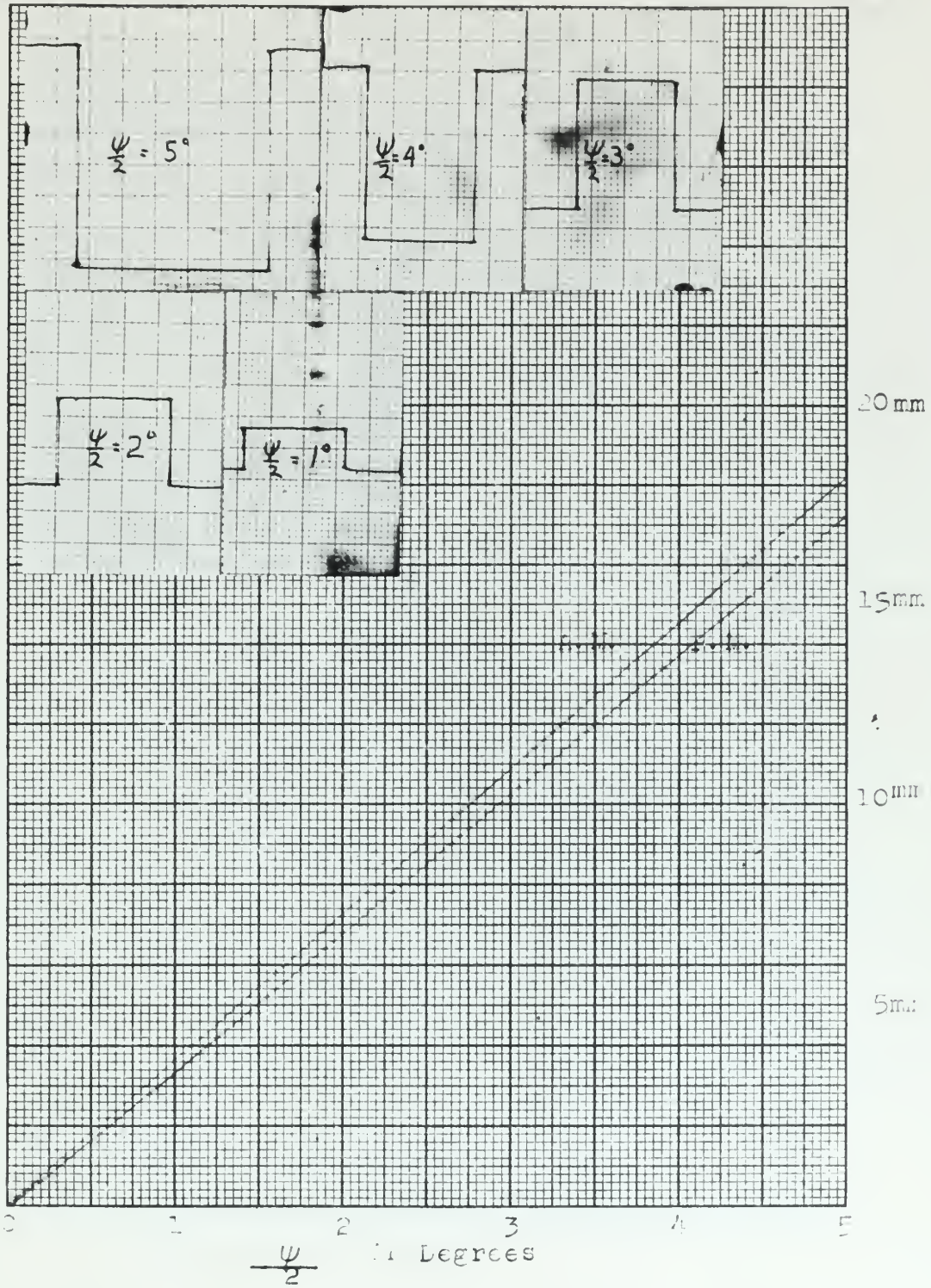

PLATE IX

SAMPLE WAVE HEIGHT CALIBRATION TAPE and CALIBRATION CURVE

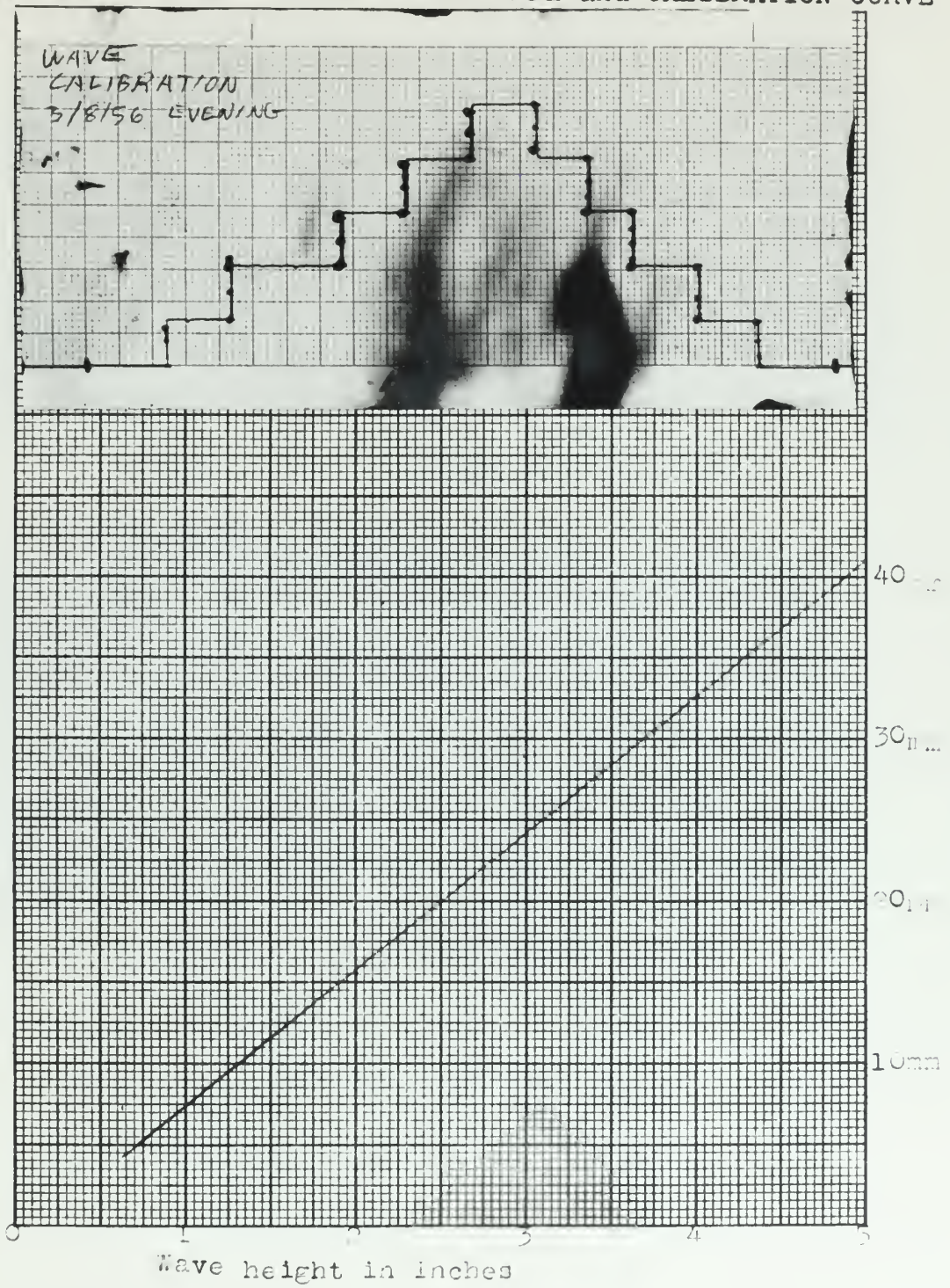

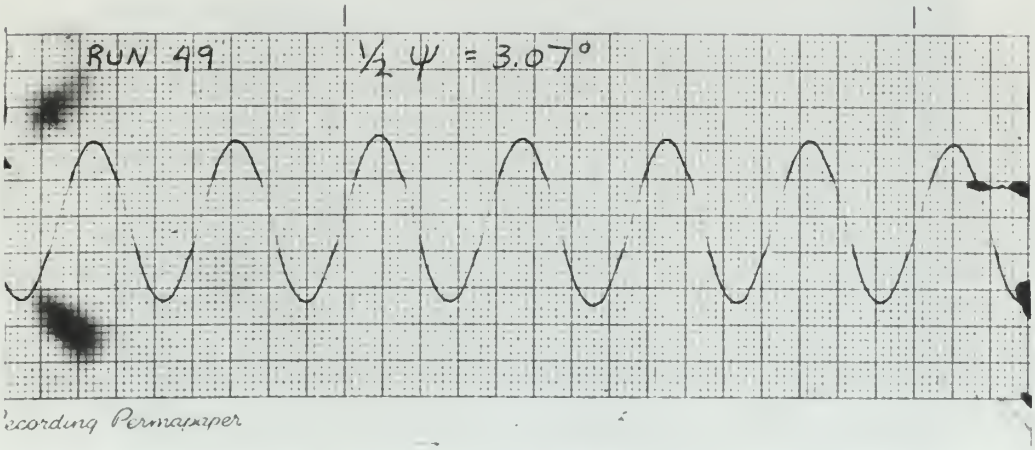

PLATE X SAMPLE PITCH RECORD

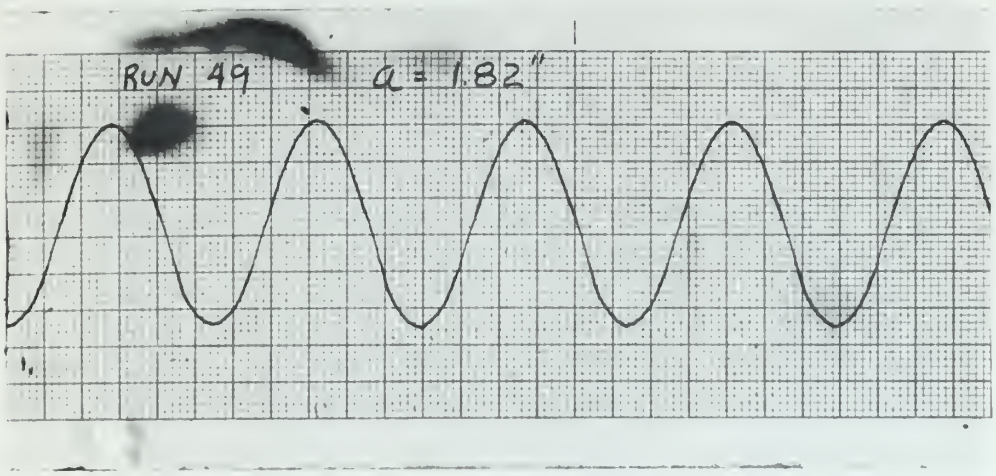

PLATE XI SAMPLE WAVE RECORD

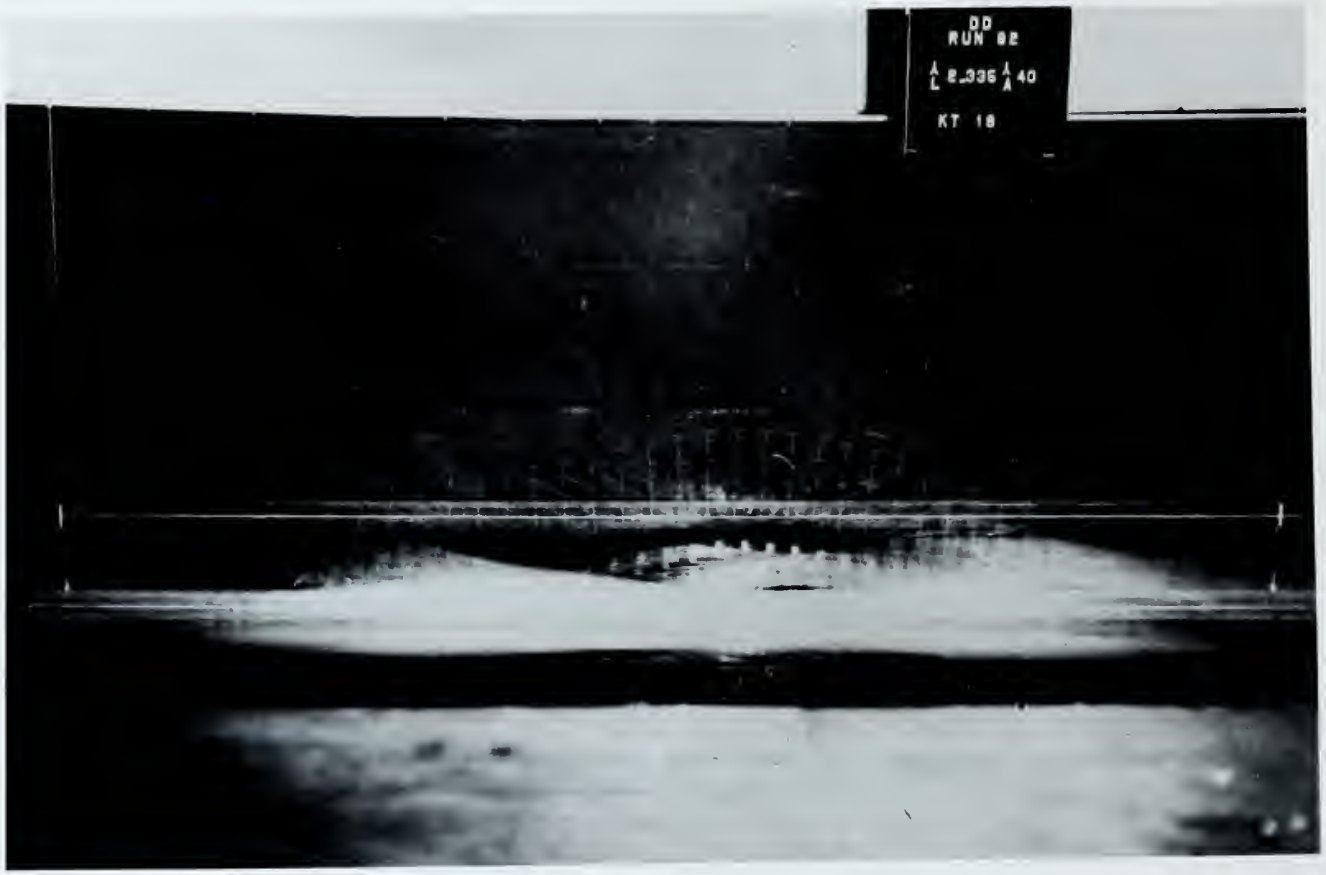

PLATE XII TYPICAL MULTI-EXPOSURE PHOTOGRAPH

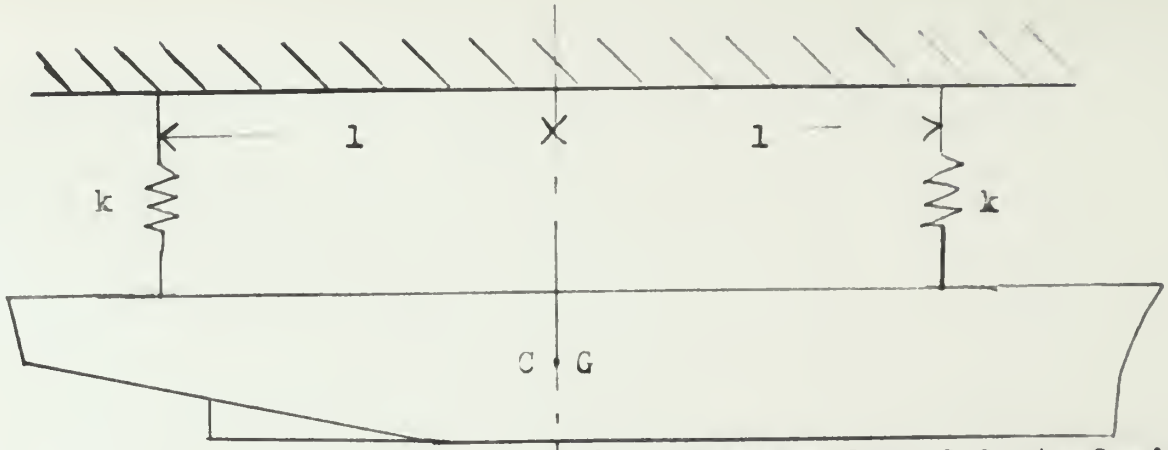

$$\omega_t^2 = \frac{2k}{m}$$

$$\omega_r^2 = \frac{k\,(2l)^2}{2I}$$

$$k_y = \left(T_r / T_t\right) l$$

l	Distance from C.G. to Spring
m	Mass of Model
I	Longitudinal Moment of Inertia
k	Spring Constant
k_y	Longitudinal Radius of Gyration

PLATE XIII METHOD OF DETERMINATION OF LONGITUDINAL RADIUS OF GYRATION

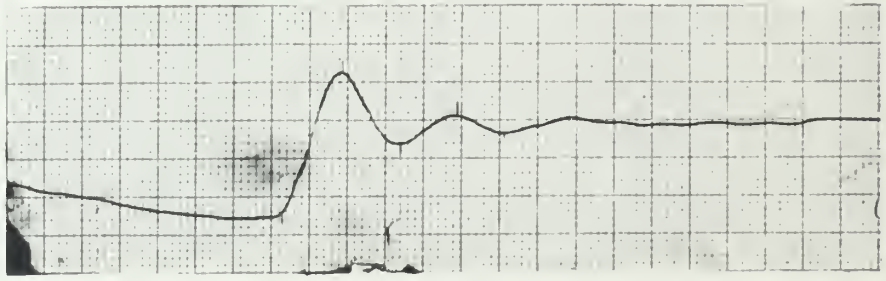

PLATE XIV PITCH EXTINCTION CURVE FOR MODEL NO. 2